

Solar Energetic Proton Events Observed by the High Energy Telescopes on the STEREO Spacecraft or at the Earth During the First Solar Orbit of STEREO A (2006–2023)

Ian G. Richardson^{1,2}  · Tycho T. von Rosenvinge^{1,3}  · O. Chris St. Cyr^{1,3}  · David Lario¹  · J. Grant Mitchell¹  · Eric R. Christian¹ 

© The author(s) ••••

Abstract

The twin STEREO A and B spacecraft were launched in October 2006 into heliocentric orbits at ~ 1 AU, advancing ahead of or lagging behind Earth, respectively, at $\sim 22^\circ/\text{year}$. The spacecraft provide in-situ observations of the solar wind and energetic particle populations, as well as remote sensing observations of solar activity and the corona. In particular, the High Energy Telescopes (HETs) on the STEREO spacecraft observe 0.7–4 MeV electrons and 13–100 MeV protons. This paper summarizes observations of solar energetic particle (SEP) events made by the STEREO HETs from the beginning of the mission through Solar Cycle 24 to December 2023, approaching the maximum of Solar Cycle 25 and

✉ I.G Richardson
 irichard@umd.edu
 T.T. von Rosenvinge
 tycho@rcn.com
 O.C. St. Cyr
 oestcyr2@gmail.com
 D. Lario
 david.lario@nasa.gov
 J.G. Mitchell
 john.g.mitchell@nasa.gov
 E.R. Christian
 eric.r.christian@nasa.gov

¹ Dept. of Astronomy, University of Maryland, College Park, MD 20742, USA

² Heliophysics Science Division, NASA Goddard Space Flight Center, Greenbelt, MD 20771, USA

³ Retired

encompassing STEREO A's first full orbit of the Sun relative to Earth, completed in August 2023; contact with STEREO B was lost in October 2014. Specifically, the catalog of SEP events including ~ 25 MeV protons observed by the STEREO HETs and/or instruments on spacecraft near Earth in Richardson et al. (2014) is updated to include ~ 450 SEP events and a total of ~ 1000 separate observations of these events from the various spacecraft locations. These extensive observations can provide unique insight into the propagation of energetic protons in the inner heliosphere and how the properties of the particle events are related to those of the associated solar eruptions. In particular, we examine the association of coronal mass ejections (CMEs) and SEP events with all 397 M and X-class solar X-ray flares in June 2010-January 2014 and demonstrate that, for these events, the occurrence of a CME accompanying a flare is required for the detection of a ~ 25 MeV proton event. On the other hand, many flares accompanied by CMEs are not followed by detected SEP events. The longitudinal width and intensity of the associated SEP events generally increase with the CME speed and the flare intensity. We also note evidence for a ~ 150 day "Rieger-like" periodicity in the SEP occurrence rate in 2020-2023 during the rising phase of Solar Cycle 25.

Keywords: Solar energetic particles; STEREO; SOHO; Coronal mass ejection; solar flare.

1. Introduction

The twin STEREO (Solar TERrestrial RElations Observatory) A ("Ahead") and B ("Behind") spacecraft (Kaiser et al. 2008) were launched on 26 October 2006 into heliocentric orbits at approximately 1 AU, advancing ahead of, or lagging Earth in its orbit, respectively. Separating from Earth by $\sim 22^\circ$ /year, in February 2011, STEREO A and B were 180° apart above the west and east limbs of the Sun, respectively, as viewed from Earth, allowing observations of the complete solar surface to be made for the first time. STEREO A passed directly behind the Sun as viewed from Earth in May 2015, and then approached Earth above the east limb of the Sun. In August, 2023, STEREO A finally returned to the vicinity of Earth. However, contact was lost with STEREO B on October 1, 2014 when on the far side of the Sun and has not been restored.

Each STEREO spacecraft carries a High Energy Telescope (HET) (von Rosenvinge et al. 2008) making observations of 0.7–4 MeV electrons and 13–100 MeV protons. The aim of this paper is to summarize observations of solar energetic particle (SEP) events made by the STEREO spacecraft, focusing on proton observations made by the HETs. In particular, we update to December 2023 the catalog of SEP events of Richardson et al. (2014) that include ~ 25 MeV protons observed at one or both of the STEREO spacecraft and/or by spacecraft located near Earth, encompassing the first STEREO A orbit of the Sun relative to Earth. The updated catalog includes information on the associated solar phenomena (e.g., location, flare, radio, and CME associations). Some 450 individual SEP events and their solar sources are identified.

As discussed in Section 2, the STEREO spacecraft were widely separated both from each other and spacecraft near Earth during the rising and maximum phases of Solar Cycle 24 (see also, for example, Lario et al. (2013) and Richardson et al. (2014)). Therefore, they were ideally located to investigate particle acceleration and transport in longitudinally-extended SEP events, some apparently filling the inner heliosphere. STEREO A was approaching Earth during the ascending phase of Solar Cycle 25, commencing in December 2019 when the spacecraft was $\sim 80^\circ$ east of Earth. When approaching closer to Earth, the observations of SEP events from STEREO A become more similar to those from near-Earth spacecraft. Nevertheless, the combined observations can be used, for example, to investigate smaller-scale variations in the features of SEP events that are related to local solar wind structures. An example is the October 9, 2021 event discussed by Lario et al. (2022) and Palmerio et al. (2024). These studies also included observations from the more recently launched missions into the inner heliosphere, including Parker Solar Probe (PSP) (Fox et al. 2016), Solar Orbiter (SolO) (Müller et al. 2020), and Bepi-Colombo (Benkhoff et al. 2021). They clearly demonstrated the impact of a corotating interaction region (CIR; e.g., Richardson 2018) on the development of an SEP event at the different spacecraft locations, as modeled by Wijsen et al. (2023). Other recent papers discussing SEP events during the rising phase of Solar Cycle 25 observed by STEREO A, near-Earth spacecraft and these inner heliosphere spacecraft include Kollhoff et al. (2021), who summarized observations of the first widespread SEP event of Cycle 25 in November 2020, and Lario et al. (2022), Palmerio et al. (2022), Dresing et al. (2023) and Khoo et al. (2024), among others. In particular, significant SEP events with multispacecraft analyses include October 28, 2021 (e.g., Papaioannou et al. 2022; Cohen et al. 2025), September 5, 2022 (e.g. Paouris et al. 2023; Kouloumvakos et al. 2025), and March 13, 2023 (e.g. Dresing et al. 2025). Also, Farwa et al. (2025) discuss electron to proton intensity ratios during 45 SEP events in 2020–2023 observed at five locations.

The focus of this paper is on the STEREO HET observations, and we do not attempt to provide a comprehensive review of SEP events observed by the current fleet of spacecraft. Nevertheless, in some cases, observations from the inner heliosphere spacecraft can help identify the source of an SEP event on the far side of the Sun relative to Earth or STEREO A. Such observations considered include the “living catalog” of SEP events observed by PSP (Mitchell et al. 2023), the catalog of X-ray flares observed by the Spectrometer/Telescope for Imaging X-rays (STIX, Krucker et al. 2020) on board SolO (<https://datacenter.stix.i4ds.net>), observations from the Energetic Particle Detector (EPD) on SolO (Rodríguez-Pacheco et al. 2020) and the catalog of multi-spacecraft SEP events in Solar Cycle 25 (Dresing et al. 2024) compiled as part of the SERPENTINE (Solar EneRgetic ParticLE aNalysis plaTform for the INner hEliosphere) project (<https://serpentine-h2020.eu/>). The end of 2023 provides a natural time to update the published STEREO ~ 25 MeV proton event list to include an additional ten years of observations beyond those summarized in Richardson et al. (2014) that encompass the first solar orbit of STEREO A with respect to Earth.

There are several reasons why observations of SEP events at HET energies are of interest. First, it is often easier to identify SEP event onsets at such

energies than at lower energies, where new solar particle events can be obscured by particles accelerated by interplanetary shocks (cf., Figure 1 of Richardson, von Rosenvinge, and Cane 2017), the effects of solar wind structures on low-energy ion intensity-time profiles, and by extended periods with elevated low-energy ion intensities. A further reason is that SEP events including ~ 25 MeV protons have been routinely identified in observations since 1967 from the Goddard Space Flight Center (GSFC) (and other) instruments on various spacecraft and used in several studies. These include: Van Hollebeke, Ma Sung, and McDonald (1975), Kahler, Hildner, and Van Hollebeke (1978), Cane, Reames, and von Rosenvinge (1988), where observations from 235 events in 1967–1985 were used to demonstrate clearly the contribution of interplanetary shocks to the distribution of SEPs in longitude, and Cane, Richardson, and von Rosenvinge (2010), who discussed 280 events in 1997–2006 during Solar Cycle 23. A summary of more than a thousand such events since 1967, including observations from STEREO, is presented in Richardson, von Rosenvinge, and Cane (2017). Also, as noted above, this paper updates the catalog of ~ 25 MeV proton events observed by STEREO and near-Earth spacecraft of Richardson et al. (2014). These near-Earth observations included proton observations from the Energetic and Relativistic Nuclei and Electron (ERNE) Sensor (Torsti et al. 1995) and proton and electron observations from the Electron, Proton Helium Instrument (EPHIN, Müller-Mellin et al. 1995), both on board the Solar and Heliospheric Observatory (SOHO, Domingo, Fleck, and Poland 1995).

Proton events extending to tens of MeV are also of space weather interest, including radiation hazards to astronauts (e.g. Cucinotta et al. 2010) and spacecraft systems (e.g., Iucci et al. 2005). Observations from the HETs have contributed to the development of the SEPSTER (SEP predictions based on STEReo observations) (Richardson, Mays, and Thompson 2018) and SEPSTER2D (Bruno and Richardson 2021) empirical SEP prediction models (see also Sections 3.26 and 3.27 in Whitman et al. 2023, for summaries of these models) that are providing near real-time predictions to the Coordinated Community Modeling Center (CCMC) SEP Scoreboard (<https://sep.ccmc.gsfc.nasa.gov/intensity/>).

Richardson et al. (2014) provided a comprehensive summary of the properties of over 200 individual SEP events up to December 2013, only 10 months before the loss of contact with STEREO B, and in particular focused on 25 widespread SEP events seen at both STEREO spacecraft and at Earth. An extended set of 43 such events is discussed by von Rosenvinge et al. (2015), including examples after December 2013. However, the STEREO spacecraft were then converging on the far side of the Sun from Earth prior to the loss of contact with STEREO B and thus less favorably configured to provide a widespread view of SEP events. Therefore, in this paper, we do not extend the analysis of widespread events of Richardson et al. (2014) and von Rosenvinge et al. (2015). Among the studies referring to the Richardson et al. (2014) catalog (including the updated version discussed in this paper), recent modeling by Strauss et al. (2023) suggests that the differences in electron and proton arrival times at the different spacecraft locations reported by Richardson et al. (2014) might be accounted for by diffusive particle transport from a single particle source, while Posner, Richardson, and Strauss (2024) argue that the dependence on the solar event longitude of proton

energy dispersion during the onsets of the most widespread SEP events is inconsistent with a source associated with an expanding CME-driven shock. Posner, Richardson, and Zeitlin (2025) note that all the 19 “ground level enhancements” observed on the surface of Mars by the Radiation Assessment Detector on the Mars Science Laboratory (MSL/RAD Hassler et al. 2012) from August 2012 to 2024 were associated with widespread SEP ~ 25 MeV proton events, including events reported in this paper. Richardson et al. (2023) used the catalog of Richardson et al. (2014) to identify SEP events up to 2013 associated with CMEs observed in the low corona by the Mauna Loa Solar Observatory (MLSO) Mk3/4 Coronameters, while around 27 SEP events associated with CMEs observed by the MLSO K-coronagraph (K-Cor) in 2013–2022 have been identified using the extended catalog described here (Burkepile et al. 2025; St. Cyr et al. 2025).

The outline of this paper is as follows: Section 2 summarizes HET SEP observations during the STEREO mission up to the end of 2023. The expanded SEP event catalog is introduced in Section 3 and is included in Appendix A. The intercalibration of the STEREO A HET and SOHO instruments at the beginning of the mission and end of the first STEREO orbit is discussed in Section 4. We then summarize examples of statistical studies of the relationship between SEP events and the properties of their solar sources using this data set in Section 5. We also consider where the highly energetic SEP events observed by the Payload for AntiMatter Exploration and Light-nuclei Astrophysics (PAMELA) reported by Bruno et al. (2018) and the events associated with long duration gamma ray flares (Bruno et al. 2023) lie in the longitudinal distribution of ~ 25 MeV proton events. In Section 6, we investigate the CME/flare/SEP association for a large sample of 397 M/X flares. Section 7 discusses evidence of periodicity in the SEP occurrence rate during the rise phase of Cycle 25. The results are summarized in Section 8. Finally several individual SEP events are discussed in Appendices B and C.

2. STEREO and Near-Earth SEP Observations in 2006–2023

Figure 1 shows an overview of the proton intensities at 14–24 MeV measured by the STEREO A and B HETs and, in a similar energy range (17–22 MeV)¹, by the ERNE instrument on SOHO located at L1 upstream of Earth (note that ERNE saturates in the largest events in Figure 1). The observations cover the period from STEREO launch (October 2006) to December 2023, shortly after STEREO A returned to near the Earth in August 2023; Figure 2 shows the STEREO spacecraft locations relative to Earth on January 1 of 2010, 2016, 2019 and 2023. The period in Figure 1 extends from the late declining phase of Solar Cycle 23 to the ascending phase of Cycle 25, as shown by the monthly-averaged

¹The ERNE data used are level 2 “export data” served by the NASA Space Physics Data Facility Virtual Energetic Particle Observatory (VEPO, <https://spdf.gsfc.nasa.gov/research/vepo/>). However, VEPO provides the approximate on-board energy channel ranges, and these have been corrected to the revised energy ranges given in https://export.srl.utu.fi/export_data_description.txt.

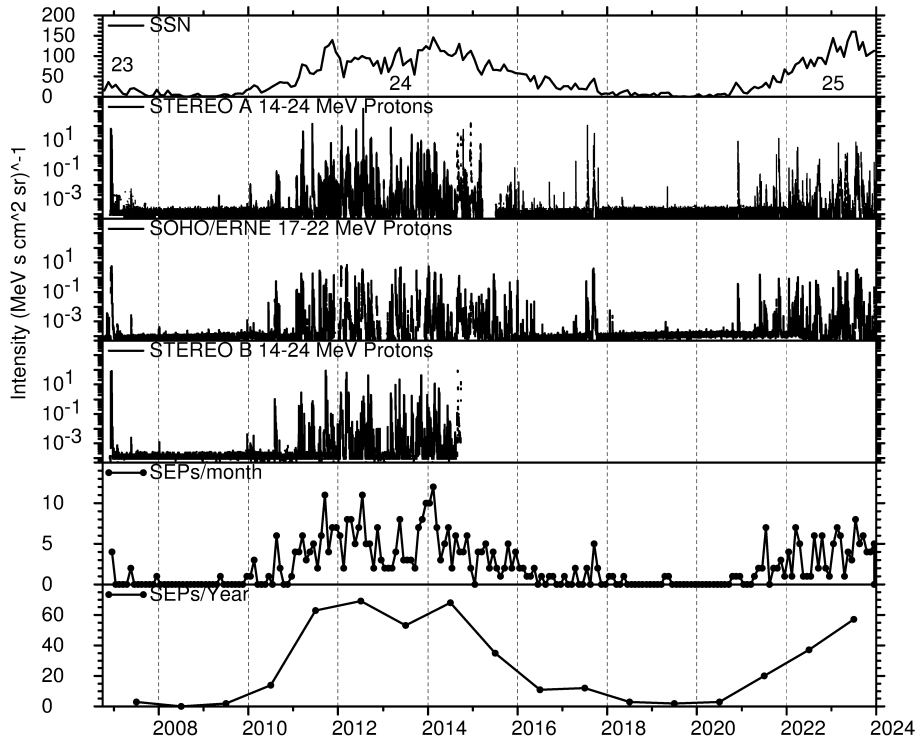


Figure 1. Summary of STEREO A (panel 2) and B (panel 4) 14-24 MeV proton intensities and SOHO ERNE 17-22 MeV proton intensities (panel 3) from STEREO launch in October 2006 to December 2023, just beyond the end of the first solar orbit (relative to Earth) of STEREO A in August 2023. Contact with STEREO B was lost on October 1 2014, when the STEREO spacecraft were both $\sim 180^\circ$ heliolongitude from Earth. The top panel shows the monthly sunspot number, extending from the late declining phase of Solar Cycle 23 to the ascending phase of Solar Cycle 25. The bottom two panels show the number of individual ~ 25 MeV proton events per month and per year cataloged in Tables 1 to 11. Note that these SEP rates are influenced by the loss of STEREO B observations and STEREO A approaching Earth in Cycle 25 (cf., Figure 2).

sunspot number (from the World Data Center for the Sunspot Index and Long-term Solar Observations (WDC-SILSO), <https://www.sidc.be/SILSO/datafiles>) in the top panel. The occurrence of SEP events in Figure 1 clearly follows the ~ 11 year solar activity cycle. The final large SEP events of Solar Cycle 23, in December 2006, occurred just after STEREO launch (e.g., von Rosenvinge et al. 2009). Only isolated particle enhancements were observed during the next ~ 3 years in the extended solar minimum between Solar Cycles 23 and 24. Then, following brief intervals of activity in early and mid-2010, the SEP rate finally increased in early 2011, more than two years into Solar Cycle 24 (beginning in December, 2008). By this time, the STEREO spacecraft were already above the limbs of the Sun when viewed from Earth, allowing observations of SEP events at widely-separated locations (e.g., Richardson et al. 2014). A notable feature of Solar Cycle 24 in Figure 1 is the temporary reduction in the occurrence of

STEREO HET First Orbit

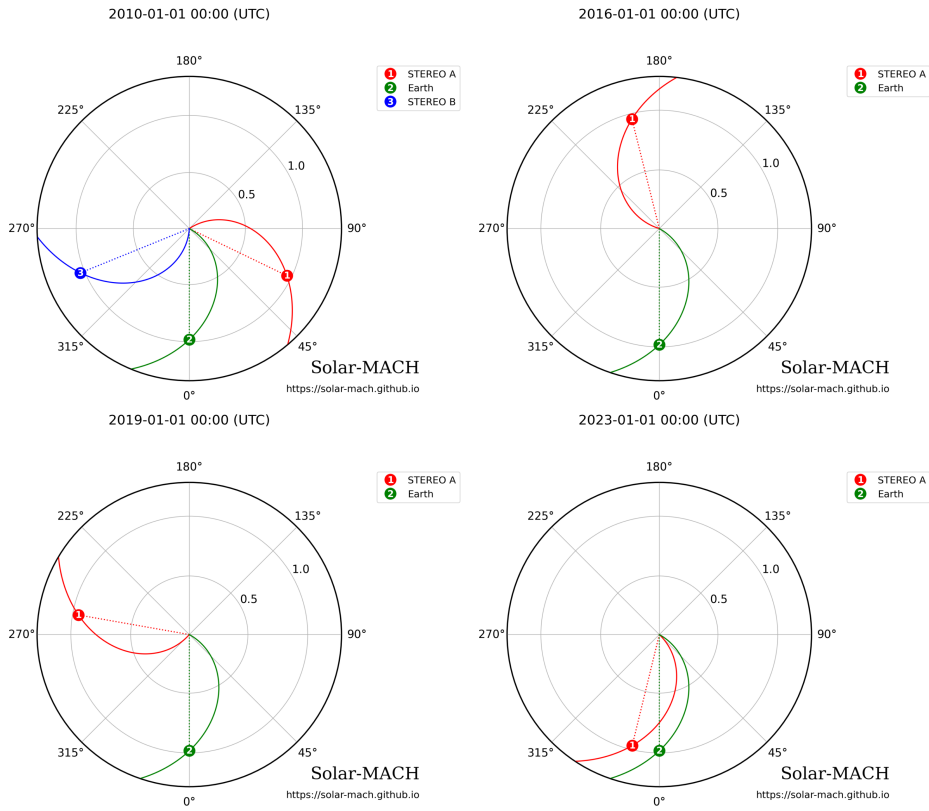


Figure 2. Locations of STEREO A (1, red) and B (3, blue) relative to Earth (2, green) on January 1 of 2010, 2016, 2019 and 2023. Contact was lost with STEREO B in October 2014. Nominal Parker spiral magnetic field lines (assuming a solar wind speed of 400 km/s) passing each location are also shown. Figures produced using Solar-MACH (Solar MAgnetic Connection Haus, Gieseler et al. 2023).

SEP events in late 2012-2013, evident in the monthly and yearly numbers of individual SEP events shown in the bottom two panels (the identification of these events is discussed below in Section 3 and Appendix A). Such a temporary decrease in the rate of energetic solar events, associated with the “Gnevyshev Gap” (e.g., Gnevyshev 1967, 1977; Storini et al. 2003), is a frequent feature near the maxima of solar activity cycles. Loss of contact with STEREO B occurred on October 1, 2014, so there are no STEREO B data after this time.

Occasional proton events occurred during the late decay phase of Solar Cycle 24. Most notably, a burst of activity in July-October, 2017, similar to that in December 2006 near the end of Cycle 23, produced some of the largest SEP events of Cycle 24. In particular, the SEP events on 4-10 September, 2017 have been discussed for example by Bruno et al. (2019), Mishev and Usoskin (2018), Mavromichalaki et al. (2018), Matthiä, Meier, and Berger (2018) and Jiggens et al. (2019). Rare small events occurred during the solar activity minimum between Solar Cycles 24 and 25, when STEREO A was returning towards

Earth above the east limb of the Sun (Figure 2); an example is highlighted in Appendix B. SEP activity then increased following the onset of Cycle 25. As noted above, the first widespread event of Cycle 25, on November 29, 2020, was discussed by Kollhoff et al. (2021). At this time, STEREO A was 70° east of Earth, and the event was also detected by near-Earth and inner heliosphere spacecraft. Figure 2 shows that STEREO A continued to approach Earth during the rising phase of Cycle 25, finally passing the longitude of Earth in August 2023.

3. SEP Catalog

As mentioned above, Richardson et al. (2014) cataloged the ~ 25 MeV proton events observed at the STEREO spacecraft and/or at Earth during the first seven years of the STEREO mission up to December 2013 and summarized their properties, including the associated solar phenomena (flares, radio emission and CMEs). Tables 1 to 11 in Appendix A update this catalog to December 2023, slightly beyond the end of the first STEREO A orbit in August 2023. For completeness, and because parameters for a few events have been updated or corrected, we have included the events identified by Richardson et al. (2014). The catalog is also available at the Harvard Dataverse (Richardson 2024) and will be further updated as data availability permits. “ ~ 25 MeV” as a description of the proton events aligns with that used in previous similar catalogs such as Cane, Richardson, and von Rosenvinge (2010). In addition, the intensities are based on observations from various spacecraft instruments around this energy that cover different energy ranges, as discussed below and in Appendix A.

The SEP events are predominantly identified from examination of ~ 1 hour-averaged (and also higher cadence) electron and proton observations from the STEREO HETs and the ERNE and EPHIN instruments on SOHO in orbit around the L1 point upstream of Earth. In a few cases (e.g., to identify SEP onsets during occasional SOHO data gaps), observations from the Advanced Composition Explorer (ACE, Stone et al. 1998) and Wind (Wilson III et al. 2021) spacecraft, also at L1, as well as the GOES (Geostationary Operational Environmental Satellite) spacecraft in geosynchronous Earth orbit, have also been considered.

Although integral proton flux data from the GOES spacecraft are widely used for near-Earth SEP studies and compiling event catalogs (e.g., Rotti et al. 2022), as well as operations (e.g., Bain et al. 2021), we do not focus on GOES data here for the following reasons, also discussed by Richardson et al. (2023): Figure 3 compares GOES > 10 MeV and > 30 MeV proton fluxes with 7.8–25 MeV and 25–41 MeV proton intensities from EPHIN during a representative period in June–July, 2012. It illustrates how the high background in the GOES observations obscures many small SEP events that are evident in EPHIN, which has a much lower background, similar to that in the HETs (see Figure 1). Although unimportant for space weather or operations, such events form part of the SEP population, and, as discussed further below, may include both small events that nonetheless have clear solar sources, such as that discussed in Appendix B, and

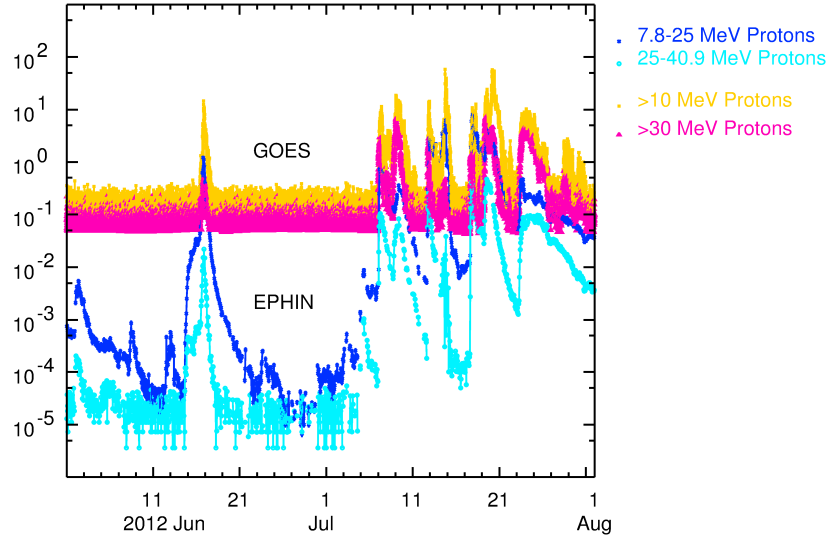


Figure 3. Comparison of GOES > 10 and > 30 MeV proton fluxes in $(\text{s cm}^2 \text{ sr})^{-1}$ (= proton flux unit, pfu) and 7.8-25 MeV and 25-40.9 MeV proton intensities (in $(\text{MeV s cm}^2 \text{ sr})^{-1}$) from SOHO/EPHIN for an interval in June-July, 2012, illustrating how the high background in the GOES fluxes obscures all but the largest SEP events that are observed by EPHIN. Using the standard/operational SEP event definition of > 10 pfu at > 10 MeV further limits the number of “SEP events”, and these are unrepresentative of the large dynamic range of SEP event intensities evident in the EPHIN observations. From Richardson et al. (2023).

particles from large events originating at distant locations on the Sun that are important for understanding particle acceleration and transport. Furthermore, the standard National Oceanic and Atmospheric Administration (NOAA) list of solar proton events affecting the Earth environment (<ftp://ftp.swpc.noaa.gov/pub/indices/SPE.txt>) requires a threshold of $10 (\text{s cm}^2 \text{ sr})^{-1}$ (= proton flux unit, pfu) in the GOES > 10 MeV proton flux to be exceeded. Many studies use this criterion, which corresponds to the lowest level (S1) of the NOAA Space Weather Prediction Center Solar Radiation Storm Scale (<https://www.swpc.noaa.gov/noaa%2Dscales%2Dexplanation>), to determine whether an SEP event or “no event” is present. However, Figure 3 clearly illustrates that these events are literally the “tip of the iceberg” of the range of SEP event size. Although this criterion may be suitable for identifying events of space weather interest (e.g., Bain et al. 2021) including spacecraft operations, and is a focus of many efforts to predict SEP events (e.g., Whitman et al. 2023), considering just a limited sample of relatively large events (which may also suffer from the “Big Flare Syndrome” (Kahler 1982)) is extremely restrictive for studies aimed at understanding the nature of SEP events and their solar sources. In addition, SEP event onsets in GOES-based SEP event lists are often based on the time when the 10 pfu threshold is crossed, which may be considerably delayed from the time of the related solar event, especially when the intensity is slowly rising. Here, we select any SEP event that is evident at proton energies of ~ 25 MeV above the low instrumental backgrounds of the HETs and SOHO instruments

while also recognizing that there are many additional SEP events that do not reach such energies that are worthy of study. Furthermore, we acknowledge that the GOES instruments, designed for operations, do have the advantage that they are less likely to saturate in exceptionally intense SEP events.

Details of the parameters included in the proton event catalog are given in Appendix A. These include the peak proton intensities at ~ 25 MeV during the “first peak” of the SEP event at STEREO A/B and near the Earth (i.e., not including any later “energetic storm particle (ESP)” intensity peak associated with interplanetary shock passage), the longitudes of the associated solar event/flare relative to Earth and the STEREO spacecraft, the GOES soft X-ray flare peak intensity (for frontside or near limb events with respect to Earth), type II and III radio emissions observed by instruments on Wind and the STEREO spacecraft and the associated CME speed and width (mainly from the CDAW (Coordinated Data Analysis Workshop) SOHO Large Angle and Spectrometric Coronagraph Experiment (LASCO) CME catalog, https://cdaw.gsfc.nasa.gov/CME_list/) for each SEP event, where available. As in the Richardson et al. (2014) catalog extending to December, 2013, the updated catalog again shows that essentially every ~ 25 MeV proton event can be associated with an identifiable solar eruption, a CME observed by LASCO (51% are identified as LASCO “halo CMEs” in the CDAW CME catalog indicating that the CME front surrounded the C2 occultor, though not necessarily symmetrically), and also with type III radio emissions observed by Wind and/or the STEREO spacecraft. Where information is available, 48% of these events were accompanied by type II emissions observed by these spacecraft. Three “problematic” events, where the solar event associations are more challenging to discern are discussed in Appendix C.

Several other SEP catalogs exist that are complementary to our catalog. These include:

- The STEREO SEP event list available at https://stereo-ssc.nascom.nasa.gov/data/ins_data/impact/level3/. This includes the subset of events meeting the criterion that the flux of 13–100 MeV protons from HET measurements is greater than 10 pfu, mimicking the NOAA Solar Proton Event list based on GOES > 10 MeV proton data. Event intensity-time plots are also provided;
- The catalog of 55–80 MeV solar proton events extending through Solar Cycles 23 and 24 of Paassilta et al. (2017);
- The catalog of > 55 MeV wide-longitude solar proton events observed by SOHO, ACE, and the STEREOs at ~ 1 AU during 2009 - 2016 compiled by Paassilta et al. (2018);
- Kühn et al. (2017) discuss 42 SEP events with protons above 500 MeV in 1995–2015 measured with SOHO/EPHIN;
- The SEPServer (<https://sepserver.eu/>) event catalog (Vainio et al. 2013; Papaioannou et al. 2014);
- The multi-spacecraft solar energetic particle event catalog for Cycle 25 produced by the SERPENTINE project (Dresing et al. 2024, <https://data.serpentine-h2020.eu/catalogs/sep-sc25/>);

- The Wind/EPACT(Energetic Particles Acceleration, Composition, Transport) Proton Event Catalog (1996–2016) compiled by Miteva, Samwel, and Costa-Duarte (2018);
- Pande et al. (2018) include 35 SEP events observed by GOES or SOHO/ERNE associated with $\geq M$ flares in 2010-2014;
- The “Integrated Geostationary Solar Energetic Particle Events Catalog” of Rotti et al. (2022) based on GOES data;
- The “Catalogues of Solar Proton Events in the 20-25 Cycles of Solar Activity” compiled by Moscow State University (https://swx.sinp.msu.ru/apps/sep_events.cat/; and
- The “Catalog of Solar Proton Events in the 24th Cycle of Solar Activity (2009–2019)” by Logachev et al. (2022).

4. HET Calibration Check in December 2006 and August 2023.

As discussed by Richardson et al. (2014), the occurrence of the last large SEP events of Solar Cycle 23 in December, 2006 (von Rosenvinge et al. 2009), around two months after STEREO launch when the STEREO spacecraft were still close to Earth, allowed the HET calibration to be checked relative to instruments on near-Earth spacecraft over a large dynamic range in particle intensity. This timing was extremely fortuitous since (Figure 1) comparable SEP events were only again observed after an interval of several years when the STEREO spacecraft were already widely separated from the Earth. While the proton responses of the HETs and instruments on near-Earth spacecraft were found to be similar, an unexpected factor of ~ 14 reduction in the 0.7-4 MeV electron intensity measured by HET relative to these other instruments was noted, as also discovered independently by Lario et al. (2013).

STEREO A returned to the vicinity of Earth during the rising phase of Solar Cycle 25 and hence observations of SEP events are available to check whether the HET and SOHO instrument responses remained consistent. Several such events are illustrated in Figure 4, which compares one-hour averaged proton intensities from SOHO/EPHIN, SOHO/ERNE and STEREO A HET on July 23-August 15, 2023 when STEREO A moved from 1.9° east of Earth to 0.3° west. The observations show that similar intensities were measured in comparable energy channels of the STEREO A HET and SOHO instruments during these events.

Another way of comparing the observations in these instruments is to investigate the correlation between the intensities measured in similar energy channels, as in Richardson et al. (2014). As an example, the top panels of Figure 5 compare the proton intensities measured by STEREO A HET (SOHO/ERNE) at 13.6-15.1 MeV (14-17 MeV) and 20.8-23.8 MeV (21-28 MeV) using simultaneous hourly-averaged data from July 19 (avoiding a large SEP event commencing late on July 17 in which ERNE saturated) to September 3, 2023. During this interval, STEREO A moved from 2.3° east to 2.0° west of Earth. Black lines indicate the least squares fits to the data, which are close to the lines of equality (red). The bottom panels show the essentially identical correlations using the

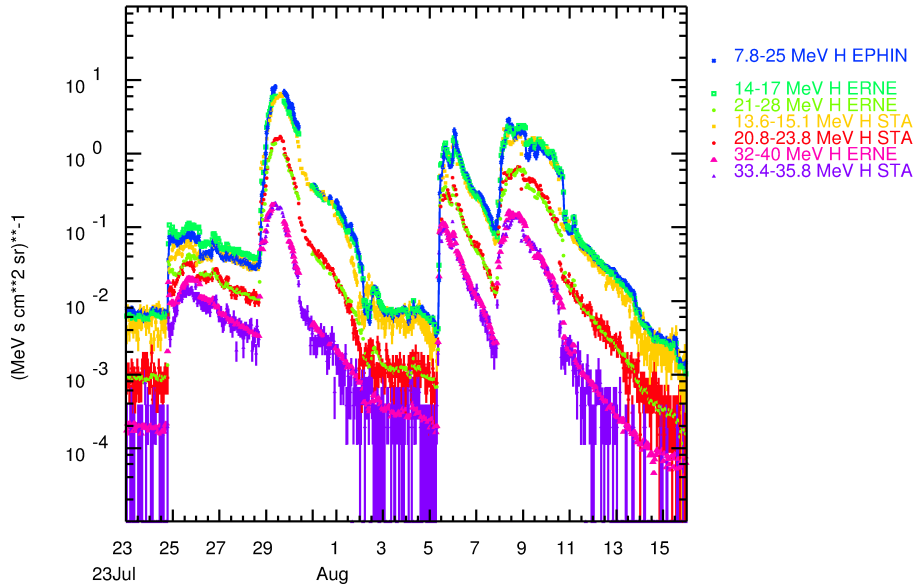


Figure 4. Comparison of hourly-averaged proton intensities observed by SOHO/EPHIN (7.8-25 MeV), SOHO/ERNE (14-17 MeV, 21-28 MeV and 32-40 MeV) and STEREO A HET (13.6-15.1, 20.8-23.8 MeV and 33.4-35.8 MeV) during a sequence of SEP events between July 23 and August 15, 2023 when STEREO A moved from 1.9° east of Earth to 0.3° west. The intensities are consistent in channels of similar energy ranges.

same energy channels for December 2006, when, as noted above, several SEP events occurred while the STEREO spacecraft were still close to Earth shortly after launch (e.g., von Rosenvinge et al. 2009; Richardson et al. 2014). These results again indicate that, at least at proton energies around ~ 20 MeV, the HET and ERNE proton inter-calibration at the end of the first STEREO A orbit is consistent with that in the early stages of the mission.

Another comparison may be made using particle spectra. Figure 6 compares proton spectra at ~ 13 -100 MeV from SOHO/EPHIN, SOHO/ERNE and the STEREO A HET for the period in Figure 5. Again the proton response of the different instruments appears to remain in excellent agreement. Based on these comparisons, and assuming that they represent the instrument responses throughout the first STEREO A orbit, and that the STEREO B HET also behaved similarly until loss of spacecraft contact, we conclude that it is not necessary to correct the proton intensities in Tables 1 to 11 in Appendix A for any drift in the calibration of HET relative to the SOHO instruments during the first STEREO A orbit.

We do not consider the electron response here since the electron response of the EPHIN instrument has changed since the December 2006 events (B. Heber, private communication, 2023). Therefore, the equivalent comparison cannot be made for the 2023 period and requires further analysis that is beyond the scope of this paper. We note however, that Farwa et al. (2025) (see their Appendix B) estimated a factor of 10 difference in the electron calibrations of the Solo HET

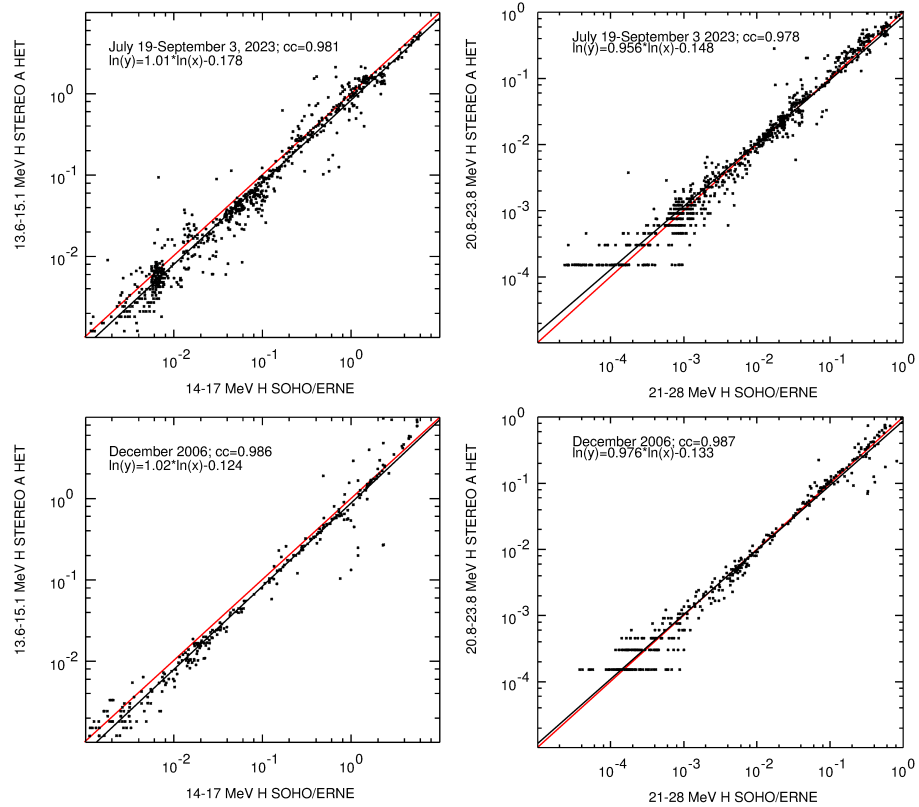


Figure 5. The top panels shows the correlation of SOHO/ERNE and STEREO A HET hourly-averaged proton intensities ($(\text{MeV s cm}^2 \text{ sr})^{-1}$) in two energy ranges during July 19–September 3, 2023 when STEREO A moved from 2.3° east of Earth to 2.0° west. The red lines indicate equal intensities. The bottom panels show essentially identical correlations in December 2006 near the start of the STEREO mission. The energy channels for SOHO/ERNE (STEREO A HET) are 13–17 (13.6–15.1) MeV in the left panels and 21–28 (20.8–23.8) MeV in the right panels. The “quantization” in the HET data in the right panels is due to low particle counts.

(an instrument unrelated to the STEREO HETs) and STEREO A HET during the decay phases of several SEP events, which is reasonably consistent with the factor of ~ 14 difference between the SOHO–STEREO HET electron calibrations at the beginning of the STEREO mission.

5. Comparison of SEP Events With the Properties of the Associated Solar Events

Richardson et al. (2014) discussed several properties of the SEP events and the associated solar events observed up to December 2013, and typically the conclusions from that study also apply to the expanded set of events. One difference is that, as noted above, the events in Richardson et al. (2014) were mainly

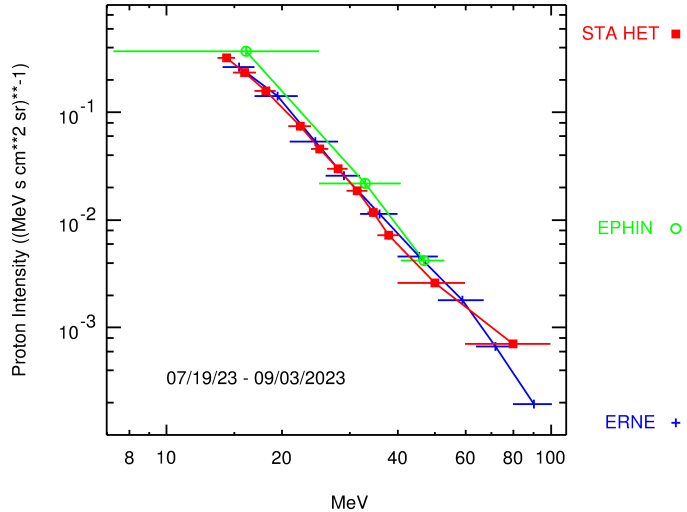


Figure 6. Comparison of proton spectra at ~ 13 - 100 MeV from SOHO EPHIN (green circles) and ERNE (blue crosses), and STEREO A HET (red squares) for July 19-September 3, 2023, showing excellent agreement between the STEREO A HET and the SOHO instruments. (Data generated by the VEPO with the ERNE energy channels corrected.)

observed when the STEREO spacecraft and Earth were approximately evenly-spaced in longitude around the Sun. Hence, for example, the number of locations at which an SEP event was detected gave a reasonable idea of how widespread an event was. With the loss of contact with STEREO B, and STEREO A making an orbit of the Sun relative to Earth, instead we consider the observations in Tables 1 to 11 as a large ensemble of SEP observations made over a wide range of heliolongitudes relative to the location of the related solar event, a single SEP event providing one to three observations depending on the number of spacecraft locations at which the SEP event was detected. Here, we summarize some of the basic properties of this ensemble of SEP events and their associated solar events. We also point out some biases that are inherent in these observations.

Figure 7 summarizes, in the top panel, ~ 25 MeV proton intensities vs. the solar event longitude relative to the observing spacecraft when an SEP event was detected (i.e., we omit cases where observations are available from a particular spacecraft location, but no SEP event was detected, or there was a high background or a data gap). This figure again emphasizes the result from Richardson et al. (2014) and Richardson, von Rosenvinge, and Cane (2017) that SEPs may be detected at all longitudes relative to a solar eruption, though the largest, and also frequent small events, tend to be observed when the eruption is on the western hemisphere (0 - 90° longitude) relative to the observing spacecraft, and hence likely to be well-connected to the spacecraft by the nominal spiral interplanetary magnetic field (IMF). The color and size of the symbols indicate the speed of the associated CME. The fastest CMEs (~ 2000 km/s and above), indicated by the larger red and purple symbols, tend to be associated with the largest SEP events at all longitudes. However, somewhat slower CMEs are also apparently

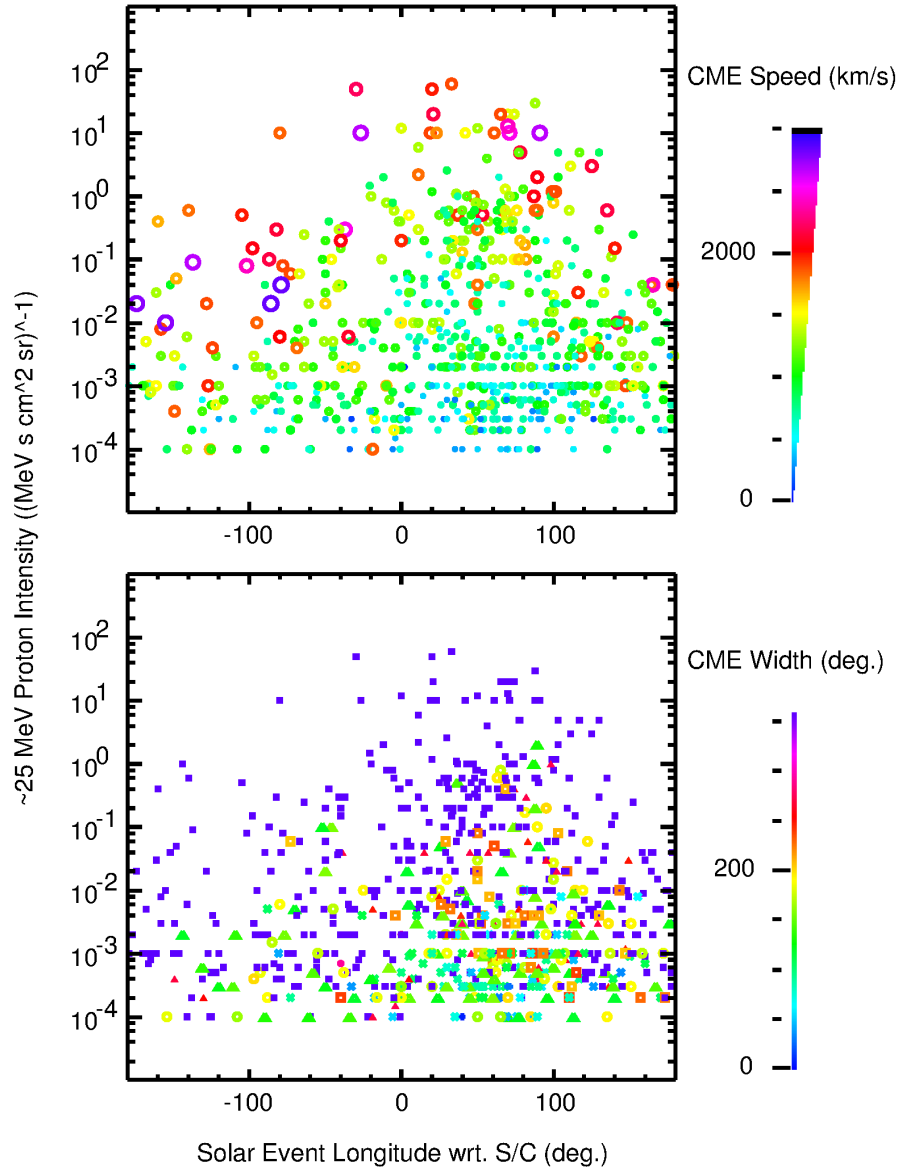


Figure 7. ~ 25 MeV proton intensity vs. solar event longitude relative to the observing spacecraft for the events in Tables 1-11. Colors/symbols indicate the speed of the associated CME in the top panel and the width of the CME in the bottom panel (blue squares indicate halo (360° width) CMEs). CME parameters are from Tables 1-11 in Appendix A and, with a few exceptions, from the CDAW LASCO CME catalog.

associated with SEP events detected far from the spacecraft, suggesting that an exceptionally fast CME in the mid-corona is not a requirement for SEPs to be detected far from the associated solar event. On the other hand, the SEPs associated with the slowest CMEs (small blue symbols) tend to be weak and predominantly detected within $\sim 60^\circ$ of the nominal magnetic connection at $\sim W60^\circ$.

We should emphasize that the low speeds for many of these SEP-associated CMEs are not due to, for example, projection effects from using the CDAW plane of the sky speeds. In particular, Richardson, von Rosenvinge, and Cane (2015) show many clear examples of ~ 25 MeV proton events associated with slow CMEs using CME parameters from several catalogs, including three-dimensional speeds from the DONKI (Database Of Notifications, Knowledge, Information) database (<https://kauai.ccmc.gsfc.nasa.gov/DONKI/>), and CME parameters inferred using coronagraph observations from spacecraft in quadrature to the solar event, reducing projection effects. We also note that MLSO K-Cor observations suggest that some SEP-associated CMEs do have higher speeds in the low corona than in the middle corona observed by LASCO (St. Cyr et al. 2025).

Although these results may not necessarily implicate particle acceleration at the expanding CME-driven shock as the sole mechanism for distributing protons in widespread events, they do indicate that the intrinsically largest SEP events, typically associated with fast CMEs, tend to be detected at large longitudinal distances from the solar event, as was also noted by Richardson et al. (2014). This study, as well as several others (e.g., Lario et al. 2013; Cohen, Mason, and Mewaldt 2017; Richardson, von Rosenvinge, and Cane 2017; Paassilta et al. 2018; Bruno and Richardson 2021), found that the longitudinal intensity dependence in individual SEP events may be expressed as a Gaussian with a standard deviation of $\sim 40^\circ$ relative to the IMF footprint, and qualitatively, the “Gaussian-like” dependence is evident in Figure 7.

In the bottom panel of Figure 7, the symbol color indicates the CME width from the CDAW SOHO/LASCO catalog. As noted above, a large fraction of the SEP-associated CMEs are “halo” (360° width) CMEs in this catalog (though not in other catalogs, e.g., Richardson, von Rosenvinge, and Cane (2015)) and these are associated with SEPs detected at all longitudes relative to the solar event. The narrower CMEs tend to be associated with SEPs from western events that are reasonably well connected with the observer. However, there is a bias introduced into this figure because the LASCO CME widths are projected against the plane of the sky. In particular, a halo designation in the CDAW catalog indicates that some signature of the CME surrounds the LASCO C2 occultor, but the CME is frequently asymmetric and associated with a solar event away from central meridian. The blue graph in the left panel of Figure 8 shows that the locations of the related solar events for the SEP-associated halo CMEs in Tables 1 to 11 of Appendix A are approximately evenly distributed in longitude relative to Earth. This clearly demonstrates that these halo CMEs are not generally directed towards or away from the Earth (as is often erroneously assumed for CDAW “halo” CMEs, as discussed by St. Cyr et al. (2005)) but are approximately equally likely to have any direction relative to the Sun-Earth line. This result is consistent with Kwon, Zhang, and Olmedo (2014) who noted

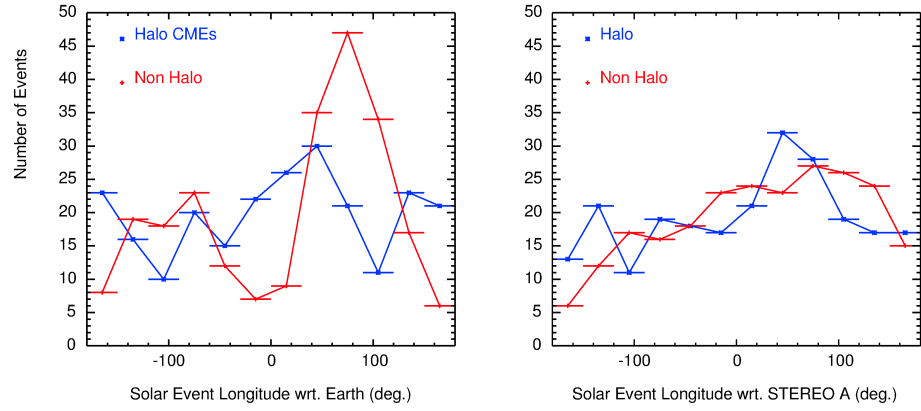


Figure 8. Left: Number of SEP-associated CDAW catalog “halo” (blue graph) and “non-halo” (red graph) SOHO/LASCO CMEs for the events in this study vs. the longitude of the associated solar event relative to Earth. The solar events associated with halo CMEs are approximately evenly distributed in longitude whereas non-halo CMEs tend to be associated with solar events located around the east and west limbs relative to Earth (longitudes $\sim \pm 90^\circ$). This pattern for the non-halo CMEs is removed when the event longitude relative to STEREO A is used (right panel) due to the changing spacecraft location relative to Earth (and similarly for STEREO B, not shown). The biases in the left panel due to the use of CME widths from the CDAW LASCO catalog are included in the bottom panel of Figure 7.

that SEP-associated CMEs tend to be halo-like even when observed well away from the direction of propagation. On the other hand, the solar events associated with non-halo CMEs (red graph in the left panel) tend to cluster near the limbs relative to Earth (longitudes $\sim \pm 90^\circ$), although with a western bias presumably because of the required association with SEP events and the influence of the spiral IMF, and are rarely located near central meridian. This distribution suggests that CMEs are more likely to be classified as non-halo, with a width less than 360° , when originating towards the limbs, where projection effects on the width are reduced. In the right panel of Figure 8, the distribution of non-halo CMEs is more uniform when plotted vs. the solar event location relative to STEREO A because the spacecraft was separated from Earth and SOHO (a similar plot could be made for STEREO B). Since the bottom panel of Figure 7 includes results from both STEREO and near-Earth spacecraft, the different longitudinal distributions of halo and non-halo CMEs at each spacecraft and the bias in CME widths from the CDAW catalog will be incorporated into this figure.

Figure 9 summarizes the relationship between the LASCO CME speed and the ~ 25 MeV proton intensity in various longitude ranges relative to the observing spacecraft. The symbols indicate whether the WAVES or SWAVES (STEREO WAVES) instruments on the Wind or STEREO spacecraft, respectively, detected interplanetary (IP) type II radio emission extending below 1 MHz (e.g., Cane and Erickson 2005, solid blue squares), type II emission that did not reach 1 MHz (red open circles), or no type II emission was detected (green crosses), as reported in the CDAW Type II catalog (https://cdaw.gsfc.nasa.gov/CME_list/radio/waves_type2.html) and indicated in Tables 1 to 11. Cases where no SEP

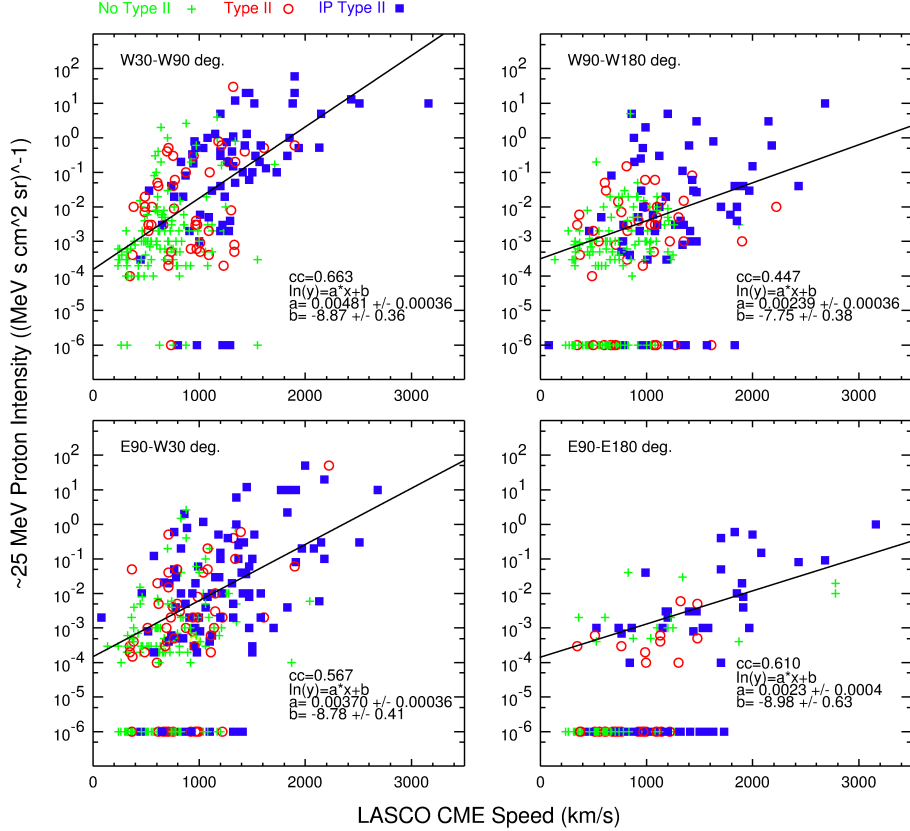


Figure 9. ~ 25 MeV proton intensity vs. LASCO CME speed (from the CDAW catalog) for events in different longitude ranges relative to the observing spacecraft. The symbols indicate whether type II (red open circles), IP type II radio emission, extending below 1 MHz (solid blue squares) or no emission (green crosses) observed by spacecraft is reported (events where this information is not available are excluded from the figure). Cases where no SEP event was detected at the observing spacecraft or there was a high background from previous events are shown at an intensity of 10^{-6} . These are excluded from the least squares fits and correlations shown.

event was detected at the observing spacecraft, or there was a high background from previous events, are shown at an intensity of 10^{-6} . These are excluded from the least squares fits and correlations shown. The top left panel shows a reasonable correlation (correlation coefficient = 0.663) between proton intensity and CME speed for well-connected events ($W30-W90^\circ$), as reported in many previous studies (e.g., Kahler, Hildner, and Van Hollebeke 1978; Reames 1999; Richardson et al. 2014). As also noted by Richardson et al. (2014) for a smaller sample of events, SEP events without type II emissions tend to be weaker and associated with slower CMEs than those with type II emissions, with the larger events typically associated with IP type II emission. Similar patterns are evident in events originating in other longitude ranges though the correlations with CME speed become weaker. The top right panel of Figure 9 shows results for behind-

the-west-limb events (all locations are relative to the observing spacecraft), the bottom right for behind-the-east-limb events, and the bottom left, front side events located between the east limb and $W30^\circ$. Thus, at all longitudes, the SEP intensity shows some correlation with the CME speed.

Figure 10 summarizes the ~ 25 MeV proton intensity vs. the longitude of the associated soft X-ray flare relative to the SEP-observing spacecraft reported in Tables 1 to 11 of Appendix A. (The flare longitude here is to be distinguished from the solar event location relative to the observing spacecraft used in other figures which does not require the observation of an X-ray flare.) The X-ray flare observations are from GOES except for twelve cases from SolO/STIX. The GOES X-ray intensities have been corrected for instrumental changes and correspond to pre-GOES-R (pre-December 18, 2017) intensities, as discussed further in Appendix A and indicated in the figure caption. The three panels show cases where SEP events are associated with C-class, M-class or X- (and higher) class flares. Again, there is a clear western hemisphere bias in the number of proton events and the largest events associated with each class of flares. For SEP events associated with western C and M-class flares, there is a wide spread in intensities, and overall, even C-class flares may be associated with SEP events that extend far from the flare location. Considering SEP events associated with X-class flares, the weak SEP events that are associated with smaller flares are generally absent, and the SEP events extend to distant longitudes. Note that these results require the detection of an SEP event, but as discussed below and in Section 6, there are significant numbers of X-ray flares that are not associated with detected SEP events.

Figure 10 also includes biases due to uneven coverage in the X-ray flare longitude with respect to the observing spacecraft. Figure 11 shows the locations of the SEP-associated soft X-ray flares observed by GOES or SolO/STIX relative to Earth or the STEREO spacecraft in 2006 to 2023. (In the following discussion, we neglect the few SolO events.) The GOES flares are only observed when on the front side or just over the limbs relative to Earth (green squares in Figure 11) and so lie predominantly in the longitude range $+90^\circ$ to -90° . Considering STEREO A (red circles) moving ahead of Earth, most of the GOES flares in Solar Cycle 24 were progressively further to the east of the spacecraft (negative longitudes), then switched to behind the west limb ($> 90^\circ$) towards the end of Solar Cycle 24 as STEREO A passed behind the Sun and began to return towards Earth (cf., Figures 1 and 2). Therefore overall, STEREO A was relatively poorly positioned to observe SEPs from X-ray flares observed at Earth in Solar Cycle 24. Then in Solar Cycle 25, the front side flares were predominantly western (longitude $> 0^\circ$) relative to STEREO A as the spacecraft approached Earth. Considering STEREO B (blue triangles), lagging behind Earth, the SEP-associated GOES soft X-ray flares were predominantly western relative to the spacecraft during Solar Cycle 24, progressing to far behind the west or east limbs just before loss of contact. The overall result of these various factors is a deficiency of cases where the GOES X-ray flare is east of the spacecraft location, and this accentuates the western bias evident in Figure 10 beyond that expected because of preferential magnetic connection to the western hemisphere.

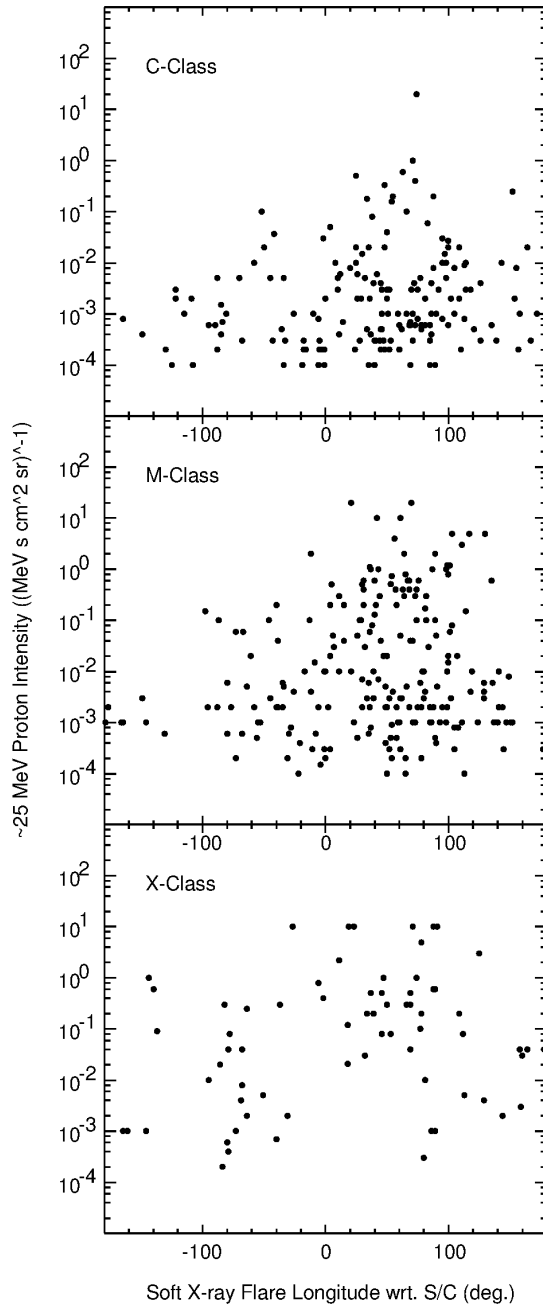


Figure 10. SEP proton intensities vs. the longitude of the associated GOES soft X-ray flare relative to the SEP-observing spacecraft for cases where a C, M, or X (and higher)-class flare is reported. Flare intensities for events after December 18, 2017 have been multiplied by 0.7 to make them consistent with earlier flare intensities. Twelve events associated with flares observed by SolO/STIX are also included based on the estimated equivalent GOES flare size.

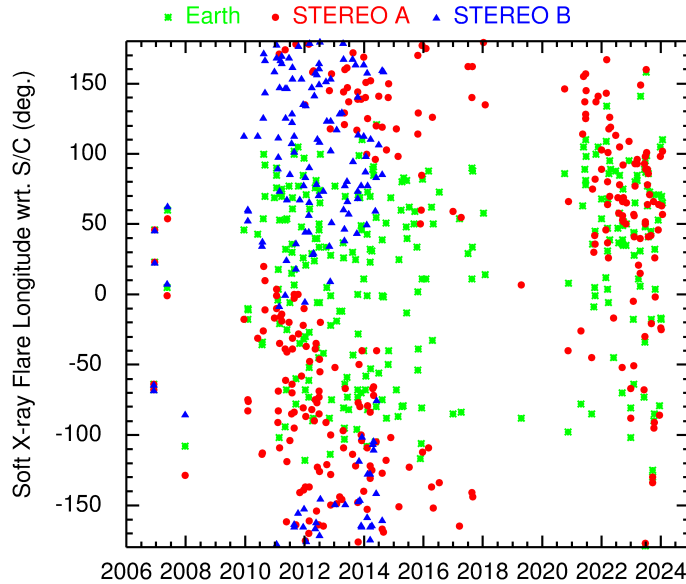


Figure 11. Locations of SEP-associated GOES soft X-ray flares in 2006-2023 relative to Earth (green squares), STEREO A (red circles) or STEREO B (blue triangles), illustrating the bias towards western events (positive longitudes) in this sample arising from the loss of contact with STEREO B, the solar cycle variation in the occurrence of SEP-associated flares, and the unfavorable (eastern/far western) locations of these flares relative to STEREO A in Cycle 24. This bias is reflected in Figure 10. Twelve flares observed by SolO/STIX are also included in the figure.

Considering just the SEP events detected at Earth, Figure 12 shows the proton intensity vs. solar event longitude for events associated with GOES soft X-ray flares (open circles) and with no clearly-associated flare (solid circles). (Again, several SEP events at Earth associated with far side flares observed by SolO/STIX are included in Figure 12 but not considered in this discussion.) This figure emphasizes that a significant fraction of the ~ 25 MeV proton events detected at Earth are not associated with GOES soft X-ray flares, which has implications for SEP prediction schemes (e.g., Whitman et al. 2023, and references therein) requiring direct observations of the related solar activity either at X-ray or other wavelengths. For this sample of 331 SEP events detected at Earth, 91 (27%) have no clearly-associated soft X-ray flare, with 19% associated with solar events behind the west limb at longitudes $\geq 90^\circ$ and 6.3% associated with solar events behind the east limb (longitudes $< 90^\circ$), consistent with the results of Richardson et al. (2014) (see their Figure 11) and Cane, Richardson, and von Rosenvinge (2010). The few front side events with no associated flare are cases where the flare association is uncertain or the SEP event appears to be associated with an eruption (often of a filament) that is not accompanied by significant soft X-ray emission.

Figure 13 summarizes the ~ 25 MeV proton intensity vs. the GOES soft X-ray flare intensity for the same solar event longitude ranges relative to the observing spacecraft as in Figure 9. Again, the GOES X-ray intensities have

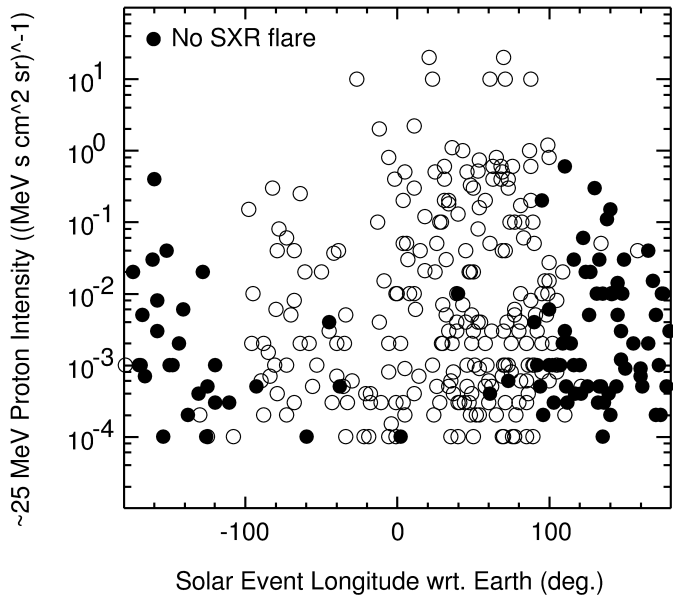


Figure 12. \sim 25 MeV proton intensity observed at Earth vs. solar event longitude relative to Earth. Filled circles indicate the 27% of these SEP events at Earth that are not associated with GOES soft X-ray (SXR) flares (typically these events originate on the far side) or, in a few cases, the association is uncertain. Several SEP events associated with far side X-ray flares observed by SolO/STIX are also shown.

been corrected for instrumental changes and correspond to pre-GOES-R (pre-December 18, 2017) intensities, as discussed further in Appendix A and indicated in the figure caption. Note that this figure includes SEP observations from the STEREO spacecraft and hence the X-ray flares are located over a more extended longitude range relative to the observing spacecraft than for the near-Earth observations in Figure 12, as previously discussed in relation to Figure 11. For well-connected events at $W30$ - 90° in the top left panel, there is a modest ($cc=0.543$) correlation between the SEP and flare intensities, as has been noted in some other studies (e.g., Richardson, von Rosenvinge, and Cane 2017). (Again, the correlation does not include cases where no SEP event was detected, or there was a high background, at a particular spacecraft, shown at an intensity of 10^{-6} .) While the upper envelope of the distribution indicates a clear correlation between the X-ray flare and SEP event size, there are also weaker SEP events for a given flare intensity, including relatively weak events that are associated with high M and low X-class flares. Correlations between the X-ray and SEP intensities are also present for other longitude ranges, though these are weaker except for the small number of cases when the flare is behind the east limb relative to the observing spacecraft (bottom right panel of Figure 13). Thus, even when the flare is well behind the east limb of the Sun relative to the spacecraft, the SEP intensity may show some dependence on the X-ray flare intensity, as is also evident in Figure 10.

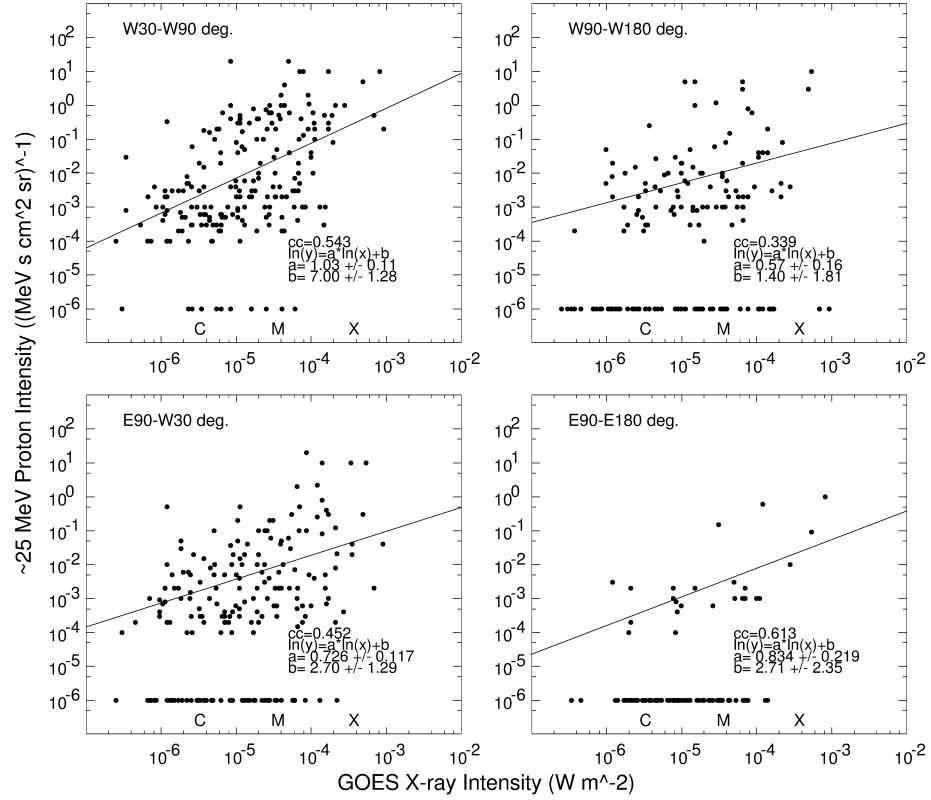


Figure 13. SEP intensity vs. GOES X-ray intensity for different ranges of solar event longitude with respect to the observing spacecraft. Cases when no SEP event was detected or there was a high background at a particular spacecraft location are shown at an intensity of 10^{-6} and are not included in the calculation of the least squares fits and correlations. X-ray intensities after December 18, 2017 have been multiplied by 0.7 to make them consistent with earlier event intensities (see Appendix A for details).

Correlations such as those in Figures 9 and 13 might be used to argue for the CME- or flare-acceleration of SEPs, respectively. For this group of ~ 25 MeV proton events, the correlation coefficients are generally larger in each longitude range for the SEP intensity vs CME speed in Figure 9. This is to be expected since, as already noted, relatively weak SEP events may be associated with relatively strong flares, but not with especially fast CMEs. On the other hand, the correlations are not comparable. In particular, the SEP intensity-X-ray correlations are double-logarithmic and cover a larger dynamic range. Therefore, a simple comparison with the values of the log-linear intensity-CME speed correlation coefficients may not provide meaningful insight into whether the observations favor SEP acceleration by either flares or CMEs. We also note that Lario and Karelitz (2014) reported “triangular” proton intensity vs. CME speed distributions when plotted using a double-logarithmic scale and GOES proton data, similar to those found for the X-ray intensity in Figure 13, and emphasized the positive correlations between SEP intensity and the CME speed

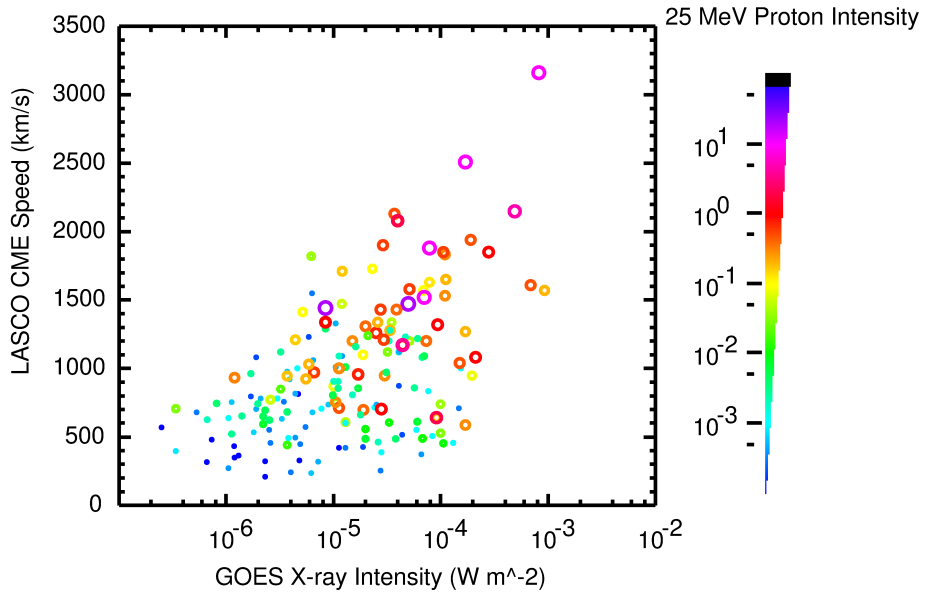


Figure 14. LASCO CME speed vs. GOES X-ray intensity for 200 SEP-associated solar events at W30-90° relative to the observing spacecraft. The symbol size and color indicates the intensity of ~ 25 MeV protons. X-ray intensities after December 18, 2017 have been multiplied by 0.7 to be consistent with earlier event intensities.

(and also the X-ray intensity) along the upper envelope of the distributions. They also suggested that the SEP intensities are influenced by solar wind structures, including at the observing spacecraft, an aspect that we do not consider here.

Figure 14 summarizes the relationship between the combination of X-ray flare intensity and CME speed, and the 25 MeV proton intensity, for 200 events with well-connected solar flares at W30-90° relative to the observing spacecraft. The symbol size and color indicate the proton intensity. Consistent with the previous discussion, the larger SEP events (intensities above $\sim 10^{-1}$) tend to be associated with CME speeds above ~ 1000 km/s and M class and larger X-ray flares. There is also clearly an overall correlation between CME speed and X-ray intensity, as is well established (e.g., Vršnak, Sudar, and Ruždjak 2005).

Bruno et al. (2018) reported the spectra of 30 high-energy SEP events in December 2006–September 2014 detected by the Payload for Antimatter Matter Exploration and Light-nuclei Astrophysics (PAMELA) instrument on the Resurs-DK1 satellite at energies of 80 MeV – few GeV. Figure 15 shows, for SEP events during this period, the ~ 25 MeV proton intensity observed by STEREO A, B, or at Earth vs. the longitude of the related solar event relative to the spacecraft. The large filled circles indicate ~ 25 MeV proton observations made by STEREO A, B and SOHO of the PAMELA events of Bruno et al. (2018). At ~ 25 MeV, the SEP events that were observed by PAMELA at higher energies generally extended to all longitudes and were among the highest intensity events observed at any longitude, although in a few cases, the PAMELA events were not detected at 25 MeV by distant spacecraft. This is consistent with

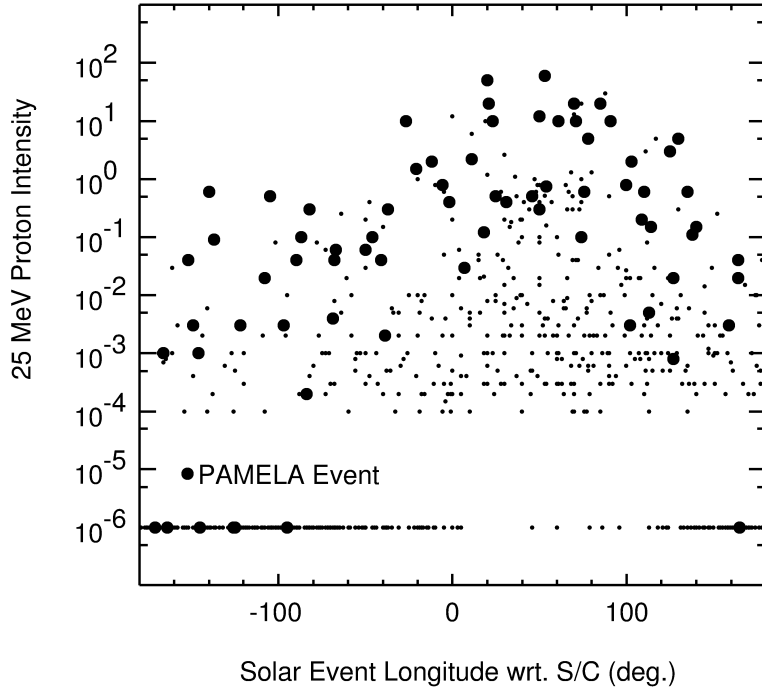


Figure 15. 25 MeV proton intensity ($(\text{MeV s cm}^{-2} \text{ sr})^{-1}$) vs. solar event longitude relative to the observing spacecraft in December 2006–September 2014 with observations related to the high energy events detected by PAMELA at 80 MeV-few GeV during the same period (Bruno et al. 2018) indicated by large circles. Observations without a detectable 25 MeV proton event are plotted at an intensity of 10^{-6} . Where such a data point is indicated as a PAMELA event, this means that, although the SEP event was observed by PAMELA, it was not detected at 25 MeV by a spacecraft widely separated from the related solar event.

the conclusion of Bruno et al. (2018) that SEP events observed at the highest energies, including ground level enhancements observed by neutron monitors, are just the most intense events in a population of SEPs with similar spectra and are not a separate/special class of events. There are also other events that have intensities at ~ 25 MeV that are comparable to those of the PAMELA events, suggesting that their spectra were softer and did not extend into the PAMELA energy range.

Figure 16 indicates, in a similar format, those SEP events that are related to the long duration gamma ray flares (LDGRFs) observed by the Fermi/LAT (Large Area Telescope) and compiled from several studies in Table 3 of Bruno et al. (2023). The SEP events shown cover the period of March 2011–September 2017 that encompasses these LDGRF observations. Again, the LDGRF events tend to be associated with larger SEP events at ~ 25 MeV, but there are exceptions. There are also many comparable SEP events that are not associated with reported LDGRFs. Given the lower proton energy that we are considering, it is unclear whether these observations directly contribute to the debate as to whether LDGRFs are caused by high energy (> 300 MeV) protons back-

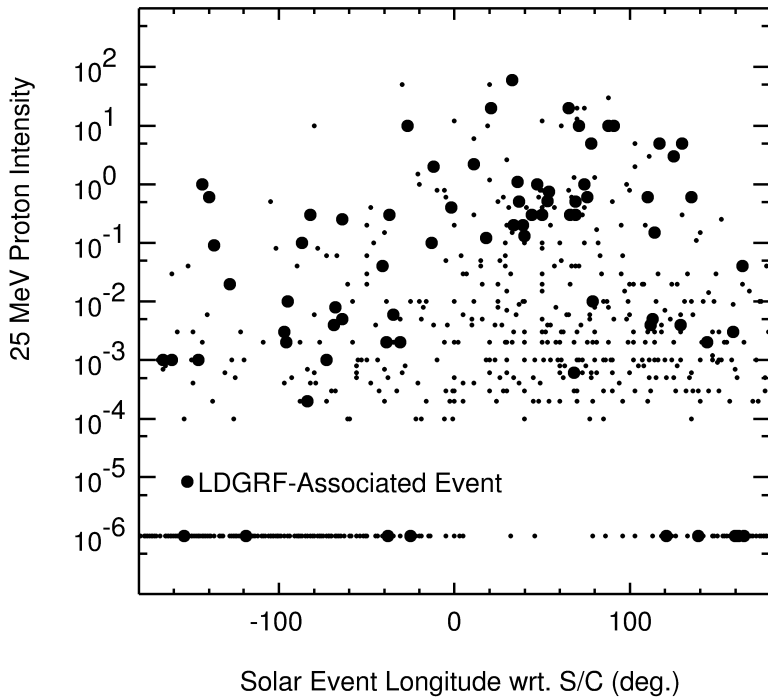


Figure 16. 25 MeV proton intensity $((\text{MeV s cm}^2 \text{ sr})^{-1})$ vs. solar event longitude relative to the observing spacecraft in March 2011–September 2017. Large circles indicate observations of the events associated with the long duration gamma ray flares (LDGRFs) observed by FERMI/LAT during this period summarized in Table 3 of Bruno et al. (2023). Observations without a detectable SEP event are plotted at an intensity of 10^{-6} .

streaming onto the photosphere from CME-driven shocks (Bruno et al. (2023) present arguments against this scenario) or by processes in the corona such as the acceleration of particles trapped in large coronal loops (e.g., Ryan and Lee 1991). Recently, Bruno et al. (2025) have discussed an LDGRF on July 16, 2024 associated with a slow CME and weak SEP event extending only to a few tens of MeV where such coronal loops were present, that might favor the latter scenario.

6. Association of M/X Flares With SEP Events

The results summarized above consider cases where an SEP event was detected at least at one location (the STEREO spacecraft or near Earth) following a solar event typically associated with a CME and evidence of flaring. However, there are many flares and CMEs that are not accompanied by observed SEP events, even when observations are made at multiple locations. For example, Richardson, Mays, and Thompson (2018) noted that 85% of the 334 CMEs in the DONKI database during October 2011–July 2012, near the peak of Solar Cycle 24, were not associated with a ~ 25 MeV proton event observed at the widely-spaced STEREO or near-Earth spacecraft. This low SEP association rate

poses challenges for SEP prediction schemes based on CME observations, as discussed by Whitman et al. (2023) and also by Richardson, Mays, and Thompson (2018). They demonstrated how various filtering schemes (for example, making SEP predictions only for CMEs exceeding a specified speed threshold) may be applied to reduce the “false prediction” rate for the CME-triggered SEPSTER model. However, Lario et al. (2020) noted that even “fast and wide” CMEs occasionally may not be associated with SEP events, and considered the factors that might lead to the absence of SEPs. An even larger imbalance with SEP events exists for solar flares. Here, we start with a large sample of soft X-ray flares and use a subset of the SEP events identified in Tables 1 to 11 in Appendix A to investigate the relationship between SEP events, eruptive solar events, flares and CMEs, specifically including solar events that are not associated with SEP events.

To examine the relationship between flares, CMEs and ~ 25 MeV SEP proton events, we have considered all the 397 X or M class soft X-ray flares observed by the GOES spacecraft from June 2010 (shortly after the launch of the Solar Dynamics Observatory (SDO, Pesnell, Thompson, and Chamberlin 2012)) to January 2014, encompassing much of the peak of Solar Cycle 24 (Figure 1). During this interval, STEREO A(B) moved from $\sim 70^\circ$ to $\sim 150^\circ$ west (east) of Earth. These flares have also formed the basis of a series of papers on the “global energetics” of solar flares (Aschwanden, Xu, and Jing 2014; Aschwanden et al. 2015, 2016; Aschwanden 2016; Aschwanden et al. 2017). In Aschwanden et al. (2017), the total energy in SEPs ($1.3\text{--}68 \times 10^{30}$ erg) was estimated for ten solar flares where the associated SEPs were observed at both STEREO spacecraft and near the Earth, and for which the associated particles could be isolated from those related to other solar events. The total SEP energy was then estimated using the SEP spectra at each location and assumptions about the spatial distribution of the SEPs. The limited number of energy estimates, even when starting from such a large sample of X-ray flares, reflects the challenges in identifying multi-spacecraft SEP events suitable for this analysis and, as will be discussed below, the paucity of flares associated with detectable SEP events. As a first step in the event identification for Aschwanden et al. (2017), a survey of the association of SEP events with these flares was made, and forms the basis of the following discussion. As is evident from Tables 1 to 11 in Appendix A and Figure 10, SEP events can be associated with <M class flares, but just considering X/M class flares gives a more manageable number of events and focuses on the stronger flares. The interval considered ends before the loss of contact with STEREO B.

One frequent challenge when associating X-ray flares and SEP events is that an unrelated SEP event may already be in progress when a flare occurs. In the absence of any signature in the particle intensity-time profile, it may be uncertain whether the flare was not associated with an SEP event, or whether an SEP event was present but obscured by the ongoing event. This can be a significant problem since multiple flares may occur during the duration of a large SEP event which may extend for several days, and flares also tend to occur in clusters at times of high solar activity. Such a situation is shown in the top panel of Figure 17, where around 20 M/X flares (indicated by the red

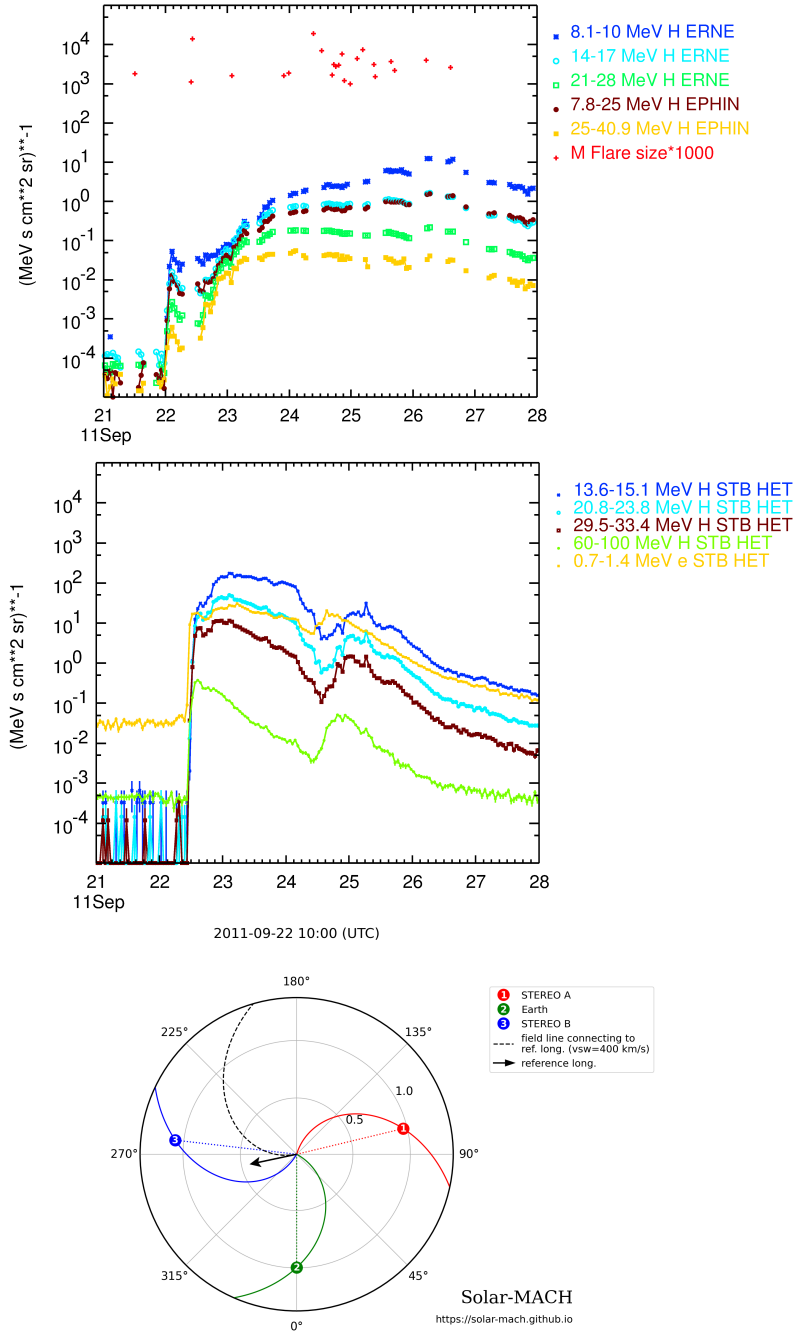


Figure 17. Top: An extended-duration widespread SEP event commencing on September 22, 2011 at ~ 10 UT (proton data are from SOHO ERNE and EPHIN), associated with an X1.4 flare at E78°. During the SEP event, a cluster of 20 M/X class flares was observed; the flare intensities (red crosses) are plotted at 1000 times the M intensity. A small preceding SEP event commencing at ~ 22 UT on September 21, is also evident, originating from a source behind the west limb at W109°, and hence with no associated flare. Center: STEREO B HET proton and electron observations for the same period, showing the prompt onset of the September 22 SEP event and a second SEP event associated with an X1.9 flare on September 24, at E60° relative to Earth and W37° relative to STEREO B. Note that at STEREO B, the profile of the first event at lower energies is also modulated by an ICME-driven shock at 09:06 UT on this day (https://stereo-ssc.nascom.nasa.gov/data/ins_data/impact/level3/STEREO_Level3_Shock.pdf). Bottom: The spacecraft configuration at the time of the flare on September 22 at the location indicated by the black arrow.

crosses near the top of the panel) occurred during the first ~ 4 days of the SEP event observed by SOHO ERNE and EPHIN commencing at ~ 10 UT on September 22, 2011 associated with an X1.4 flare at $E78^\circ$. (This was preceded by a small SEP event late on the previous day from behind the west limb with no associated X-ray flare; see Table 2.) Fourteen of these flares were from Active Region 1302, also the origin of the X1.4 flare and SEP event. Thus, around 5% of our sample of 397 X/M flares occurred just in the period in Figure 17. We are unable to determine whether any other flare was associated with an SEP event based on observations at Earth. However, the center panel of Figure 17 shows STEREO B HET observations during the same period (the bottom panel shows the spacecraft configuration). As noted in Table 2 and evident in this figure, an additional SEP event associated with an X1.9 flare on September 24 at $E60^\circ$ was observed by STEREO B; the flare was at $W37^\circ$ relative to STEREO B above the east limb. This period illustrates how multi-spacecraft observations can help to determine whether a flare was associated with an SEP event, although SEP events that are narrow in longitude might still be overlooked. As discussed above, the requirement here for a GOES flare to be observed tends to bias the detection of SEP events in Solar Cycle 24 towards Earth and STEREO B, which was favorably placed to detect SEPs associated with eastern hemisphere GOES flares. On the other hand, STEREO A was poorly connected to front side flares and only detected the more widespread SEP events such as the September 22, 2011 event (STEREO A observations for this event are not shown in Figure 17, but see Table 2).

Considering SEP observations at Earth and both STEREO spacecraft for the 397 M/X flares, these together provide potentially 1191 (i.e., 3×397) *independent* SEP observations. Of these observations, in 602 cases (51%), we could not determine whether an SEP event was detected because of an ongoing SEP event at the observing spacecraft or other factors, such as a data gap. For 462 cases (39%), SEP observations are available but there is no evidence of a ~ 25 MeV proton event above the prevailing low background. For the remaining 127 cases (11%), an SEP event was observed that was clearly associated with the X-ray flare. Considering just these last two groups with suitable SEP observations, a ~ 25 MeV proton event was only detected in 21.6% (127/589) of the observations. Thus, even when considering SEP events above the low instrumental threshold and relatively large M/X flares, an SEP (~ 25 MeV proton) event was detected in only around a quarter of STEREO or near-Earth observations without ongoing events or data gaps.

Considering just SEP observations at Earth for the 397 M/X flares, in 235 (59%) of cases, an ongoing event or data gap was present at the time of the X-ray flare. For another 107 flares (27%), SEP observations are available but no SEP (~ 25 MeV proton) event is evident, while an SEP event was detected for 55 (14%) of the flares. Again, combining the last two groups, an SEP (~ 25 MeV proton) event was observed at Earth in 55 out of 162 (34%) cases that were not affected by a high background or data gaps. Since a front side flare is required here, this helps to explain the higher rate of SEP detection (34% vs. 22%) when considering just near-Earth SEP observations than if observations from the STEREO spacecraft, well-separated from Earth, are also included (see

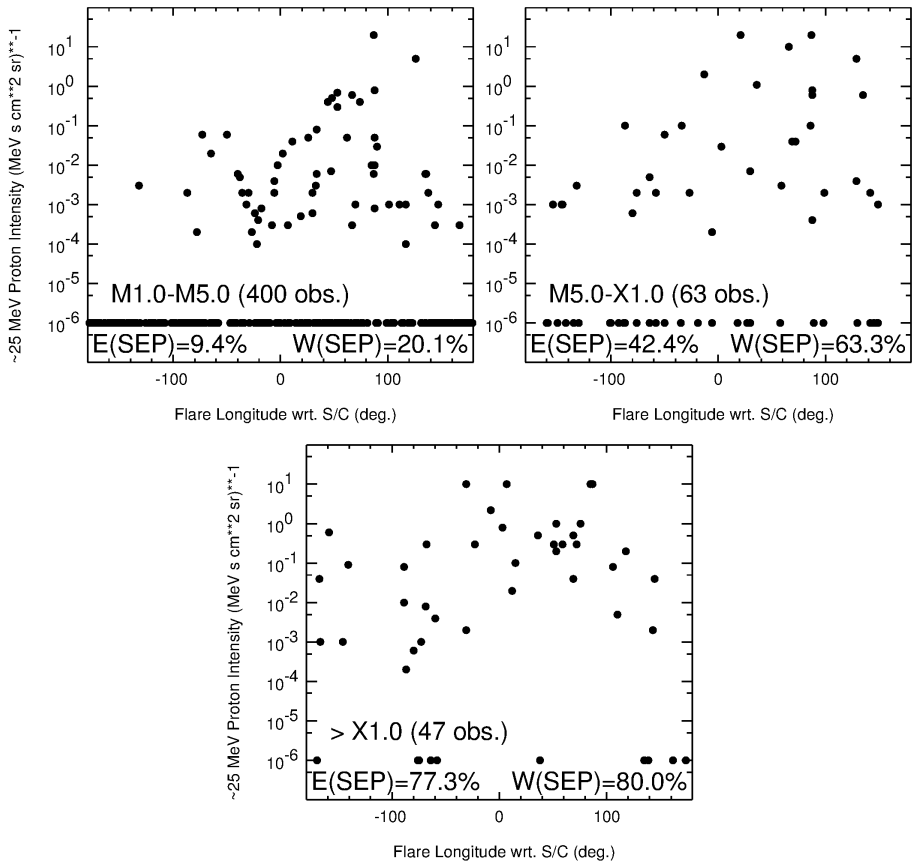


Figure 18. SEP ~ 25 MeV proton intensity vs. flare longitude with respect to the observing spacecraft for (top left) M1.0-M5.0, (top right) M5.0-X1.0, and bottom $>X1.0$ flares between June 2010 to January 2014 with suitable SEP observations (e.g., no ongoing events or data gaps) at the STEREO spacecraft or at Earth (502 observations in total). When there is no SEP event detected at the observing spacecraft, an intensity of 10^{-6} is plotted. The probability of an SEP event being detected (indicated for observations when the flare is east (E(SEP)) or west (W(SEP)) of the observing spacecraft) and over a wider longitude range, clearly increases with flare size.

Figure 11). As a comparison, the NOAA SEP list based on GOES data includes $20 > 10$ MeV proton events exceeding 10 pfu that are associated with M/X flares during the same period, around one third of the $55 \sim 25$ MeV proton events at Earth identified here.

In Figure 18, we have combined observations from the STEREO A/B and SOHO spacecraft to compare the dependence of the 25 MeV proton intensity on the flare size and longitude with respect to the observing spacecraft. Thus, a flare may be plotted up to three times if suitable SEP observations (i.e., without data gaps or large ongoing events) are available at the different spacecraft locations. In total, 502 SEP observations without data gaps or ongoing SEP events are available, considering measurements from the STEREO and near-Earth space-

craft. Cases where no SEP event is observed at a particular spacecraft are plotted at an intensity of 10^{-6} .

In the top left panel, of the 400 SEP measurements associated with M1.0-5.0 flares, an SEP event was observed in only 59 cases (14.8%). There is a clear western (longitude $> 0^\circ$) bias in the number of events and their intensity, indicating the strong influence of the spiral interplanetary magnetic field on the detection of these events. (Since observations from both STEREO spacecraft are available, the western bias introduced in the larger event sample due to the loss of contact with STEREO B (cf., Figure 11) is not a factor here.) Of the SEP measurements made when the M1.0-5.0 flares were to the west of the observing spacecraft, SEP events were detected in 20.1% of cases, compared with 9.4% of the SEP measurements made when the flare was east of the spacecraft. For M5.0-X1.0 flares (top right panel), SEP events were detected in 33 out of 63 (52.4%) of the SEP measurements, again with a clear western bias in the largest events – SEP events were detected in 63.3% of the measurements made when M5.0-X1.0 flares were to the west of the observing spacecraft and 42.4% of the cases when the flare was to the east. For $>X1.0$ flares (bottom panel), of 47 SEP observations, an SEP event was present in a majority of cases (37, 78.7%). The SEP event detections were widely distributed in longitude relative to the flare and tend to be relatively intense compared to those associated with weaker flares. SEP events were detected in 80% of cases where the $>X1.0$ flare was west of the spacecraft and 77.3% of the cases when the flare was to the east. Thus, the probability of detecting a ~ 25 MeV proton event following an X-class flare is around 80% for both eastern and western flares, and these SEP events are likely to be detectable at all longitudes relative to the flare.

In the bottom panel of Figure 18, there is one X-class flare without an SEP event despite its well-connected western location relative to the observing spacecraft. This is the brief X1.9 flare with peak intensity at 20:27 UT on November 3, 2011, located at $E65^\circ$ relative to Earth and $W38^\circ$ relative to STEREO B (see the bottom left panel of Figure 19) which, even though well-connected to the flare, did not detect any SEP event, as is evident in the STEREO B HET observations in the top panel of Figure 19. No CME associated with this flare is reported in the CDAW or DONKI catalogs or the “Dual-Viewpoint CME Catalog from the SECCHI (Sun Earth Connection Coronal and Heliospheric Investigation)/COR Telescopes” (Vourlidas et al. 2017); <http://solar.jhuapl.edu/Data-Products/COR-CME-Catalog.php>). However, a narrow, slow CME shown in the top panels of Figure 20 was evident in STEREO B COR1, but fell apart in the field of view. We estimate the CME leading edge speed in COR1 as 226 ± 42 km/s from a linear fit. Only weak type III emission (not shown) was evident. The absence of any SEP event and weak CME signatures suggests that this X-flare was probably a “confined” flare; other notable examples were found in the major active region 12192 in October 2014 (e.g., Sun et al. 2015). This flare was around three hours before a major eruption far behind the east limb (see the bottom right panel of Figure 19), and therefore not associated with a GOES soft X-ray flare, that was directly imaged by STEREO B and accompanied by a 991 km/s LASCO halo CME, also observed by STEREO B (Figure 20), and type II and bright complex type

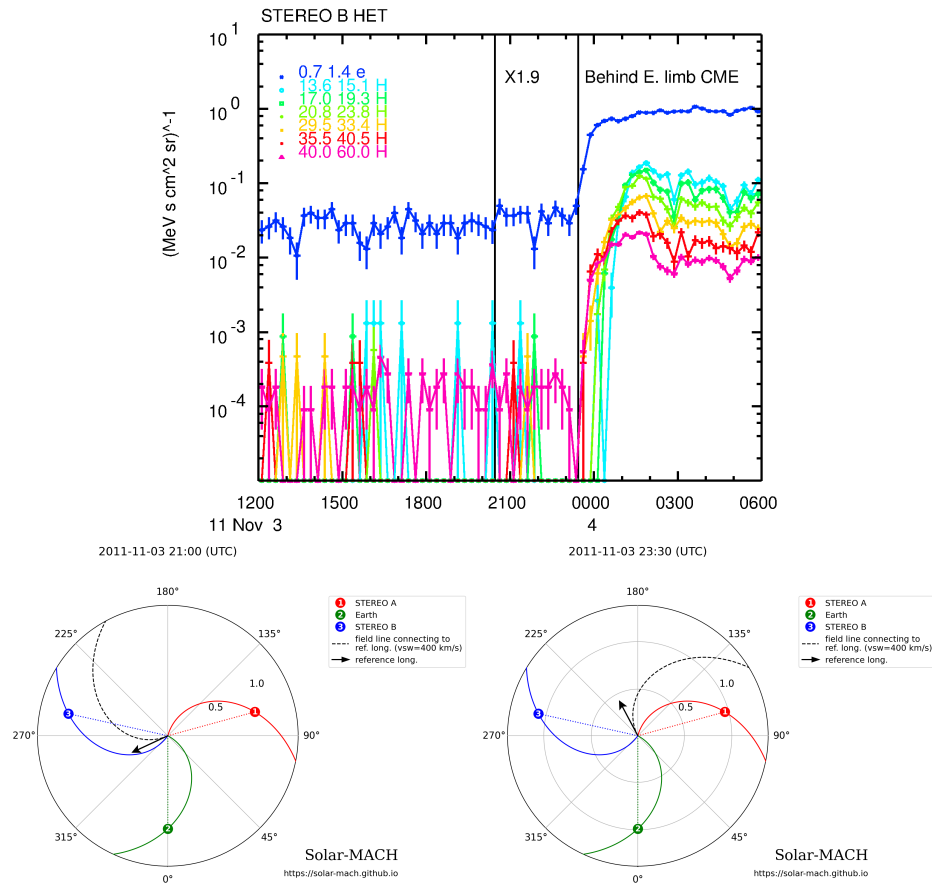


Figure 19. Top: STEREO B HET observations on November 3–4, 2011 showing the absence of an SEP event associated with the E65° X1.9 flare with peak intensity at 20:27 UT located at W38° relative to the spacecraft (bottom left). Although associated with this flare in some SEP catalogs (see text), the later major SEP event was clearly related with a separate behind-the-limb solar event (bottom right) directly observed by STEREO B and accompanied by a fast halo CME (e.g., Gómez-Herrero et al. 2015).

III radio emissions (not shown here). This eruption gave rise to the widely-studied intense SEP event (Table 2) evident in Figure 19 that rapidly propagated to both STEREO spacecraft and Earth (e.g., Richardson et al. 2014; Gómez-Herrero et al. 2015; Xie et al. 2017; Lario et al. 2017; Zhao and Zhang 2018), although we note that Park et al. (2013) and Prise et al. (2014) have suggested alternative multi-event interpretations.

Notwithstanding that these studies have demonstrated that the source of the SEP event on 3 November 2011 is not the front side X1.9 flare, we note that the catalog of Rotti et al. (2022) (available at <https://doi.org/10.7910/DVN/DZYLHK>) does associate the far side SEP event with the front side X1.9 flare. This incorrect association is also made by the “Catalog of Solar Proton Events in the 24th Cycle of Solar Activity (2009–2019)” by Logachev et al.

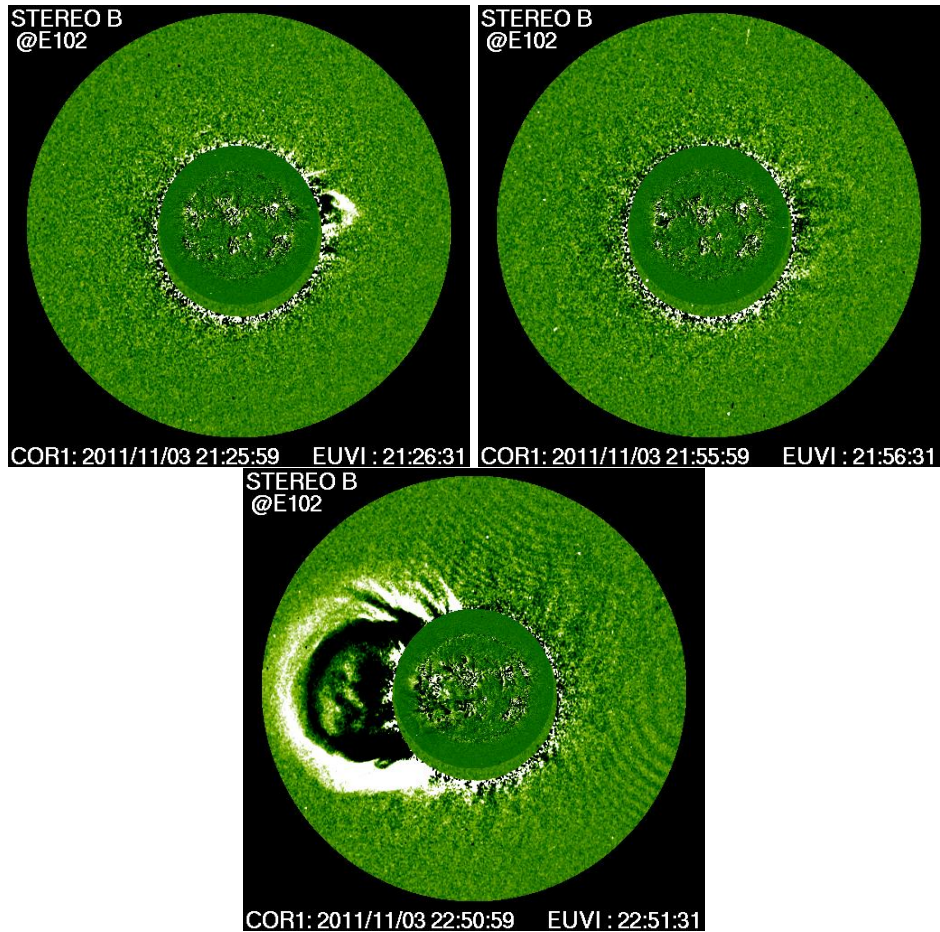


Figure 20. Top: STEREO B COR1 observations of the slow (~ 226 km/s) narrow CME above the west limb associated with the front side X1.9 flare with peak intensity at 20:27 UT on November 3, 2011 showing the CME falling apart in the COR1 field of view. Bottom: A similar view at 22:51 UT of the faster (991 km/s) wide far side CME associated with the SEP event in Figure 19. (Images from the CDAW CME catalog.)

(2022) and the “Catalogues of Solar Proton Events in the 20-25 Cycles of Solar Activity” compiled by Moscow State University (https://swx.sinp.msu.ru/apps/sep_events_cat/). This example illustrates why it is important to consider the possibility that SEP events detected at Earth may originate on the far side of the Sun, as STEREO observations have clearly demonstrated, and should not be assumed to be associated with unrelated front side flares. The SEP sources listed in Tables 1 to 11, including those on the far side, may help to reduce such errors.

We have also examined the dependence on CME speed and flare longitude of SEP occurrence and intensity for our sample of M/X flares. Figure 21, in a similar format to Figure 18, shows observations of the ~ 25 MeV proton intensity from STEREO and near-Earth spacecraft plotted against the longitude of the

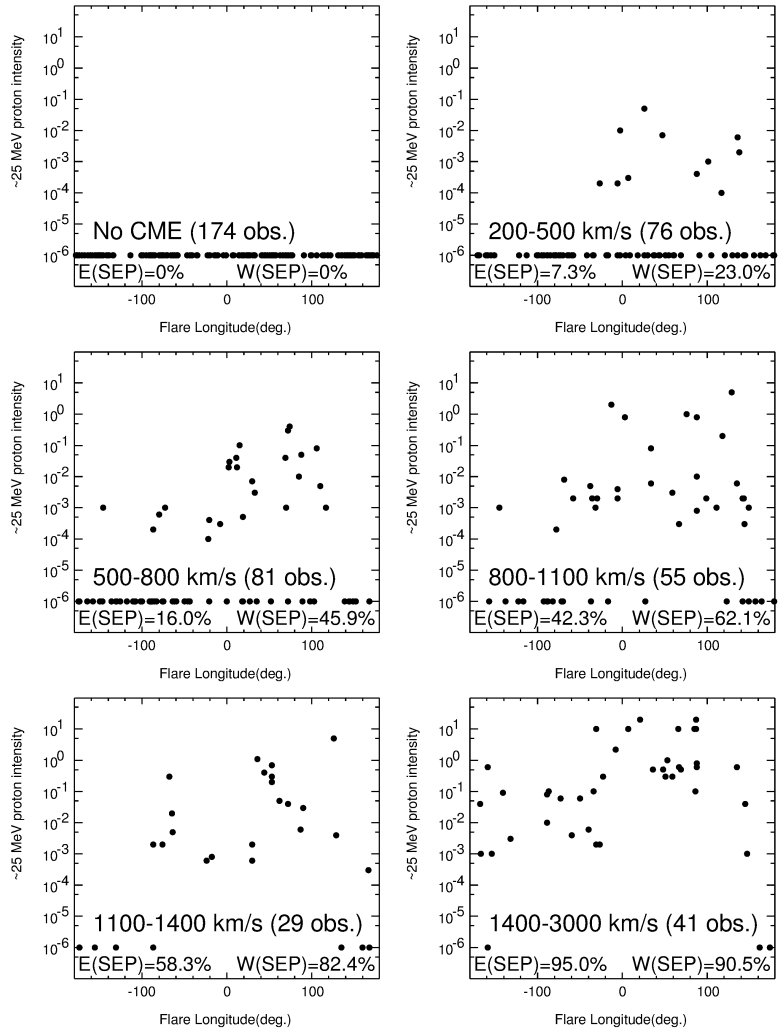


Figure 21. As in Figure 18 but for M/X flares associated with no CME (top left), when a ~ 25 MeV proton event is never detected in any of 174 observations, or associated with CMEs in several speed ranges. Again the probability of an SEP event and the size and extent of the event, increases with CME speed. E(SEP) and W(SEP) indicate the probability that an SEP event is detected for flares east or west of the observing spacecraft, respectively.

associated flare relative to the observing spacecraft for different speed ranges of the associated CME. Many of the flares are not associated with cataloged CMEs, so we have also examined movies from SOHO/LASCO and STEREO/COR1 and COR2 coronagraphs at the time of each flare to confirm that there is no evidence of an unreported CME or other eruption of material into the corona. Some 461 independent SEP measurements are available after removing cases with a data gap or high SEP background at a particular spacecraft. (Again, observations where no SEP event is detected are plotted at an intensity of 10^{-6} in Figure 21.)

At least for this sample of M/X flares, the 174 SEP observations in the top left panel of Figure 21 show that if an M/X flare is not accompanied by a CME, or evidence of erupting structures in the coronagraph observations, suggesting that the flare is confined, no ~ 25 MeV proton event is detected. Thus, based on these results, a necessary requirement for an M/X class flare to be associated with a ~ 25 MeV proton event appears to be the occurrence of an eruption evident in the corona.

The remaining panels of Figure 21 show results for flares accompanied by CMEs in increasing speed ranges. They demonstrate that even a well-connected flare (i.e., on the western hemisphere with respect to the spacecraft) accompanied by a CME does not necessarily lead to the detection of a ~ 25 MeV proton event, in particular when the CME is relatively slow. As in Figure 18, the percentage of observations when the flare is west or east of the observing spacecraft in which an SEP event was detected are given in each panel. As the CME speed progressively increases, the fraction of M/X flares with detected SEP events increases, and these events tend to increase in intensity (with a western bias due to connection) and are detected over a wider longitude range. For example, for flares with relatively slow (200-500 km/s) CMEs, a ~ 25 MeV proton event was detected for only 7.3% of observations where the flare was east of the spacecraft compared with 23% of observations where the flare was to the west. When an M/X flare was accompanied by a CME with a speed above ~ 1400 km/s, an SEP event was detected in nearly every spacecraft measurement at all longitudes relative to the flare, though the largest intensities are still associated with flares located at well-connected western longitudes.

To combine observations of the CME speed, flare intensity and SEP intensity, Figure 22 shows the LASCO CME speed vs. GOES X-ray flare intensity (in multiples of M1) for the 95 M/X flares in our sample at W30-90° relative to the SEP-observing spacecraft. The symbol size and color indicate the SEP 25 MeV proton intensity. This figure is similar to, and contains a subset of the events in Figure 14 except that here, flares without CMEs (plotted at zero CME speed) or without SEP events (small blue circles) are included. Again, the trend is for larger SEP events to be associated with larger flares and in particular faster CMEs. Flares in this subset of events for which no associated ~ 25 MeV proton event was detected generally have intensities below $\sim M5$ and either no associated CME, or if present, the CME speed was below ~ 500 km/s. However, our larger sample of SEP events in Tables 1 to 11 of Appendix A does include examples associated with weaker flares and slower CMEs, as illustrated in Figure 14.

These results, starting from a large number of M/X flares and using observations of SEPs from multiple locations with a large dynamic range in SEP intensity (unlike the standard GOES SEP events), clearly demonstrate the relationship between the energy release in a solar eruptive event, as indicated by the soft X-ray intensity or the CME speed, and the peak intensity and extent of the associated SEP event, as well as the probability of an SEP event being produced and detected following the flare.

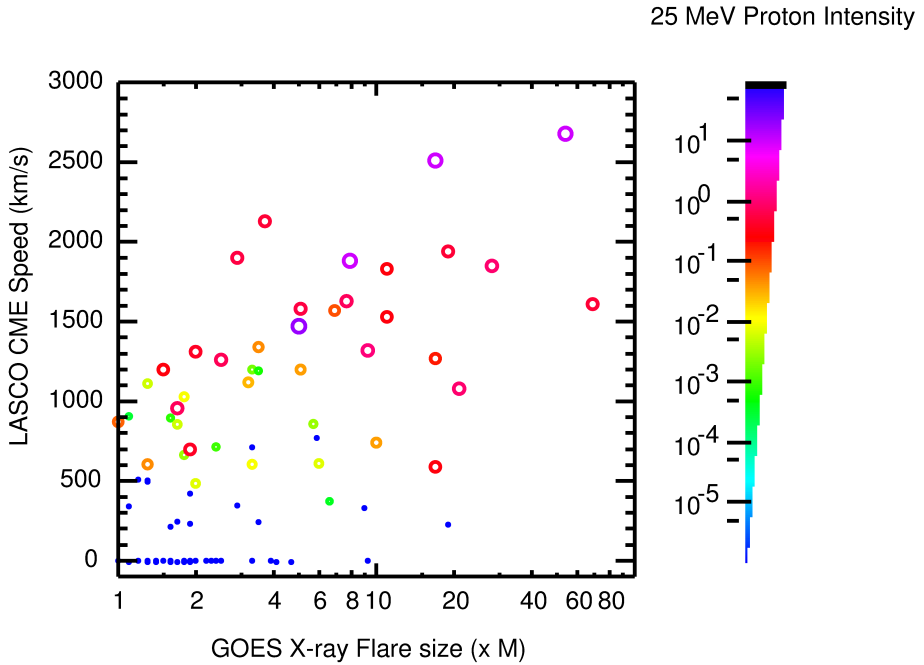


Figure 22. LASCO CME speed vs. GOES X-ray flare size expressed as multiples of M1 for 95 M/X flares at W30-90° with respect to the observing spacecraft. Cases when no CME was observed accompanying the flare are plotted at zero CME speed. The symbol size and color indicate the 25 MeV proton intensity. The small blue circles indicate cases where no SEP event was detected, which are generally associated with flares below \sim M5 and with no CME or a CME below \sim 500 km/s.

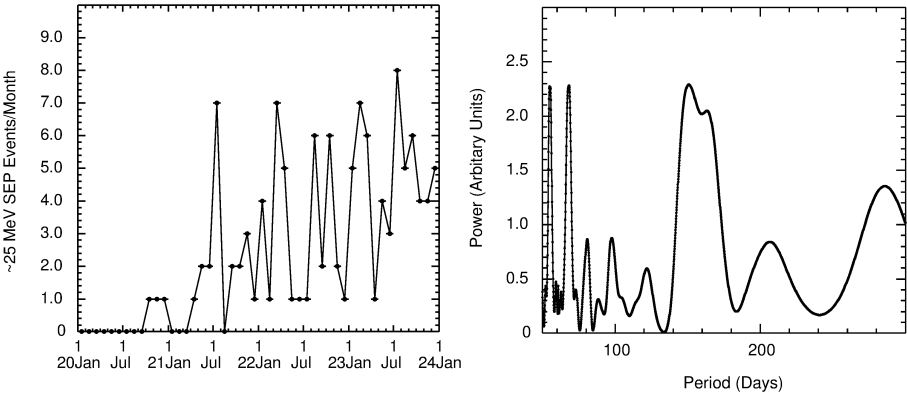


Figure 23. Left: Monthly number of \sim 25 MeV proton events (from Figure 1) in 2020-2023 during the rising phase of Solar Cycle 25 showing the tendency for intervals with enhanced numbers of SEP events to be separated by intervals with few events, possibly exhibiting evidence for quasi-periodicity. Right: Lomb periodogram in the range 50-300 days for the SEP occurrence rate in 2020-2023, showing a broad power enhancement with a peak at 150.8 days and a secondary peak at 163.3 days, consistent with a “Rieger-like” periodicity.

7. Evidence for Periodicity in the SEP Occurrence Rate During the Rising Phase of Cycle 25 (2020-2023)

Following the identification of a ~ 154 day periodicity in the occurrence rate of X-ray flares during Solar Cycle 21 by Rieger et al. (1984), “Rieger-like” quasi-periodicities have been widely reported in various solar phenomena (e.g., Lean 1990; Lou et al. 2003; Lara et al. 2008; Lobzin, Cairns, and Robinson 2012; Chowdhury et al. 2015; Gurgenashvili et al. 2021, and references therein) including SEP events (e.g., Bai and Cliver 1990; Cane, Richardson, and von Rosenvinge 1998; Dalla et al. 2001; Richardson, von Rosenvinge, and Cane 2016). In particular, Richardson, von Rosenvinge, and Cane (2016) discussed evidence for ~ 6 month periodicities in the SEP (~ 25 MeV proton) event occurrence rate during the rising and peak phases of Cycle 24 using the Richardson et al. (2014) event catalog. These periodicities were most clearly identified by separating the SEP events into those originating in the northern or southern solar hemispheres, and were shown to be related to variations in the sunspot number or area in the solar hemisphere in which the events originated. Using combined STEREO and near-Earth SEP observations also improved the event statistics significantly over using only near-Earth observations. Here, we point out evidence for a Rieger-like periodicity in the occurrence of SEP events in 2020–2023 during the rising phase of Cycle 25 that might be investigated further (e.g., by considering hemispheric occurrence rates) using a longer sequence of Cycle 25 SEP and solar observations. The left panel of Figure 23 shows the monthly number of ~ 25 MeV proton events during the rise phase of Cycle 25 in 2020–2023 identified in this study (from Figure 1), based on STEREO A and near-Earth observations. As has been noted during the onsets of some previous solar cycles (e.g., Dalla et al. 2001; Cane, Richardson, and von Rosenvinge 1998; Richardson, von Rosenvinge, and Cane 2016), the SEP rate does not ramp up gradually but shows intervals with large numbers of events (when major active regions are present) separated by periods of reduced activity with fewer SEP events. Inspection suggests that the times of peak SEP rate may occur \sim periodically starting with the first peak late in 2020. To examine this more quantitatively, the right panel shows a Lomb-Scargle (Lomb 1976; Scargle 1982) periodogram in the range 50–300 days derived from the SEP occurrence rate that includes a broad power enhancement with a peak at 150.8 days and a secondary peak at 163.3 days. These results suggest the presence of a periodicity in the SEP rate which is similar to the Rieger periodicity, though shorter than the six–seven months periodicity found by Richardson, von Rosenvinge, and Cane (2016) during the rising phase of Cycle 24. McIntosh et al. (2015) have discussed the influence of such periodicities, which may originate from Rossby waves in the Solar Tachocline (Dikpati and McIntosh 2020), on solar and heliospheric parameters and their implications for space weather.

8. Summary

- Some 450 individual SEP events including ~ 25 MeV protons were detected by the STEREO A/B spacecraft and/or by near-Earth spacecraft

between STEREO launch in October 2006 and December 2023, encompassing STEREO A's first orbit of the Sun relative to Earth completed in August 2023.

- This period includes the maximum phase of Solar Cycle 24, when the STEREO spacecraft and Earth were widely-separated in longitude, allowing observations of these events to be compared over wide longitudes near 1 AU and demonstrating that SEPs may be transported to extended regions of the inner heliosphere, including those poorly-connected to the observing spacecraft. These observations have also clearly demonstrated that solar events originating on the far side of the Sun can contribute significantly to the SEP population at Earth, with 19% of the 25 MeV proton events at Earth during our study period originating behind the west limb, and 6.3% behind the east limb. Unfortunately, contact with STEREO B was lost in 2014 when on the far side of the Sun. As a consequence, observations of activity behind the west limb became more limited as STEREO A moved towards the east limb. Following the loss of contact with STEREO B, we have used estimates of the direction of the associated CMEs in the DONKI catalog to help infer the general longitude of far side events, in particular those behind the west limb.
- During the ascending phase of Solar Cycle 25, STEREO A was approaching Earth, and complementary observations from spacecraft in the inner heliosphere, including PSP, SolO and Bepi-Colombo have enabled studies of SEPs using a constellation of spacecraft at varying longitudes and heliocentric distances relative to Earth and STEREO A. In some cases, SolO was favorably placed to directly observe the origin of an SEP event using remote sensing. In addition, SEP observations from the inner heliosphere spacecraft may help to identify the onset of an SEP event that was poorly connected to Earth or STEREO A. While such observations from an ever-changing constellation of spacecraft provide opportunities to explore different spatial and temporal variations in SEP events, the STEREO mission has proven the value of observations from spacecraft that are slowly varying in location. In particular, the STEREO spacecraft provided extended (multi-year) near-continuous observations of far side activity that are not available from inner heliosphere missions.
- As in Richardson et al. (2014), we have been able to identify the solar event associated with all but a few of the SEP events by assessing the SEP observations together with solar flare, EUV imaging from STEREO or near-Earth spacecraft (SOHO, SDO), coronal mass ejections observed by SOHO/LASCO or STEREO/SECCHI, and solar radio observations from Wind/WAVES and STEREO/SWAVES. Examples of more challenging SEP events are discussed in Appendix C, as well as a rare small event observed during solar minimum described in Appendix B. We have also pointed out that the standard list of SEP events at Earth based on GOES data and defined by thresholds widely used for operations only includes a small subset of the largest SEP events. These do not reflect the rich diversity of SEP events that should be considered, for example, when examining the relationship between solar phenomena and SEP event characteristics that may contribute to the development of models to predict SEP events.

- The combined observations from the STEREO and near-Earth spacecraft provide a large sample of ~ 1000 observations of SEP events associated with solar events at a wide range of longitudes relative to the observing spacecraft that may be useful for statistical studies. For example, we have used this large sample to investigate how the properties of the SEP event depend on those of the solar event, such as the correlation between CME speed and SEP intensity found in many other studies which is also observed at all event longitudes, and a corresponding, though generally weaker, correlation between the flare soft X-ray and SEP intensities. We have also illustrated how the energetic SEP events discussed by Bruno et al. (2018), and the SEP events associated with long-duration gamma ray flares (Bruno et al. 2023) lie in the general population at a proton energy of ~ 25 MeV. We have also pointed out some biases evident in these data sets, in particular in the longitudinal distributions, due to the locations of the STEREO spacecraft at the times of high SEP activity in Cycles 24 and 25, the loss of contact with STEREO B, and the restriction of direct X-ray flare observations to front side events (other than a few examples from SolO/STIX). We have also noted that SEP-associated CDAW LASCO “non-halo” CMEs tend to be associated with solar events near the limbs, suggesting a bias due to projection, while the “halo” CMEs are associated with solar events located at all longitudes relative to Earth, consistent with Kwon, Zhang, and Olmedo (2014).
- We have also summarized the association of ~ 25 MeV proton events observed by the STEREO or near-Earth spacecraft with a large sample of 397 M/X class GOES X-ray flares in 2010-2014 selected independently of any association with SEP events (Aschwanden et al. 2017). Considering cases with suitable SEP observations (e.g., no data gaps or ongoing SEP event), a ~ 25 MeV proton event above instrumental background was only detected in 22% of the observations, demonstrating that even for M/X flares, a majority are not associated with observed SEP events. At least for this set of flares, an SEP event was not detected if no CME or evidence of an eruption accompanied a flare. The likelihood of SEP detection and the longitudinal extent of the SEP event increased as the CME speed increased. The likelihood of an SEP event being detected and its intensity and longitudinal width also increased with increasing flare size.
- As noted above, the observations clearly demonstrate that far side solar events contribute to the SEP population at Earth. We emphasize that, as a consequence, a significant fraction of the SEP events observed at Earth are not associated with front side flares observed, for example in EUV and X-rays, and that care should be taken to avoid erroneously associating far side SEP events with front side flares. In particular, we highlight the case of the November 3, 2011 event, for which the source far behind the east limb was directly observed by STEREO B, as several studies have discussed, but has been associated with an unrelated front side X-class flare in several SEP catalogs. We suspect that further examples of such erroneous associations are also present in older SEP catalogs where SEP events originating on the far side are incorrectly associated with the most conspicuous front side solar event.

- There is evidence for a “Rieger-like” periodicity, with peak power at 150.8 days, in the SEP occurrence rate in 2020-2023 during the rising phase of Cycle 25. This could be explored further using an extended interval of observations and by separating the observations by their solar hemisphere source as in Richardson, von Rosenvinge, and Cane (2016).

Appendix

A. SEP Event Tables

The first column in Tables 1 to 11 gives the date and hour of the likely-related solar event while the second column gives the hour of SEP onset at the space-craft that first detects the event. We do not provide more detailed estimates of the particle onset times because this requires carefully specifying the instrument/energy considered and for example, possible effects of anisotropies and instrument viewing. Rather the aim is to indicate the solar source associations that may be useful for further detailed studies; several of the other catalogs noted in Section 3 include more detailed information on particle onsets that may include inferred solar release times for selected events.

The next three pairs of columns show the solar event location with respect to the observing spacecraft, and the peak ~ 25 MeV proton intensity at that space-craft, for STEREO B, the Earth, and STEREO A, respectively. The solar event location, which may be on the far side of the Sun, is inferred from examining movies of solar activity and coronal mass ejections from the STEREO spacecraft, the Solar Dynamics Observatory and SOHO, and cross-checking for consistency with catalogs of solar flares (e.g., NOAA daily solar activity reports (<https://www.swpc.noaa.gov/products/solar-and-geophysical-event-reports>, Solarmonitor.org) (<https://solarmonitor.org>), and the Solarsoft latest events archive (https://www.lmsal.com/solarsoft/latest_events_archive.html) for front side events, and CMEs (e.g., the CDAW, DONKI (Database Of Notifications, Knowledge, Information; <https://kauai.ccmc.gsfc.nasa.gov/DONKI/>) and CACTus (Computer Aided CME Tracking; <https://www.sidc.be/cactus/>) catalogs). Occasionally these catalogs do not agree on the solar event properties/location or may include apparent typographical errors, in which case, we have used our judgment guided by observations to make any necessary corrections. In twelve cases between the launch of SolO in February 2020 and December 2023, the related far side X-ray flare was directly detected by the STIX instrument on SolO. Some of the listed far side events were also directly observed by remote sensing instruments on SolO. “D” indicates a source longitude based on the CME propagation direction in the DONKI database. This is mainly used for events that occurred following the loss of STEREO B observations where the source cannot be viewed directly but appears to be behind the west limb as viewed from Earth (e.g., there is a CME above the west limb with no front side activity) and is also beyond the eastern limb as viewed from STEREO-A. In addition, in some cases, the DONKI database gives an estimate of the behind the limb flare location. The DONKI database typically gives a brief explanation of the rationale for estimating a

certain CME direction. The typical east-west asymmetry of SEP event intensity-time profiles (Cane, Reames, and von Rosenvinge 1988; Cane and Lario 2006) can also often help to corroborate the event location relative to the observing spacecraft. The solar event locations provided are likely to be accurate only to $\sim 10^\circ$ since the associated activity may cover an extended region, different flare databases often do not agree exactly on the location, and there is uncertainty in the DONKI CME directions (Bruno and Richardson (2021) indicate uncertainties of $\sim 10 - 15^\circ$ depending on the number of spacecraft used in the direction determination).

The peak ~ 25 MeV proton intensity at the observing spacecraft generally corresponds to the “first peak” during the first few (~ 12) hours of the event, in $(\text{MeV s cm}^2 \text{ sr})^{-1}$. The intensity may be higher in an “energetic storm particle” enhancement around passage of the associated interplanetary shock, which occasionally can extend above 40 MeV (Lario et al. 2023) but is typically more prominent at lower energies. However, here, we choose not to mix intensities from different stages of an SEP event. The proton intensities at ~ 25 MeV are based on observations from different spacecraft instruments around this energy. In particular, the STEREO HETs have a channel at 23.8-26.4 MeV, the SOHO/ERNE export data have a channel at 21-28 MeV. SOHO/EPHIN has rather wide channels, including 7.8-25 MeV and 25-40.9 MeV that encompass the energy of interest, and Wind/EPACT has a proton channel at 19-28 MeV; some examples of scalings between different instrument channels are discussed in Richardson et al. (2014). Due to such differences in instrumentation, the ~ 25 MeV proton intensities are typically only quoted to one significant figure, but are sufficient to indicate the relative sizes of the SEP events at the spacecraft locations. “BG” indicates that there is a background from an ongoing SEP event that may prevent the SEP event from being observed at a certain location. “...” indicates that the SEP event was not detected at ~ 25 MeV above the instrument background, typically $\sim 10^{-4}$ $(\text{MeV s cm}^2 \text{ sr})^{-1}$ in all the instruments used (see Figure 1).

Column 9 gives the GOES soft X-ray flare size (peak intensity) for front side or just over the limb events, obtained from operational GOES data and reports. Note that before December 18, 2017, the reported intensities are 43% lower than the actual intensities, due to application of a correction factor, whereas later intensities are from GOES-R with different instrumentation that provides operational data with correctly-calibrated absolute soft X-ray intensities (<https://www.goes-r.gov/users/transitionToOperations16.html>; see also the XRS Users Guide, available at <https://www.ngdc.noaa.gov/stp/satellite/goes-r.html>). Hence, after this date, the flare intensities listed should be multiplied by 0.7 to be consistent with those of earlier events or alternatively, earlier event intensities should be multiplied by 1.43 to give the absolute intensities. In analyses using the X-ray intensities discussed in Section 5, we have chosen to correct the GOES-R data to be consistent with earlier observations since most of the cataloged SEP events occurred before the GOES-R era, while recognizing that these intensities are not absolute. We have also retained the reported X-ray intensities in the catalog, rather than make any corrections, to facilitate cross referencing with other catalogs and studies that typically also quote these intensities. In a few

cases where the related far side flare was detected by the STIX instrument on SolO, the equivalent GOES intensity is obtained from the STIX flare list available at <https://datacenter.stix.i4ds.net/> and denoted by ‘S’.

Column 10 indicates whether or not (1 or 0, respectively) a type III radio burst (Wild, Smerd, and Weiss 1963) observed by the Wind/WAVES or STEREO/SWAVES instruments accompanied the solar event. Observations of type III (fast-drift) radio emissions (usually attributed to flare-accelerated electrons streaming away from the Sun) from the STEREO spacecraft and Wind can help indicate the solar event time and also corroborate the location based on the brightness of the burst at each spacecraft (see Krupar et al. (2024) for a recent discussion) and whether there is occultation of the higher frequencies by the limb of the Sun indicating a far side event relative to the observing spacecraft. As discussed for example by Cane, Erickson, and Prestage (2002), Cane, Richardson, and von Rosenvinge (2010), Laurenza et al. (2009), MacDowall et al. (2003), MacDowall et al. (2009), Winter and Ledbetter (2015), Richardson et al. (2014), and Richardson, Mays, and Thompson (2018), SEP events are highly (nearly 100%) associated with type III radio emissions observed by spacecraft, with the larger SEP events tending to be associated with brighter, longer duration type III emissions that extend to low frequencies. In particular, Richardson, Mays, and Thompson (2018) used the presence or absence of type III emissions to help distinguish CMEs that were more or less likely to be associated with SEP (specifically, ~ 25 MeV proton) events. Radio observations made by various spacecraft since November 2015 are summarized at the Coordinated Radiodiagnostics Of CMEs and Solar flares (CROCS) website (<https://parker.gsfc.nasa.gov/crocs.html>).

Column 11 indicates whether (1/2) or not (0) a type II (slow drift) radio burst, believed to be evidence for particle acceleration at a CME-driven shock (e.g., Cane et al. 1982; Nelson and Melrose 1985; Wild, Smerd, and Weiss 1963), was observed by these instruments (from the lists at https://solar-radio.gsfc.nasa.gov/wind/data_products.html and https://cdaw.gsfc.nasa.gov/CME_list/radio/waves.type2.html). If type II emissions extended below 1 MHz, indicative of an “interplanetary” (IP) type II event (e.g., Cane and Erickson 2005), this is denoted by ‘2’. “...” indicates that this information is not available at the time of writing.

Columns 12 and 13 give the plane-of-the-sky angular width and speed of the associated CME as observed by SOHO/LASCO. Values from the CDAW CME catalog (http://cdaw.gsfc.nasa.gov/CME_list/) are used if available. Other values are from the CACTus catalog (<http://sidc.oma.be/cactus/>), indicated by “**”) while “A” or “B” indicates values from the STEREO A or B CACTUS catalog, respectively.

Table 1. ~ 25 MeV Proton Events at 1 AU During the STEREO Mission

| Solar Event (UT) | SEP Event (UT) | Solar Event (°) | Solar Event-B (°) | 25 MeV I(B) | Solar Event-Earth (°) | 25 MeV I(Earth) | Solar Event-A (°) | 25 MeV I(A) | GOES X-Ray | Type III | Type II | CME dA (°) | CME V km/s |
|------------------|----------------|-----------------|-------------------|-------------|-----------------------|-----------------|-------------------|-------------|------------|----------|---------|------------|------------|
| 2006 Dec 5, 10 | Dec 5, 12 | -68 | 0.04 | -68 | 0.04 | -68 | 0.04 | X9.0 | 1 | 2 | DG | DG | |
| 2006 Dec 6, 18 | Dec 6, 19 | -64 | BG | -64 | BG | -64 | BG | X6.5 | 1 | 2 | 360 | 360 | |
| 2006 Dec 13, 02 | Dec 13, 02 | 23 | 10 | 23 | 10 | 23 | 10 | X3.4 | 1 | 2 | 360 | 1774 | |
| 2006 Dec 14, 21 | Dec 14, 22 | 46 | 0.5 | 46 | 0.5 | 46 | 0.5 | X1.5 | 1 | 2 | 360 | 1042 | |
| 2007 May 19, 12 | May 19, 14 | 08 | 0.0004 | 05 | 0.0009 | -01 | 0.0003 | B9.5 | 1 | 1 | 106 | 958 | |
| 2007 May 23, 07 | May 23, 07 | 63 | 0.0003 | 60 | 0.0003 | 54 | 0.0003 | B5.3 | 1 | 0 | 90 | 679 | |
| 2007 Dec 31, 00 | Dec 31, 02 | -85 | ... | -108 | 0.0001 | -129 | ... | C8.3 | 1 | 1 | 164 | 995 | |
| 2009 May 5, 08 | May 5, 10 | -90 | ... | -137 | ... | 175 | 0.0006 | ... | 1 | 1 | 66 B | 595 B | |
| 2009 Dec 22, 04 | Dec 22, 05 | 113 | 0.0008 | 46 | 0.0005 | -18 | 0.0002 | C7.2 | 1 | 0 | 47 | 318 | |
| 2010 Jan 17, 03 | Jan 17, 04 | -50 | 0.0003 | -120 | 0.0003 | 176 | 0.0003 | ... | 1 | 1 | 126 | 350 | |
| 2010 Feb 6, 07 | Feb 6, 08 | 53 | 0.0003 | -18 | ... | -83 | ... | C4.0 | 1 | 0 | 56 | 240 | |
| 2010 Feb 7, 02 | Feb 7, 03 | 61 | 0.0003 | -10 | ... | 75 | ... | M1.3 | 1 | 0 | 360 | 421 | |
| 2010 Feb 12, 11 | Feb 12, 12 | 60 | 0.001 | -11 | 0.0003 | -76 | ... | M8.3 | 1 | 0 | 360 | 509 | |
| 2010 Jun 12, 00 | Jun 12, 01 | 113 | 0.0001 | 43 | 0.007 | -31 | 0.0002 | M2.0 | 1 | 1 | 119 | 486 | |
| 2010 Aug 1, 07 | Aug 1, 12 | 35 | 0.02 | -36 | 0.0005 | -114 | ... | C3.2 | 0 | 2 | 360 | 850 | |
| 2010 Aug 7, 17 | Aug 7, 19 | 38 | 0.08 | -34 | 0.005 | -113 | ... | M1.0 | 1 | 2 | 360 | 871 | |
| 2010 Aug 14, 09 | Aug 14, 10 | 126 | 0.004 | 54 | 0.2 | -26 | 0.001 | C4.4 | 1 | 0 | 360 | 1205 | |
| 2010 Aug 18, 05 | Aug 18, 06 | 172 | 0.001 | 100 | 0.03 | 20 | 0.008 | C4.5 | 1 | 2 | 184 | 1471 | |
| 2010 Aug 31, 02 | Aug 31, 03 | -141 | ... | 145 | 0.005 | 64 | 0.0002 | ... | 1 | 0 | 33 | 319 | |
| 2010 Aug 31, 21 | Aug 31, 22 | -141 | 0.0001 | 145 | 0.005 | 64 | 0.008 | ... | 1 | 1 | 360 | 1304 | |
| 2010 Sep 4, 14 | Sep 4, 20 | 144 | ... | 70 | 0.0001 | -11 | ... | B2.5 | 1 | 1 | 130 | 567 | |
| 2010 Sep 8, 23 | Sep 9, 20 | 167 | 0.0003 | 92 | 0.003 | 10 | 0.003 | C3.3 | 1 | 1 | 147 | 818 | |
| 2010 Dec 31, 04 | Dec 31, 05 | 159 | ... | 69 | 0.0001 | -17 | ... | C1.3 | 1 | 0 | 45 | 363 | |
| 2011 Jan 27, 08 | Jan 27, 10 | 169 | ... | 76 | 0.0001 | -10 | ... | B6.6 | 1 | 0 | 52 | 316 | |
| 2011 Jan 27, 11 | Jan 27, 14 | 178 | ... | 85 | 0.0001 | -1 | ... | C1.2 | 1 | 1 | 43 | 349 | |
| 2011 Jan 28, 00 | Jan 28, 02 | -177 | ... | 90 | 0.05 | 04 | 0.002 | M1.3 | 1 | 1 | 119 | 606 | |
| 2011 Jan 31, 16 | Jan 31, 20 | -136 | ... | 131 | ... | 45 | 0.0002 | ... | 1 | 1 | 150 | 713 | |
| 2011 Feb 13, 17 | Feb 13, 18 | 90 | 0.0004 | -04 | 0.0002 | -91 | ... | M6.6 | 1 | 1 | 276 | 373 | |
| 2011 Feb 14, 17 | Feb 14, 18 | 98 | 0.001 | 04 | 0.0003 | -83 | ... | M2.2 | 1 | 2 | 360 | 326 | |
| 2011 Feb 15, 01 | Feb 15, 02 | 112 | 0.08 | 18 | 0.02 | -69 | ... | X2.2 | 1 | 2 | 360 | 669 | |
| 2011 Feb 24, 07 | Feb 24, 08 | -8 | 0.0006 | -102 | ... | 171 | ... | M3.5 | 1 | 0 | 158 | 1186 | |
| 2011 Mar 4, 14 | Mar 4, 15 | -85 | ... | 180 | ... | 92 | 0.0003 | ... | 1 | 0 | 60 B | 297 B | |
| 2011 Mar 7, 13 | Mar 7, 15 | 74 | 0.4 | -21 | 0.0004 | -21 | 0.0004 | M1.9 | 1 | 1 | 261 | 698 | |
| 2011 Mar 7, 19 | Mar 7, 21 | 148 | BG | 53 | 0.5 | -35 | 0.0006 | M3.7 | 1 | 2 | 360 | 2125 | |
| 2011 Mar 16, 22 | Mar 16, 22 | 167 | ... | 72 | 0.004 | -16 | 0.0002 | C3.7 | 1 | 0 | 184 | 682 | |
| 2011 Mar 21, 02 | Mar 21, 03 | -127 | 0.0008 | 138 | 0.11 | 50 | 12 | ... | 1 | 2 | 360 | 1341 | |
| 2011 Mar 29, 20 | Mar 30, 04 | -25 | 0.01 | -120 | ... | 151 | 0.003 | ... | 1 | 0 | >195 | 1264 | |
| 2011 Apr 3, 05 | Apr 3, 06 | 170 | ... | 75 | 0.0008 | -14 | ... | C1.2 | 1 | 0 | DG | DG | |
| 2011 Apr 4, 03 | Apr 4, 12 | 165 | ... | 70 | 0.001 | -19 | ... | B8.6 | 1 | 0 | DG | DG | |
| 2011 Apr 21, 00 | Apr 21, 02 | -105 | ... | 160 | 0.0007 | 70 | 0.001 | ... | 1 | 0 | 111 | 475 | |

Table 2. ~ 25 MeV Proton Events at 1 AU During the STEREO Mission

| Solar Event (UT) | SEP Event (UT) | Solar Event (°) | Solar Event-B (°) | 25 MeV I(B) | Solar Event-Earth (°) | 25 MeV I(Earth) | Solar Event-A (°) | 25 MeV I(A) | GOES X-Ray | Type III | Type II | Type CME | dA (°) | CME V km/s |
|------------------|----------------|-----------------|-------------------|-------------|-----------------------|-----------------|-------------------|-------------|------------|----------|---------|----------|--------|------------|
| 2011 May 9, 20 | May 10, 00 | 0 | 0.002 | -94 | 0.004 | 174 | ... | C5.4 | 1 | 2 | 292 | 1318 | | |
| 2011 May 11, 02 | May 11, 04 | 147 | ... | 53 | ... | -39 | ... | B8.1 | 1 | 0 | 225 | 745 | | |
| 2011 May 19, 03 | May 19, 06 | 126 | 0.01 | 32 | ... | -61 | 0.0001 | B3.0 | 1 | 0 | 132 | 626 | | |
| 2011 May 29, 20 | May 29, 22 | 25 | 0.006 | -68 | ... | -162 | ... | C8.7 | 1 | 2 | 186 | 1407 | | |
| 2011 Jun 2, 07 | Jun 2, 09 | 68 | 0.0006 | -25 | ... | -119 | ... | C3.7 | 1 | 1 | 360 | 976 | | |
| 2011 Jun 4, 06 | Jun 4, 07 | -112 | ... | 155 | 0.002 | 60 | 0.1 | ... | 1 | 2 | 360 | 1407 | | |
| 2011 Jun 4, 22 | Jun 4, 22 | -102 | 0.08 | 165 | 0.04 | 70 | 1.3 | ... | 1 | 2 | 360 | 2425 | | |
| 2011 Jun 7, 06 | Jun 7, 07 | 147 | BG | 54 | 0.7 | -41 | BG | M2.5 | 1 | 2 | 360 | 1255 | | |
| 2011 Jun 29, 00 | Jun 29, 00 | 169 | ... | 77 | 0.0001 | -20 | ... | B7.3 | 1 | 0 | 122 | 481 | | |
| 2011 Jul 11, 10 | Jul 11, 12 | 86 | ... | -06 | 0.0001 | -104 | ... | C2.6 | 1 | 0 | 53 | 266 | | |
| 2011 Jul 26, 08 | Jul 26, 10 | -82 | 0.0004 | -175 | ... | 85 | 0.01 | ... | 1 | 1 | 360 | 382 | | |
| 2011 Aug 2, 05 | Aug 2, 07 | 108 | 0.0008 | 15 | 0.04 | -85 | ... | M1.4 | 1 | 1 | 268 | 712 | | |
| 2011 Aug 3, 13 | Aug 3, 14 | 123 | ... | 30 | 0.007 | -70 | ... | M6.0 | 1 | 0 | 360 | 610 | | |
| 2011 Aug 4, 03 | Aug 4, 05 | 129 | 0.004 | 36 | 1.1 | -64 | 0.005 | M9.3 | 1 | 2 | 360 | 1315 | | |
| 2011 Aug 8, 18 | Aug 8, 19 | 154 | ... | 61 | 0.05 | -39 | ... | M3.5 | 1 | 2 | 237 | 1343 | | |
| 2011 Aug 9, 07 | Aug 9, 08 | 162 | ... | 69 | 0.5 | -31 | 0.002 | X6.9 | 1 | 1 | 360 | 1610 | | |
| 2011 Aug 23, 22 | Aug 24, 06 | -85 | ... | -179 | ... | 79 | 0.002 | ... | 0 | 0 | 360 | 312 | | |
| 2011 Sep 3, 02 | Sep 3, 03 | -95 | ... | 170 | 0.0002 | 68 | 0.0003 | ... | 1 | 0 | 105 | 325 | | |
| 2011 Sep 4, 04 | Sep 4, 05 | -163 | ... | 102 | 0.002 | 0 | ... | C9.0 | 0 | 0 | 53 | 262 | | |
| 2011 Sep 4, 23 | Sep 5, 02 | -165 | ... | 100 | 0.0006 | -03 | 0.0002 | C7.9 | 1 | 1 | 146 | 622 | | |
| 2011 Sep 6, 01 | Sep 6, 02 | 102 | 0.003 | 7 | 0.03 | -95 | ... | M5.3 | 1 | 2 | 360 | 782 | | |
| 2011 Sep 6, 22 | Sep 6, 23 | 113 | 0.005 | 18 | 0.1 | -84 | 0.0002 | X2.1 | 1 | 2 | 360 | 575 | | |
| 2011 Sep 7, 18 | Sep 7, 20 | -50 | BG | -145 | BG | 112 | 0.004 | ... | 1 | 1 | 188 | 924 | | |
| 2011 Sep 8, 22 | Sep 9, 00 | -122 | BG | 143 | BG | 40 | 0.003 | ... | 1 | 1 | 281 | 983 | | |
| 2011 Sep 13, 12 | Sep 13, 12 | -161 | ... | 103 | 0.0003 | 0 | ... | C9.0 | 0 | 0 | 199 | 746 | | |
| 2011 Sep 21, 22 | Sep 21, 23 | -155 | ... | 109 | 0.002 | 05 | 0.0004 | ... | 1 | 0 | 255 | 1007 | | |
| 2011 Sep 22, 10 | Sep 22, 10 | 19 | 10 | -78 | 0.08 | 178 | 0.04 | X1.4 | 1 | 2 | 360 | 1905 | | |
| 2011 Sep 24, 09 | Sep 24, 11 | 37 | 0.5 | -60 | BG | -164 | BG | X1.9 | 1 | 2 | 145 | 1936 | | |
| 2011 Oct 4, 12 | Oct 4, 15 | -50 | 0.2 | -148 | 0.001 | 108 | 0.02 | ... | 1 | 0 | 360 | 1101 | | |
| 2011 Oct 14, 11 | Oct 14, 15 | -40 | 0.0002 | -140 | ... | 115 | 0.0005 | ... | 1 | 0 | 241 | 814 | | |
| 2011 Oct 20, 03 | Oct 20, 04 | -155 | ... | 105 | 0.0008 | 0 | 0.0002 | M1.6 | 1 | 0 | 193 | 893 | | |
| 2011 Oct 22, 10 | Oct 22, 12 | 177 | 0.0003 | 77 | 0.006 | -28 | 0.0008 | M1.3 | 0 | 2 | 360 | 1005 | | |
| 2011 Nov 3, 22 | Nov 3, 23 | -50 | 0.06 | -152 | 0.04 | 103 | 2.0 | ... | 1 | 2 | 360 | 991 | | |
| 2011 Nov 9, 13 | Nov 9, 14 | 68 | 0.002 | -35 | 0.002 | -141 | ... | M1.1 | 1 | 2 | 360 | 907 | | |
| 2011 Nov 12, 18 | Nov 12, 18 | 0 | 0.0002 | -103 | ... | 151 | 0.0003 | ... | 1 | 0 | 192 | 654 | | |
| 2011 Nov 13, 18 | Nov 13, 22 | -70 | 0.0003 | -174 | ... | 80 | 0.001 | ... | 1 | 0 | 360 | 596 | | |
| 2011 Nov 17, 22 | Nov 17, 23 | -20 | 0.01 | -125 | ... | -129 | 0.001 | ... | 1 | 0 | 360 | 1041 | | |
| 2011 Nov 23, 15 | Nov 23, 15 | -60 | ... | -165 | ... | 90 | 0.0003 | ... | 1 | 0 | 95? | 315? | | |
| 2011 Nov 26, 06 | Nov 26, 08 | 154 | 0.002 | 48 | 0.3 | -58 | 0.01 | C1.2 | 1 | 2 | 360 | 933 | | |

Table 3. ~ 25 MeV Proton Events at 1 AU During the STEREO Mission

| Solar Event (UT) | SEP Event (UT) | Solar Event (°) | Solar Event-B (°) | 25 MeV I(B) | Solar Event-Earth (°) | 25 MeV I(Earth) | Solar Event-A (°) | 25 MeV I(A) | GOES X-Ray | Type III | Type II | Type I | CME dA (°) | CME V km/s |
|------------------|----------------|-----------------|-------------------|-------------|-----------------------|-----------------|-------------------|-------------|------------|----------|---------|--------|------------|------------|
| 2011 Dec 3, 07 | Dec 3, 08 | -117 | ... | 136 | DG | 30 | 0.0003 | ... | 1 | 0 | 155 | 454 | | |
| 2011 Dec 11, 13 | Dec 11, 14 | -76 | ... | 176 | ... | 70 | 0.0003 | ... | 1 | 0 | 32 A | 312 A | | |
| 2011 Dec 17, 10 | Dec 17, 16 | -115 | ... | 136 | 0.0003 | 30 | 0.002 | ... | 1 | 0 | 247 | 987 | | |
| 2011 Dec 24, 11 | Dec 24, 14 | -165 | ... | 85 | 0.0003 | -22 | ... | C4.9 | 1 | 2 | 102 | 447 | | |
| 2011 Dec 25, 18 | Dec 25, 19 | 136 | 0.006 | 26 | 0.05 | -81 | ... | M4.0 | 1 | 1 | 125 | 366 | | |
| 2011 Dec 27, 04 | Dec 27, 05 | 78 | 0.0006 | -32 | BG | -139 | ... | C8.9 | 1 | 0 | 84 B | 735 B | | |
| 2011 Dec 29, 16 | Dec 29, 18 | -142 | ... | 107 | 0.001 | 0 | ... | | 1 | 0 | 171 | 736 | | |
| 2012 Jan 2, 14 | Jan 2, 16 | -152 | ... | 97 | 0.02 | -10 | 0.001 | C2.4 | 1 | 1 | 360 | 1138 | | |
| 2012 Jan 12, 07 | Jan 12, 10 | -05 | 0.0003 | -118 | ... | 135 | 0.0006 | C2.5 | 0 | 0 | 360 | 814 | | |
| 2012 Jan 16, 02 | Jan 16, 08 | 45 | 0.0005 | -68 | 0.0003 | -175 | ... | C6.5 | 0 | 0 | 360 | 1060 | | |
| 2012 Jan 19, 13 | Jan 19, 15 | 84 | 0.03 | -30 | 0.0006 | -137 | ... | M3.2 | 1 | 2 | 360 | 1120 | | |
| 2012 Jan 23, 04 | Jan 23, 04 | 135 | 0.6 | 21 | 20 | -87 | 0.1 | M8.7 | 1 | 2 | 360 | 2175 | | |
| 2012 Jan 27, 17 | Jan 27, 19 | -175 | BG | 71 | 10 | -37 | 0.3 | XI.7 | 1 | 2 | 360 | 2508 | | |
| 2012 Feb 24, 04 | Feb 24, 10 | 79 | ... | -38 | 0.0005 | -147 | ... | | 0 | 2 | 189 | 800 | | |
| 2012 Feb 29, 09 | Feb 29, 10 | -118 | ... | 125 | 0.0005 | 16 | 0.005 | | 1 | 0 | 360 | 466 | | |
| 2012 Mar 3, 18 | Mar 4, 00 | 45 | 0.0002 | -73 | ... | 178 | ... | C1.9 | 1 | 1 | 192 | 1078 | | |
| 2012 Mar 4, 10 | Mar 4, 12 | 57 | 0.4 | -61 | 0.02 | -170 | ... | M2.0 | 1 | 1 | 360 | 1306 | | |
| 2012 Mar 5, 02 | Mar 5, 04 | 66 | 0.3 | -52 | BG | -161 | 0.001 | XI.1 | 1 | 2 | 360 | 1531 | | |
| 2012 Mar 7, 00 | Mar 7, 01 | 91 | 100 | -27 | 10 | -137 | 0.09 | X5.4 | 1 | 2 | 360 | 2684 | | |
| 2012 Mar 13, 17 | Mar 13, 18 | 179 | BG | 61 | 10 | -48 | BG | M7.9 | 1 | 1 | 360 | 1884 | | |
| 2012 Mar 21, 07 | Mar 21, 07 | -81 | BG | 160 | 160 | 50 | 0.8 | | 1 | 1 | 360 | 1178 | | |
| 2012 Mar 24, 00 | Mar 24, 00 | -50 | 0.03 | -169 | 0.001 | 80 | 1.3 | ... | 1 | 2 | 360 | 1152 | | |
| 2012 Mar 26, 22 | Mar 27, 00 | -5 | 0.6 | -124 | BG | 125 | BG | ... | 1 | 1 | 360 | 1390 | | |
| 2012 Apr 5, 20 | Apr 6, 00 | 148 | ... | 29 | 0.002 | -82 | ... | C1.5 | 1 | 0 | 360 | 828 | | |
| 2012 Apr 7, 16 | Apr 7, 17 | -80 | ... | 161 | 0.0005 | 50 | 0.02 | ... | 1 | 2 | 360 | 765 | | |
| 2012 Apr 9, 12 | Apr 9, 12 | -168 | ... | 73 | 0.0006 | -38 | ... | C3.9 | 1 | 1 | 360 | 921 | | |
| 2012 Apr 15, 02 | Apr 15, 03 | 29 | 0.002 | -90 | ... | 158 | 0.001 | C1.7 | 1 | 1 | 173 | 1220 | | |
| 2012 Apr 18, 02 | Apr 18, 03 | -39 | ... | -158 | ... | 90 | 0.0006 | ... | 1 | 0 | > 271 | 352 | | |
| 2012 Apr 18, 04 | Apr 18, 15 | -35 | ... | -154 | 0.0001 | 94 | 0.0004 | ... | 1 | 2 | 184 | 840 | | |
| 2012 Apr 24, 07 | Apr 24, 09 | 30 | 0.015 | -88 | 0.0002 | 159 | ... | C3.7 | 1 | 0 | 190 | 443 | | |
| 2012 Apr 27, 15 | Apr 27, 18 | -108 | ... | 133 | ... | 20 | 0.0003 | ... | 1 | 1 | 360 | 681 | | |
| 2012 May 1, 16 | May 1, 18 | -59 | ... | -177 | ... | 70 | 0.0002 | ... | 1 | 0 | 200 | 788 | | |
| 2012 May 7, 00 | May 7, 03 | 142 | ... | 24 | 0.0002 | -90 | ... | C1.3 | 1 | 0 | 124 A | 625 A | | |
| 2012 May 14, 09 | May 14, 10 | 158 | ... | 40 | 0.0003 | -75 | ... | C2.5 | 1 | 1 | 48 | 551 | | |
| 2012 May 17, 01 | May 17, 02 | -166 | 0.001 | 76 | 0.6 | -39 | 0.002 | M5.1 | 1 | 2 | 360 | 1582 | | |
| 2012 May 26, 20 | May 26, 21 | -127 | 0.001 | 116 | 0.03 | 0.0 | 0.2 | ... | 1 | 2 | 360 | 1966 | | |
| 2012 Jun 1, 22 | Jun 1, 22 | 81 | 0.0006 | -35 | ... | 154 | ... | C3.3 | 1 | 0 | 175 | 630 | | |
| 2012 Jun 3, 17 | Jun 3, 19 | 79 | 0.01 | -38 | ... | -154 | ... | M3.3 | 1 | 0 | 180 | 605 | | |
| 2012 Jun 8, 07 | Jun 8, 07 | 157 | ... | 40 | 0.0001 | -77 | ... | C4.8 | 1 | 1 | 34 | 308 | | |
| 2012 Jun 12, 05 | Jun 12, 06 | -109 | ... | 135 | 0.0001 | 18 | 0.001 | ... | 1 | 0 | 195 | 864 | | |
| 2012 Jun 14, 12 | Jun 14, 15 | 111 | 0.001 | -66 | 0.002 | -123 | ... | M1.9 | 1 | 0 | 360 | 987 | | |
| 2012 Jun 28, 07 | Jun 28, 08 | -65 | ... | 179 | ... | 60 | 0.002 | ... | 1 | 0 | 360 | 728 | | |
| 2012 Jun 28, 16 | Jun 28, 16 | 71 | 0.001 | -45 | ... | -164 | ... | M2.4 | 1 | 0 | 104 | 714 | | |

Table 4. ~25 MeV Proton Events at 1 AU During the STEREO Mission

| Solar Event (UT) | SEP Event (UT) | Solar Event-B (°) | 25 MeV I(B) | Solar Event-Earth (°) | 25 MeV I(Earth) | Solar Event-A (°) | 25 MeV I(A) | GOES X-Ray | Type III | Type II | CME Type | dA (°) | CME V km/s |
|------------------|----------------|-------------------|-------------|-----------------------|-----------------|-------------------|-------------|------------|----------|---------|----------|--------|------------|
| 2012 Jul 2, 08 | Jul 2, 09 | -10 | 0.001 | -126 | 0.0001 | 115 | 0.01 | ... | 1 | 2 | 360 | 1074 | |
| 2012 Jul 4, 16 | Jul 4, 18 | -150 | ... | 34 | 0.003 | -85 | ... | M1.8 | 1 | 1 | 360 | 662 | |
| 2012 Jul 5, 21 | Jul 5, 22 | 161 | ... | 46 | BG | -73 | 0.0002 | M1.6 | 1 | 2 | 94 | 980 | |
| 2012 Jul 6, 23 | Jul 7, 01 | 165 | ... | 50 | 0.3 | -69 | 0.004 | X1.1 | 1 | 2 | 360 | 1828 | |
| 2012 Jul 8, 16 | Jul 8, 16 | -171 | ... | 74 | 0.1 | -46 | 0.1 | M6.9 | 1 | 2 | 157 | 1572 | |
| 2012 Jul 12, 15 | Jul 12, 17 | 109 | 0.2 | -06 | 0.8 | -126 | BG | X1.4 | 1 | 2 | 360 | 885 | |
| 2012 Jul 13, 19 | Jul 13, 20 | -115 | BG | 130 | BG | -10 | 0.004 | ... | 1 | 0 | 115 | 386 | |
| 2012 Jul 17, 12 | Jul 17, 15 | 180 | ... | 65 | 0.8 | -55 | 0.001 | M1.7 | 1 | 2 | 176 | 958 | |
| 2012 Jul 18, 06 | Jul 18, 06 | -75 | 0.001 | 170 | BG | 50 | 0.1 | ... | 1 | 1 | 360 | 873 | |
| 2012 Jul 19, 04 | Jul 19, 08 | -145 | ... | 100 | 0.8 | -20 | BG | M7.7 | 1 | 2 | 360 | 1631 | |
| 2012 Jul 23, 02 | Jul 23, 03 | -105 | 0.5 | 140 | 0.2 | 20 | 0.50 | ... | 1 | 2 | 360 | 2003 | |
| 2012 Aug 10, 09 | Aug 10, 13 | -97 | ... | 147 | 0.001 | 25 | 0.008 | ... | 1 | 0 | 251 | 464 | |
| 2012 Aug 19, 04 | Aug 19, 05 | -71 | ... | 173 | 0.0002 | 50 | 0.08 | ... | 1 | 0 | 224 | 577 | |
| 2012 Aug 19, 18 | Aug 19, 18 | -71 | 0.001 | 173 | 0.0002 | 50 | 0.4 | ... | 1 | 0 | 360 | 612 | |
| 2012 Aug 21, 20 | Aug 21, 21 | -56 | 0.0008 | -172 | ... | 65 | BG | ... | 1 | 2 | 360 | 1024 | |
| 2012 Aug 31, 19 | Aug 31, 20 | 74 | 20 | -42 | 0.04 | -165 | 0.0008 | C8.4 | 1 | 2 | 360 | 1442 | |
| 2012 Sep 8, 10 | Sep 8, 11 | -99 | ... | 145 | 0.01 | 20 | 0.002 | ... | 1 | 1 | 360 | 734 | |
| 2012 Sep 19, 11 | Sep 19, 12 | -51 | ... | -168 | ... | 67 | 0.04 | ... | 1 | 1 | 360 | 616 | |
| 2012 Sep 20, 15 | Sep 20, 15 | -40 | 0.2 | -158 | 0.003 | 77 | 5 | ... | 1 | 2 | 360 | 1202 | |
| 2012 Sep 27, 10 | Sep 27, 10 | -84 | ... | 158 | 0.2 | 33 | 0.15 | ... | 1 | 2 | 360 | 1319 | |
| 2012 Sep 27, 23 | Sep 28, 00 | 152 | 0.3 | 34 | 0.2 | -91 | BG | C3.7 | 1 | 0 | 360 | 947 | |
| 2012 Oct 7, 06 | Oct 7, 12 | -124 | ... | 5 | 0.0002 | -121 | ... | B4.5 | 1 | 0 | 149 | 663 | |
| 2012 Oct 14, 00 | Oct 14, 01 | -18 | 0.008 | -138 | 0.0002 | 96 | 0.06 | ... | 1 | 1 | 360 | 987 | |
| 2012 Nov 8, 02 | Nov 8, 03 | 35 | 0.006 | -88 | ... | 145 | 0.0003 | M1.7 | 1 | 0 | 360 | 855 | |
| 2012 Nov 8, 11 | Nov 8, 11 | -68 | BG | 168 | 0.02 | 41 | 0.4 | ... | 1 | 2 | 360 | 972 | |
| 2012 Nov 16, 06 | Nov 17, <19 | 10 | 0.005 | -114 | ... | 118 | ... | C1.4 | 1 | 0 | 360 | 775 | |
| 2012 Nov 20, 12 | Nov 20, 13 | 103 | ... | -22 | 0.0001 | -150 | ... | M1.7 | 1 | 0 | 360 | 619 | |
| 2012 Nov 21, 15 | Nov 21, 17 | 124 | 0.001 | -1 | 0.0003 | -128 | ... | M3.5 | 0 | 0 | 360 | 529 | |
| 2012 Nov 23, 23 | Nov 23, 23 | -102 | ... | 132 | 0.0003 | -5 | 0.03 | ... | 1 | 2 | 360 | 1186 | |
| 2012 Nov 24, 13 | Nov 24, 14 | -154 | ... | 28 | 0.0003 | -100 | ... | C3.3 | 1 | 0 | 84 | 237 | |
| 2012 Dec 2, 15 | Dec 2, 16 | -56 | ... | 177 | 0.0005 | 50 | 0.005 | ... | 1 | 0 | 360 | 678 | |
| 2012 Dec 5, 00 | Dec 5, 03 | 52 | 0.003 | -75 | ... | 157 | 0.0002 | C1.7 | 1 | 1 | 231 | 963 | |
| 2012 Dec 14, 01 | Dec 14, 03 | -169 | ... | 40 | 0.01 | -88 | ... | ... | 1 | 0 | 149 | 763 | |
| 2013 Jan 6, 22 | Jan 6, 23 | -40 | ... | -173 | ... | 58 | 0.008 | ... | 1 | 0 | 211 | 667 | |
| 2013 Jan 16, 18 | Jan 16, 20 | -149 | ... | 77 | 0.005 | -52 | ... | C2.2 | 1 | 0 | 250 | 648 | |
| 2013 Feb 6, 00 | Feb 6, 03 | 118 | 0.002 | -19 | 0.0001 | -149 | 0.0004 | C8.7 | 1 | 0 | 271 | 1867 | |
| 2013 Feb 26, 09 | Feb 26, 13 | -89 | ... | 131 | 0.01 | 0 | 0.002 | ... | 1 | 1 | 360 | 987 | |
| 2013 Mar 5, 03 | Mar 5, 03 | -1 | 0.4 | -141 | 0.006 | 88 | 30 | ... | 1 | 1 | 360 | 1316 | |
| 2013 Mar 15, 05 | Mar 15, 07 | -129 | 0.006 | -12 | 0.004 | -144 | ... | M1.1 | 1 | 2 | 360 | 1063 | |
| 2013 Apr 11, 06 | Apr 11, 07 | -130 | 5 | -12 | 2 | -146 | 0.001 | M6.5 | 1 | 2 | 360 | 861 | |
| 2013 Apr 21, 06 | Apr 21, 08 | -94 | ... | 124 | 0.02 | -10 | 0.001 | ... | 1 | 0 | 360 | 919 | |
| 2013 Apr 24, 21 | Apr 24, 22 | -44 | 0.001 | 175 | 0.01 | 40 | 0.1 | ... | 1 | 0 | 360 | 594 | |
| 2013 Apr 28, 20 | Apr 28, 22 | -179 | ... | 37 | 0.0004 | -97 | ... | C4.4 | 1 | 0 | 91 | 497 | |

Table 5. ~ 25 MeV Proton Events at 1 AU During the STEREO Mission

| Solar Event (UT) | SEP Event (UT) | Solar Event (°) | 25 MeV I(B) | Solar Event-Earth (°) | 25 MeV I(Earth) | Solar Event-A (°) | 25 MeV I(A) | GOES X-Ray | CME Type III | CME Type II | CME dA (°) | CME V km/s |
|------------------|----------------|-----------------|-------------|-----------------------|-----------------|-------------------|-------------|------------|--------------|-------------|------------|------------|
| 2013 May 1, 02 | May 1, 04 | 37 | 0.009 | -105 | ... | 120 | 0.007 | ... | 1 | 1 | 360 | 762 |
| 2013 May 2, 04 | May 2, 06 | 168 | BG | 26 | 0.0005 | -109 | BG | ML.1 | 1 | 0 | 99 | 671 |
| 2013 May 3, 17 | May 3, 20 | 61 | 0.003 | -81 | ... | 144 | 0.002 | ML.7 | 0 | 0 | 274 | 858 |
| 2013 May 10, 18 | May 10, 20 | -78 | ... | 140 | 0.0002 | 5 | 0.006 | ... | 1 | 0 | 120 | 6.7 |
| 2013 May 13, 01 | May 13, 02 | 39 | 0.2 | -103 | BG | 121 | ... | X1.7 | 1 | 1 | 360 | 1270 |
| 2013 May 13, 15 | May 13, 16 | 47 | 1.0 | -95 | 0.01 | 129 | 0.004 | X2.8 | 1 | 2 | 360 | 1850 |
| 2013 May 15, 01 | May 15, 06 | 78 | BG | -64 | 0.3 | 160 | BG | X1.2 | 1 | 2 | 360 | 1366 |
| 2013 May 22, 12 | May 22, 13 | -149 | 0.003 | 70 | 20 | -67 | 0.06 | ML5.0 | 1 | 2 | 360 | 1466 |
| 2013 Jun 17, 02 | Jun 17, 03 | 81 | 0.002 | -59 | ... | 161 | ... | C1.2 | 0 | 0 | ... | ... |
| 2013 Jun 21, 02 | Jun 21, 03 | 67 | 0.6 | -73 | 0.06 | 147 | 0.001 | M2.9 | 1 | 1 | 207 | 1900 |
| 2013 Jun 23, 20 | Jun 23, 20 | 78 | BG | -62 | ... | 159 | 0.0004 | M2.9 | 1 | 0 | 101 | 339 |
| 2013 Jul 1, 20 | Jul 1, 20 | 50 | 0.015 | -90 | ... | 130 | 0.004 | ... | 1 | 0 | 208 | 819 |
| 2013 Jul 3, 07 | Jul 3, 07 | 58 | 0.002 | -82 | ... | 137 | ... | ML.5 | 1 | 0 | 267 | 807 |
| 2013 Jul 22, 06 | Jul 22, 06 | -50 | 0.001 | 172 | 0.001 | 29 | 0.04 | ... | 1 | 0 | 360 | 1004 |
| 2013 Aug 17, 19 | Aug 17, 19 | 168 | ... | 30 | 0.002 | -114 | ... | M3.3 | 1 | 2 | 360 | 1202 |
| 2013 Aug 19, 23 | Aug 19, 23 | -48 | 0.4 | 174 | 0.01 | 30 | 3 | ... | 1 | 0 | 360 | 877 |
| 2013 Aug 30, 02 | Aug 30, 02 | 95 | 0.03 | -43 | 0.0003 | 172 | ... | C8.2 | 1 | 2 | 360 | 949 |
| 2013 Sep 24, 19 | Sep 25, 00 | 79 | 0.0002 | -60 | 0.0001 | 153 | ... | ... | 1 | 0 | 360 | 919 |
| 2013 Sep 29, 21 | Sep 29, 22 | 164 | 0.02 | 25 | 0.5 | -122 | 0.003 | C1.2 | 1 | 2 | 360 | 1179 |
| 2013 Oct 5, 08 | Oct 5, 08 | 16 | 0.02 | -123 | ... | 90 | 0.5 | ... | 1 | 2 | 360 | 964 |
| 2013 Oct 11, 07 | Oct 11, 07 | 44 | 0.3 | -96 | 0.002 | 117 | 5 | ML.5 | 1 | 2 | 360 | 1200 |
| 2013 Oct 22, 21 | Oct 22, 22 | 141 | 0.002 | 00 | 0.01 | -148 | ... | M4.2 | 1 | 2 | 360 | 459 |
| 2013 Oct 25, 08 | Oct 25, 08 | 69 | 0.3 | -73 | 0.001 | 139 | ... | X1.7 | 1 | 0 | 360 | 587 |
| 2013 Oct 25, 14 | Oct 25, 15 | 74 | 1.0 | -68 | 0.008 | 144 | 0.002 | M2.1 | 1 | 2 | 360 | 1081 |
| 2013 Oct 28, 04 | Oct 28, 04 | -147 | BG | 71 | 0.04 | -77 | 0.002 | M5.1 | 1 | 2 | 156 | 1201 |
| 2013 Oct 28, 15 | Oct 28, 16 | 114 | 0.2 | -28 | BG | -176 | BG | M4.4 | 1 | 1 | 360 | 812 |
| 2013 Nov 2, 04 | Nov 2, 04 | -90 | 0.04 | 127 | 0.02 | -21 | 1.5 | ... | 1 | 0 | 360 | 828 |
| 2013 Nov 4, 05 | Nov 4, 06 | -49 | BG | 168 | BG | 20 | 1.2 | ... | 1 | 2 | 360 | 1040 |
| 2013 Nov 6, 23 | Nov 7, 01 | -118 | BG | 99 | 0.01 | -50 | BG | M1.8 | 1 | 0 | 360 | 1033 |
| 2013 Nov 7, 10 | Nov 7, 10 | 0 | 12 | -143 | BG | 68 | 1.3 | ... | 1 | 2 | 360 | 1405 |
| 2013 Nov 19, 11 | Nov 19, 11 | -146 | 0.001 | 69 | 0.04 | -80 | 0.0006 | X1.0 | 1 | 2 | 360 | 740 |
| 2013 Nov 26, 15 | Nov 26, 15 | -44 | ... | 169 | ... | 20 | 0.0006 | ... | 1 | 0 | ... | ... |
| 2013 Nov 30, 05 | Nov 30, 06 | -63 | ... | 150 | 0.0009 | 0 | 0.0005 | ... | 1 | 0 | 98* | 371* |
| 2013 Nov 30, 14 | Nov 30, 15 | 0 | 0.002 | -146 | BG | 63 | ... | ... | 0 | 0 | 251 | 723 |
| 2013 Dec 5, 14 | Dec 5, 14 | 40 | 0.003 | -108 | BG | 102 | 0.001 | ... | 0 | 1 | 148 | 549 |
| 2013 Dec 7, 07 | Dec 7, 09 | -164 | ... | 49 | 0.0004 | -100 | ... | M1.2 | 1 | 1 | 360 | 1085 |
| 2013 Dec 9, 19 | Dec 9, 23 | 78 | 0.0005 | -70 | ... | 139 | 0.0003 | C1.9 | 0 | 0 | 146 | 702 |
| 2013 Dec 12, 03 | Dec 12, 04 | -165 | ... | 46 | 0.001 | -104 | ... | C4.6 | 1 | 2 | 276 | 1002 |
| 2013 Dec 13, 20 | Dec 13, 20 | 0 | ... | -149 | ... | 61 | 0.001 | ... | 1 | 0 | 360 | 518 |
| 2013 Dec 14, 02 | Dec 14, 02 | 3 | ... | -146 | ... | 64 | 0.006 | ... | 1 | 0 | 92 | 512 |
| 2013 Dec 14, 06 | Dec 14, 06 | 5 | ... | -144 | 0.002 | 66 | 0.02 | ... | 1 | 0 | 121 | 611 |
| 2013 Dec 16, 21 | Dec 16, 22 | -101 | ... | 110 | 0.0002 | -40 | ... | C3.1 | 1 | 0 | 240 | 779 |
| 2013 Dec 26, 03 | Dec 26, 04 | -10 | 0.8 | -161 | 0.03 | 49 | 0.8 | ... | 1 | 0 | 360 | 1336 |
| 2013 Dec 28, 17 | Dec 28, 18 | -78 | BG | 130 | 0.3 | -20 | BG | ... | 1 | 2 | 360 | 1118 |

Table 6. ~ 25 MeV Proton Events at 1 AU During the STEREO Mission

| Solar Event (UT) | SEP Event (UT) | Solar Event (°) | Event-B (B) | 25 MeV I(B) | Solar Event-Earth (°) | 25 MeV I(Earth) | Solar Event-A (°) | 25 MeV I(A) | GOES X-Ray | Type III | Type II | Type CME | dA (°) | CME V km/s |
|------------------|----------------|-----------------|-------------|-------------|-----------------------|-----------------|-------------------|-------------|------------|----------|---------|----------|--------|------------|
| 2014 Jan 4, 18 | Jan 4, 21 | 113 | 0.003 | -40 | 0.002 | 169 | 0.04 | M4.0 | 1 | 2 | 360 | 977 | | |
| 2014 Jan 6, 07 | Jan 6, 08 | -97 | 0.04 | 110 | 0.6 | -41 | 0.6 | ... | 1 | 2 | 360 | 1402 | | |
| 2014 Jan 7, 18 | Jan 7, 19 | 164 | 0.04 | 11 | 2.2 | -140 | 0.6 | X1.2 | 1 | 2 | 360 | 1830 | | |
| 2014 Jan 20, 14 | Jan 20, 17 | -20 | ... | -176 | ... | 33 | 0.002 | ... | 1 | 0 | 360 | 675 | | |
| 2014 Jan 21, 05 | Jan 21, 06 | -94 | ... | 111 | 0.0005 | -40 | ... | ... | 1 | 0 | 125 | 496 | | |
| 2014 Jan 21, 10 | Jan 21, 11 | -91 | ... | 114 | 0.002 | -37 | ... | ... | 1 | 0 | 157 | 554 | | |
| 2014 Jan 21, 18 | Jan 21, 19 | -85 | ... | 120 | 0.001 | -31 | ... | ... | 1 | 0 | 113 | 1035 | | |
| 2014 Jan 21, 20 | Jan 22, 07 | -4 | 0.004 | -159 | ... | 50 | 0.02 | ... | 1 | 0 | 221 | 1065 | | |
| 2014 Jan 28, 22 | Jan 28, 22 | 88 | 0.002 | -68 | ... | 140 | ... | M2.6 | 1 | 0 | 91 | 462 | | |
| 2014 Jan 30, 15 | Jan 30, 17 | 99 | 0.002 | -58 | 0.002 | 151 | 0.001 | M6.6 | 1 | 0 | 360 | 1087 | | |
| 2014 Feb 9, 15 | Feb 9, 16 | 50 | 0.002 | -108 | ... | 100 | 0.02 | M1.0 | 1 | 0 | 360 | 908 | | |
| 2014 Feb 11, 13 | Feb 11, 14 | -89 | ... | 112 | 0.0003 | -40 | 0.002 | BG | 1 | 0 | 208 | 330 | | |
| 2014 Feb 11, 19 | Feb 11, 22 | -85 | ... | 116 | 0.001 | -36 | 0.002 | ... | 1 | 0 | 208 | >271 | | |
| 2014 Feb 14, 08 | Feb 14, 10 | -54 | ... | 147 | 0.003 | -05 | 0.0004 | ... | 1 | 0 | 360 | 1165 | | |
| 2014 Feb 15, 01 | Feb 15, 06 | -158 | ... | 43 | 0.002 | -109 | 0.002 | C2.1 | 1 | 0 | 138 | 362 | | |
| 2014 Feb 16, 09 | Feb 16, 11 | 158 | ... | -01 | 0.0003 | -153 | 0.002 | M1.1 | 1 | 0 | 360 | 634 | | |
| 2014 Feb 18, 01 | Feb 18, 03 | 114 | 0.001 | -45 | 0.004 | 163 | ... | ... | 1 | 2 | 360 | 779 | | |
| 2014 Feb 19, 04 | Feb 19, 05 | 5 | ... | -155 | BG | 53 | 0.002 | ... | 1 | 0 | 360 | 612 | | |
| 2014 Feb 20, 07 | Feb 20, 08 | -127 | ... | 73 | 0.3 | -79 | 0.002 | M3.0 | 1 | 1 | 360 | 948 | | |
| 2014 Feb 21, 01 | Feb 21, 04 | 125 | 0.002 | -35 | BG | 172 | ... | ... | 1 | 0 | 143 | 646 | | |
| 2014 Feb 21, 15 | Feb 21, 16 | 40 | 0.2 | -120 | 0.001 | 87 | 0.01 | ... | 1 | 0 | 360 | 1252 | | |
| 2014 Feb 25, 00 | Feb 25, 01 | 78 | 5 | -82 | 0.3 | 125 | 3 | X4.9 | 1 | 2 | 360 | 2147 | | |
| 2014 Mar 4, 18 | Mar 4, 18 | -31 | 0.005 | 168 | BG | 15 | 0.05 | ... | 1 | 1 | 360 | 794 | | |
| 2014 Mar 5, 13 | Mar 5, 13 | -16 | 0.01 | -177 | BG | 30 | 0.2 | ... | 1 | 2 | 360 | 828 | | |
| 2014 Mar 12, 14 | Mar 12, 14 | 04 | 0.06 | -158 | ... | 48 | 0.6 | ... | 1 | 0 | 360 | 972 | | |
| 2014 Mar 14, 00 | Mar 14, 00 | -64 | BG | 134 | 0.0005 | -20 | BG | ... | 1 | 0 | 155 | 331 | | |
| 2014 Mar 25, 05 | Mar 25, 05 | -127 | ... | 70 | 0.003 | -84 | ... | C1.4 | 0 | 2 | 223 | 651 | | |
| 2014 Mar 28, 23 | Mar 29, 01 | -174 | ... | 23 | 0.001 | -131 | 0.0006 | M2.6 | 1 | 1 | 138 | 514 | | |
| 2014 Mar 29, 17 | Mar 29, 19 | -165 | 0.001 | 32 | 0.03 | -122 | BG | X1.0 | 1 | 2 | 360 | 528 | | |
| 2014 Apr 2, 13 | Apr 2, 14 | 111 | 3 | -53 | 0.001 | 152 | 0.001 | M6.5 | 1 | 2 | 360 | 1471 | | |
| 2014 Apr 18, 12 | Apr 18, 14 | -164 | ... | 31 | 0.4 | -125 | ... | M7.3 | 1 | 2 | 360 | 1203 | | |
| 2014 Apr 25, 00 | Apr 25, 02 | -106 | ... | 89 | 0.001 | -67 | ... | X1.3 | 0 | 0 | 296 | 456 | | |
| 2014 May 6, 17 | May 6, 18 | -110 | ... | 85 | 0.0001 | -72 | ... | C4.7 | 1 | 0 | 201 | 815 | | |
| 2014 May 7, 16 | May 7, 18 | -104 | ... | 91 | 0.005 | -66 | 0.005 | M1.2 | 1 | 2 | 360 | 923 | | |
| 2014 May 9, 02 | May 9, 03 | -85 | ... | 110 | 0.003 | -48 | 0.0004 | ... | 1 | 2 | 360 | 1099 | | |
| 2014 May 15, 20 | May 15, 21 | 65 | 0.006 | -100 | ... | 102 | 0.02 | ... | 1 | 0 | 275 | 655 | | |
| 2014 May 29, 08 | May 29, 10 | 60 | 0.0008 | -105 | ... | 96 | ... | B3.4 | 1 | 0 | 224 | 398 | | |
| 2014 Jun 6, 13 | Jun 6, 14 | 123D? | 0.005 | -41D? | ... | 159D? | 0.009 | ... | 1 | 0 | 360 | 1200 | | |
| 2014 Jun 7, 16 | Jun 7, 17 | 40 | 0.002 | -124 | ... | 76 | 0.002 | ... | 1 | 0 | 155 | 675 | | |
| 2014 Jun 10, 12 | Jun 10, 12 | 84 | 0.15 | -80 | ... | 120 | 0.03 | X2.2 | 1 | 2 | 360 | 1469 | | |
| 2014 Jun 12, 21 | Jun 12, 23 | -141 | ... | 55 | 0.004 | -105 | ... | BG | 1 | 1 | 58 | 970 | | |
| 2014 Jun 17, 08 | Jun 17, 14 | -75 | ... | 121 | 0.0005 | -40 | ... | C3.0 | 1 | 0 | 360 | 1198 | | |
| 2014 Jun 24, 04 | Jun 24, 08 | -75 | ... | -179 | ... | 20 | 0.001 | ... | 1 | 0 | 177 | 633 | | |
| 2014 Jun 29, 12 | Jun 29, 15 | 20 | 0.0003 | -143 | ... | 55 | 0.001 | ... | 1 | 0 | 173 | 546 | | |

Table 7. ~ 25 MeV Proton Events at 1 AU During the STEREO Mission

| Solar Event (UT) | SEP Event (UT) | Solar Event-B ($^{\circ}$) | 25 MeV I(B) | Solar Event-Earth ($^{\circ}$) | 25 MeV I(Earth) | Solar Event-A ($^{\circ}$) | 25 MeV I(A) | 25 MeV GOES X-Ray | Type III | Type II | Type dA | CME V km/s |
|-------------------------------|----------------|------------------------------|-------------|----------------------------------|-----------------|------------------------------|-------------|-------------------|----------|---------|---------|------------|
| 2014 Jul 8, 16 | Jul 8, 17 | 107 | 0.02 | -56 | 0.0005 | 141 | DG | M6.5 | 1 | 0 | 360 | 773 |
| 2014 Jul 10, 07 | Jul 10, 08 | -81 | BG | 116D | 0.001 | -47 | DG | ... | 1 | 0 | 275 | 928 |
| 2014 Aug 8, 16 | Aug 8, 18 | -44 | 0.001 | 155 | ... | -10 | 0.001 | B7.0 | 0 | 0 | 360 | 1137 |
| 2014 Aug 12, 20 | Aug 13, 03 | 30 | 0.001 | -132 | ... | 63 | 0.0008 | C2.2 | 1 | 1 | 187 | 599 |
| 2014 Aug 22, 10 | Aug 22, 12 | 160 | ... | -01 | 0.0001 | -167 | DG | M5.9 | 1 | 0 | 360 | 600 |
| 2014 Aug 24, 12 | Aug 24, 14 | 86 | 0.001 | -75 | ... | 119 | DG | M2.0 | 1 | 1 | 360 | 551 |
| 2014 Aug 25, 14 | Aug 25, 17 | -160 | ... | 39 | 0.01 | -127 | DG | ... | 1 | 2 | 360 | 555 |
| 2014 Aug 28, 17 | Aug 28, 17 | -5 | 0.05 | -166 | 0.0007 | 28 | >0.6 | ... | 1 | 2 | 360 | 766 |
| 2014 Sep 1, 10 | Sep 1, 11 | 33 | 60 | -128 | 0.02 | 65 | >20 | ... | 1 | 2 | 360 | 1901 |
| 2014 Sep 10, 17 | Sep 10, 21 | 159 | 0.003 | -02 | 0.4 | -169 | BG | X1.6 | 1 | 2 | 360 | 1267 |
| 2014 Sep 22, 06 | Sep 22, 07 | -50 | ... | 149 | 0.03 | -19 | 0.005 | ... | 1 | 1 | 252 | 618 |
| 2014 Sep 24, 20 | Sep 24, 22 | -20 | 1.0 | 179 | 0.003 | 11 | >6 | ... | 1 | 2 | 360 | 1350 |
| 2014 Oct 2, 04 | Oct 2, 06 | ... | DG | -93D | 0.0005 | 98 | 0.005 | ... | 1 | 0 | 186 | 875 |
| 2014 Oct 10, 16 | Oct 10, 18 | ... | DG | 51 | 0.001 | -118 | ... | C3.0 | 1 | 0 | >210 | 782 |
| 2014 Oct 13, 00 | Oct 13, 05 | ... | DG | 96 | 0.0002 | -73 | ... | ... | 0 | 0 | 125 | 521 |
| 2014 Oct 14 ^b , 18 | Oct 14, 21 | ... | DG | -88 | 0.002 | 103 | ... | M1.1 | 1 | 0 | 360 | 848 |
| 2014 Nov 1, 04 | Nov 1, 08 | ... | DG | -50 | 0.02 | 140 | ... | C2.7 | ... | ... | 159 | 1628 |
| 2014 Nov 1, 18 | Nov 1, 19 | ... | DG | -161D | BG | 29 | 0.06 | ... | 1 | ... | 216 | 659 |
| 2014 Nov 2, 10 | Nov 2, 10 | ... | DG | -110D | BG | 80 | 0.008 | ... | ... | ... | >168 | 461 |
| 2014 Nov 7, 17 | Nov 8, 00 | ... | DG | -40 | 0.0007 | 150 | ... | X1.6 | 1 | 0 | 233 | 795 |
| 2014 Nov 11, 04 | Nov 11, 05 | ... | DG | -95D | ... | 95 | 0.02 | ... | 1 | 0 | 266 | 792 |
| 2014 Nov 25, 11 | Nov 25, 15 | ... | DG | <-90 | ... | 0.001 | 0.001 | ... | ... | ... | 194 | 454 |
| 2014 Dec 5, 06 | Dec 5, 06 | ... | DG | 69 | 0.0007 | -102 | ... | C1.8 | 1 | 0 | 172 | 534 |
| 2014 Dec 13, 14 | Dec 13, 15 | ... | DG | 142 | 0.01 | -30 | ... | ... | 1 | 1 | 360 | 2222 |
| 2015 Feb 8, 22 | Feb 8, 22 | ... | DG | <-90 | ... | 0.001 | 0.004 | M2.4 | 1 | ... | 132 | 315 |
| 2015 Feb 9, 23 | Feb 10, 01 | ... | DG | -68 | ... | 118 | 0.004 | ... | 1 | 2 | 360 | 1106 |
| 2015 Feb 21, 09 | Feb 21, 11 | ... | DG | 135D | 0.01 | -39 | 0.01(ESP) | ... | 1 | 2 | 360 | 1120 |
| 2015 Feb 28, 21 | Feb 28, <24 | ... | DG | -162D | ... | 23 | 0.004 | ... | 1 | ... | 360 | 999 |
| 2015 Mar 3, 15 | Mar 3, 16 | ... | DG | -128D | ... | 57 | 0.04 | ... | 1 | ... | 268 | 732 |
| 2015 Mar 6, 07 | Mar 6, 08 | ... | DG | -87 | ... | 98 | 1.0 | ML5 | 0 | 2 | 275 | 880 |
| 2015 Mar 15, 02 | Mar 15, 02 | ... | DG | 25 | 0.02 | -151 | ... | C9.1 | 1 | 2 | 360 | 719 |
| 2015 Mar 24, 08 | Mar 24, 10 | ... | DG | 100D | 0.006 | ... | DG | ... | 1 | 2 | 360 | 1794 |
| 2015 Apr 12, 23 | Apr 13, 00 | ... | DG | 60 | 0.0006 | ... | DG | C6.4 | 1 | 0 | 175 | 678 |
| 2015 Apr 14, 02 | Apr 14, 04 | ... | DG | -150D | 0.001 | ... | DG | ... | 1 | 0 | 360 | 1198 |
| 2015 Apr 21, 10 | Apr 21, 19 | ... | DG | -80 | 0.006 | ... | DG | M2.2 | 1 | 0 | 191 | 2039 |
| 2015 Apr 23, 09 | Apr 23, 12 | ... | DG | 80 | 0.003 | ... | DG | M1.1 | 1 | 0 | 360 | 857 |
| 2015 Apr 26, 03 | Apr 26, 03 | ... | DG | 165D | 0.002 | ... | DG | ... | 1 | 1 | 360 | 820 |
| 2015 May 5, 22 | May 6, 04 | ... | DG | -79 | 0.0004 | ... | DG | X2.7 | 1 | 2 | 360 | 715 |
| 2015 May 12, 02 | May 12, 03 | ... | DG | 83 | 0.06 | ... | DG | C2.6 | 1 | 1 | 250 | 772 |
| 2015 Jun 14, 03 | Jun 14, 06 | ... | DG | 48 | 0.0002 | ... | DG | C5.9 | 1 | 1 | 195 | 1228 |
| 2015 Jun 18, 00 | Jun 18, 02 | ... | DG | 81 | 0.17 | ... | DG | ML2 | 1 | 0 | 195 | 1714 |
| 2015 Jun 21, 02 | Jun 21, 02 | ... | DG | -13 | 0.1 | ... | DG | M2.6 | 1 | 2 | 360 | 1366 |
| 2015 Jun 25, 08 | Jun 25, 09 | ... | DG | 40 | 0.13 | ... | DG | M7.9 | 1 | 2 | 360 | 1627 |

Table 8. ~25 MeV Proton Events at 1 AU During the STEREO Mission

| Solar Event (UT) | SEP Event (UT) | Solar Event-B (°) | 25 MeV I(B) | Solar Event-Earth (°) | 25 MeV I(Earth) | Solar Event-A (°) | 25 MeV I(A) | GOES X-Ray | Type III | Type II | CME dA (°) | CME V km/s |
|------------------|----------------|-------------------|-------------|-----------------------|-----------------|-------------------|-------------|------------|----------|---------|------------|-------------|
| 2015 Jul 1, 14 | Jul 1, 15 | ... | DG | 133D | 0.03 | ... | DG | ... | 1 | 2 | 360 | 1435 |
| 2015 Jul 19, 09 | Jul 19, 11 | ... | DG | 62 | 0.005 | -123 | ... | C2.1 | 1 | 0 | 194 | 782 |
| 2015 Aug 16, 08 | Aug 16, 09 | ... | DG | -133 | ... | 40 | 0.005 | ... | 1 | 0 | 114 | 544 |
| 2015 Sep 20, 17 | Sep 20, 18 | ... | DG | 50 | 0.02 | ... | DG | M2.1 | 1 | 2 | 360 | 1239 |
| 2015 Sep 30, 10? | Sep 30, 17 | ... | DG | 59? | 0.001 | ... | DG | M1.3? | 0 | 0 | ? | ? (2+ CMEs) |
| 2015 Oct 12, 16 | Oct 12, 17 | ... | DG | -149 | ... | 20 | 0.002 | ... | 1 | 0 | 83 | 365 |
| 2015 Oct 22, 02 | Oct 22, 05 | ... | DG | -34 | 0.005 | ... | DG | C4.4 | 1 | 0 | 360 | 817 |
| 2015 Oct 25, 04 | Oct 25, <07 | ... | DG | -139 | ... | 30 | 0.006 | ... | 1 | 0 | 77 | 326 |
| 2015 Oct 29, 02 | Oct 29, 02 | ... | DG | 95 | 0.2 | -97 | ... | ... | 1 | 0 | 202 | 530 |
| 2015 Oct 30, 16 | Oct 31, <2 | ... | DG | -54 | BG | 114 | 0.003 | C5.2 | 1 | .. | 131 | 609 |
| 2015 Nov 4, 13 | Nov 4, 14 | ... | DG | 02 | 0.002 | 170 | ... | M3.7 | 1 | 2 | 360 | 578 |
| 2015 Nov 9, 12 | Nov 9, 14 | ... | DG | -39 | 0.04 | 129 | 0.006 | M3.9 | 1 | 1 | 273 | 1041 |
| 2015 Dec 7, 14 | Dec 7, 15 | ... | DG | -117 | ... | 50 | 0.03 | B3.4 | 1 | 0 | >176 | 707 |
| 2015 Dec 19, 12 | Dec 19, 16 | ... | DG | -106 | ... | 60 | 0.002 | C1.7 | 1 | 0 | 158 | 797 |
| 2015 Dec 21, 00 | Dec 21, 01 | ... | DG | -81 | ... | 85 | 0.001 | M2.8 | 1 | 0 | 71 | 389 |
| 2015 Dec 28, 11 | Dec 28, 12 | ... | DG | 11 | 0.01 | 177 | ... | M1.9 | 1 | 2 | 360 | 1212 |
| 2016 Jan 1, 23 | Jan 1, 23 | ... | DG | 82 | 0.1 | -112 | ... | M2.3 | 1 | 2 | 360 | 1730 |
| 2016 Jan 6, 14 | Jan 7, ~12 | ... | DG | 138 | ... | -56 | 0.006 | ... | 1 | 0 | 360 | 969 |
| 2016 Feb 11, 21 | Feb 12, 00 | ... | DG | 11 | 0.004 | 175 | ... | C8.9 | 1 | 0 | 360 | 719 |
| 2016 Feb 15, 14 | Feb 15, 16 | ... | DG | -144? | ... | 0.001 | ... | ... | 1 | 0 | 90 | 383 |
| 2016 Mar 16, 06 | Mar 16, 07 | ... | DG | 88 | 0.008 | -109 | ... | C2.2 | 1 | 0 | 154 | 592 |
| 2016 Apr 18, 00 | Apr 18, 01 | ... | DG | 62 | 0.003 | -137 | ... | M6.7 | 1 | 0 | 162 | 1084 |
| 2016 May 2, 08 | May 2, 15 | ... | DG | -33 | 0.003 | 126 | ... | C3.5 | 1 | 0 | 61 | 262 |
| 2016 May 15, 15 | May 15, 16 | ... | DG | 50 | 0.003 | -152 | ... | C3.2 | 1 | 0 | 176 | 1118 |
| 2016 Jul 23, 05 | Jul 23, 05 | ... | DG | 73 | 0.001 | -134 | ... | M7.6 | 1 | 0 | 117 | 835 |
| 2016 Sep 14, 23 | Sep 15, 01 | ... | DG | -122? | ... | 27 | 0.004 | ... | 1 | 0 | >156 | 742 |
| 2016 Oct 25, 18 | Oct 25, 21 | ... | DG | -147 | ... | 0 | 0.0003 | ... | 1 | 0 | 162 | 470 |
| 2017 Jan 12, 16 | Jan 12, 18 | ... | DG | -85 | ... | 59 | 0.001 | C3.8 | 1 | 0 | 98 | 493 |
| 2017 Apr 1, 21 | Apr 1, 22 | ... | DG | 54 | 0.002 | -165 | ... | M4.4 | 1 | 0 | 115 | 516 |
| 2017 Apr 18, 19 | Apr 18, 20 | ... | DG | -84 | 0.0007 | 55 | 0.2 | C5.5 | 1 | 0 | 360 | 926 |
| 2017 Jul 14, 01 | Jul 14, 02 | ... | DG | 29 | 0.1 | 162 | ... | M2.4 | 1 | 2 | 360 | 1200 |
| 2017 Jul 23, 04 | Jul 23, 07 | ... | DG | 148 | 0.01 | -80 | 10 | ... | 1 | 2 | 360 | 1848 |
| 2017 Sep 2, 15 | Sep 2, 16 | ... | DG | 90 | 0.001 | -141 | ... | C7.7 | 1 | 0 | 94 | 705 |
| 2017 Sep 4, 20 | Sep 4, 21 | ... | DG | 11 | 0.3 | 140 | 0.001 | M5.5 | 1 | 2 | 360 | 1418 |
| 2017 Sep 6, 12 | Sep 6, 13 | ... | DG | 34 | 0.2 | 162 | ... | X9.3 | 1 | 2 | 360 | 1571 |
| 2017 Sep 10, 15 | Sep 10, 16 | ... | DG | 88 | 10 | -144 | 1 | X8.2 | 1 | 2 | 360 | 3163 |
| 2017 Sep 17, 11 | Sep 17, 13 | ... | DG | -169 | BG | -41 | 0.3 | ... | 1 | 2 | 360 | 1385 |
| 2017 Oct 11, 14 | Oct 11, 15 | ... | DG | 139D | 0.0004 | -95D | ... | ... | 1 | 0 | 109 | 741 |
| 2017 Oct 18, 05 | Oct 18, 06 | ... | DG | -126 | 0.005 | 0 | 0.01 | B9.5 | 1 | 2 | 360 | 1576 |
| 2018 Jan 22, 03 | Jan 22, 04 | ... | DG | 58 | 0.002 | 179 | ... | ... | 1 | 0 | 116 | 462 |
| 2018 Feb 12, 01 | Feb 12, 04 | ... | DG | 14 | 0.0007 | 135 | ... | C1.5 | 1 | 0 | 360 | 661 |
| 2018 May 3, 16 | May 3, 19 | ... | DG | -136 | ... | -20 | 0.0004 | ... | 1 | 0 | 302 | 533 |

Table 9. ~ 25 MeV Proton Events at 1 AU During the STEREO Mission

| Solar Event (UT) | SEP Event (UT) | Solar Event-B ($^{\circ}$) | 25 MeV I(B) | Solar Event-Earth ($^{\circ}$) | 25 MeV I(Earth) | Solar Event-A ($^{\circ}$) | 25 MeV I(A) | GOES X-Ray | Type III | Type II | Type I | CME dA | CME V km/s |
|------------------|----------------|------------------------------|-------------|----------------------------------|-----------------|------------------------------|-------------|-------------|----------|---------|--------|--------|------------|
| 2019 Apr 21, 04 | Apr 21, 05 | ... | DG | 117D | 0.0004 | -147D | ... | C1.0 | 1 | 0 | 93 | 463 | |
| 2019 May 3, 23 | May 4, 01 | ... | DG | -88 | 0.0004 | 7 | 0.001 | C1.5 | 1 | 1 | 113 | 692 | |
| 2020 Oct 16, 12 | Oct 16, 13 | ... | DG | 86 | 0.0004 | 146 | ... | ... | 0 | 0 | 55 | 271 | |
| 2020 Nov 29, 12 | Nov 29, 13 | ... | DG | -98 | 0.15 | -40 | 0.2 | M4.4 | 1 | 2 | 360 | 2077 | |
| 2020 Dec 7, 15 | Dec 7, 16 | ... | DG | 8 | 0.01 | 66 | 0.1 | C7.4 | 1 | 2 | 360 | 1407 | |
| 2021 Apr 17, 16 | Apr 17, 20 | ... | DG | -111 | 0.0003 | -58 | 0.0005 | C5.0S | 1 | 1 | 146 | 763 | |
| 2021 May 18, 18 | May 17, 23 | ... | DG | -78 | ... | -26 | 0.004 | M3.9 | 1 | 1 | 114 | 754 | |
| 2021 May 28, 22 | May 28, 23 | ... | DG | 63 | 0.6 | 114 | 0.01 | C9.4 | 1 | 2 | 197 | 971 | |
| 2021 Jun 9, 12 | Jun 9, 12 | ... | DG | 105D | 0.008 | 155D | 0.008 | C1.7 | 1 | 0 | 65 | 441 | |
| 2021 Jun 25, 13 | Jun 25, 14 | ... | DG | 89 | 0.0001 | 137 | ... | C1.7 | 1 | 0 | 90 | 433 | |
| 2021 Jul 3, 07 | Jul 3, 07 | ... | DG | 78 | 0.0002 | 125 | ... | M2.7 | 1 | 1 | 0 | 67 | |
| 2021 Jul 3, 14 | Jul 3, 14 | ... | DG | 81 | 0.01 | 128 | ... | X1.5 | 1 | 0 | 69 | 455 | |
| 2021 Jul 5, 16 | Jul 5, 17 | ... | DG | 110 | 0.0002 | 157 | ... | B5.3 | 1 | 0 | 83 | 545 | |
| 2021 Jul 9, 17 | Jul 9, 17 | ... | DG | 98 | 0.005 | 145 | ... | C4.7 | 1 | 0 | 668 | ... | |
| 2021 Jul 13, 19 | Jul 13, 22 | ... | DG | 170 | 0.005 | -144 | ... | M2.8S | 1 | 1 | 110 | 1101 | |
| 2021 Jul 15, 21 | Jul 16, 00 | ... | DG | -168 | 0.005 | -122 | 0.0005 | M4.6S | 1 | 1 | 360 | 1476 | |
| 2021 Jul 17, 05 | Jul 17, 11 | ... | DG | -139 | BG | -93 | 0.002 | M2.8S | 1 | 1 | 360 | 1228 | |
| 2021 Sep 17, 04 | Sep 17, 15 | ... | DG | -85 | 0.0015 | -45 | 0.005 | \geq C3.5 | 1 | 0 | 264 | 1349 | |
| 2021 Sep 28, 06 | Sep 28, 06 | ... | DG | 36 | 0.002 | 75 | 0.003 | C1.6 | 1 | 1 | 265 | 524 | |
| 2021 Oct 09, 06 | Oct 09, 06 | ... | DG | -9 | 0.015 | 30 | 0.05 | M1.6 | 1 | 1 | 360 | 712 | |
| 2021 Oct 28, 15 | Oct 28, 15 | ... | DG | 5 | 0.5 | 42 | 10 | X1.0 | 1 | 2 | 360 | 1519 | |
| 2021 Nov 01, 01 | Nov 01, 02 | ... | DG | 45 | 0.04 | 82 | 0.3 | M1.5 | 1 | 1 | 274 | 753 | |
| 2021 Nov 02, 01 | Nov 02, 04 | ... | DG | -1 | 0.01 | 36 | 0.06 | M1.7 | 1 | 2 | 360 | 1473 | |
| 2021 Nov 09, 16 | Nov 09, 17 | ... | DG | 100 | 0.015 | 137 | 0.001 | M2.0 | 1 | 1 | 176 | 1350 | |
| 2021 Dec 05, 07 | Dec 05, 07 | ... | DG | 105 | 0.001 | 141 | ... | M1.4 | 1 | 0 | 110 | 628 | |
| 2022 Jan 18, 17 | Jan 18, 17 | ... | DG | 54 | 0.0009 | 89 | 0.0005 | M1.5 | 1 | 1 | 153 | 1014 | |
| 2022 Jan 20, 05 | Jan 20, 06 | ... | DG | 68 | 0.4 | 103 | 0.08 | M5.5 | 1 | 1 | 211 | 1431 | |
| 2022 Jan 29, 23 | Jan 30, 00 | ... | DG | -6 | 0.0001 | 29 | 0.0005 | M1.1 | 1 | 1 | 360 | 530 | |
| 2022 Jan 31, 23 | Feb 01, 00 | ... | DG | 92D | 0.001 | 127D | ... | ... | 1 | 0 | 52 | 469 | |
| 2022 Feb 02, 01 | Feb 02, 07 | ... | DG | 99D | 0.0002 | 134D | ... | ... | 1 | 0 | 43 | 467 | |
| 2022 Feb 15, 21 | Feb 15, 23 | ... | DG | -158D | 0.008 | -124D | 0.004 | ... | 1 | 2 | 360 | 1905 | |
| 2022 Mar 10, 18 | Mar 10, 21 | ... | DG | 12 | 0.006 | 46 | 0.003 | C2.8 | 1 | 0 | 360 | 742 | |
| 2022 Mar 14, 17 | Mar 14, 18 | ... | DG | 109D | 0.02 | 143D | 0.01 | M1.4S | 1 | 0 | 225 | 740 | |
| 2022 Mar 19, 06 | Mar 19, 12 | ... | DG | 100D | 0.001 | 133D | ... | ... | 1 | 0 | 82 | 329 | |
| 2022 Mar 21, 06 | Mar 21, 06 | ... | DG | 134 | 0.05 | 167 | 0.005 | C1.4S | 1 | 0 | 360 | 916 | |
| 2022 Mar 28, 10 | Mar 28, 11 | ... | DG | 4 | 0.2 | 37 | 2.0 | M4.0 | 1 | 0 | 360 | 702 | |
| 2022 Mar 30, 17 | Mar 30, 17 | ... | DG | 31 | 0.2 | 64 | 2.0 | X1.3 | 1 | 0 | 360 | 641 | |
| 2022 Mar 31, 19 | Mar 31, 20 | ... | DG | 47 | 0.02 | 80 | 0.01 | M9.6 | 1 | 1 | 360 | 489 | |
| 2022 Apr 02, 13 | Apr 02, 14 | ... | DG | 68 | 0.6 | 101 | 0.06 | M3.9 | 1 | 2 | 360 | 1433 | |
| 2022 Apr 11, 05 | Apr 11, 05 | ... | DG | -6 | 0.0008 | 26 | 0.002 | \geq C1.6 | 1 | 1 | 360 | 940 | |
| 2022 Apr 20, 03 | Apr 20, 04 | ... | DG | 86 | 0.001 | 118 | ... | X2.2 | 1 | 0 | 139 | 1001 | |
| 2022 Apr 29, 07 | Apr 29, 07 | ... | DG | 39 | 0.004 | 70 | ... | M1.2 | 1 | 2 | 245 | 1292 | |
| 2022 Apr 30, 13 | Apr 30, 14 | ... | DG | 95 | 0.002 | 126 | ... | X1.1 | 1 | 1 | 187 | 498 | |

Table 10. ~ 25 MeV Proton Events at 1 AU During the STEREO Mission

| Solar Event (UT) | SEP Event (UT) | Solar Event-B (°) | 25 MeV I(B) | Solar Event-Earth (°) | 25 MeV I(Earth) | Solar Event-A (°) | 25 MeV I(A) | GOES X-Ray | Type III | Type II | Type CME | dA (°) | CME V km/s |
|------------------|----------------|-------------------|-------------|-----------------------|-----------------|-------------------|-------------|------------|----------|---------|----------|--------|------------|
| 2022 May 11, 18 | May 11, 18 | ... | DG | 105 | 0.1 | 135 | 0.01 | M2.7 | 1 | 1 | 194 | 1100 | |
| 2022 Jun 13, 02 | Jun 13, 06 | ... | DG | -45 | 0.003 | -17 | 0.01 | M3.4 | 1 | 1 | 360 | 1150 | |
| 2022 Jul 09, 13 | Jul 09, 13 | ... | DG | 88 | 0.2 | 113 | 0.009 | C8.4 | 1 | 1 | 148 | 1034 | |
| 2022 Aug 05, 06 | Aug 05, 09 | ... | DG | 47 | 0.0003 | 69 | ... | C4.9 | 1 | 0 | 90 | 756 | |
| 2022 Aug 18, 10 | Aug 18, 11 | ... | DG | 37 | 0.0008 | 58 | 0.0005 | M1.5 | 1 | 1 | 360 | 1327 | |
| 2022 Aug 26, 12 | Aug 26, 17 | ... | DG | 58 | 0.0005 | 78 | ... | M3.6 | 1 | 1 | 184 | 737 | |
| 2022 Aug 27, 02 | Aug 27, 03 | ... | DG | 58 | 0.2 | 78 | 0.002 | M4.8 | 1 | 2 | 360 | 1284 | |
| 2022 Aug 28, 16 | Aug 28, 21 | ... | DG | 85 | 0.002 | 105 | 0.0003 | M6.7 | 1 | 0 | 360 | 1232 | |
| 2022 Aug 30, 18 | Aug 31, 00 | ... | DG | 121D | 0.0004 | 141D | DG | X1.0S | 1 | 0 | 360 | 1247 | |
| 2022 Sep 05, 16 | Sep 06, 18 | ... | DG | -174 | 0.02 | -155 | 0.01 | M9.0S | 1 | 0 | 360 | 2776 | |
| 2022 Sep 24, 17 | Sep 24, 17 | ... | DG | -70 | 0.005 | -52 | 0.1 | C7.2 | 1 | 1 | 123 | 1063 | |
| 2022 Oct 01, 20 | Oct 01, 20 | ... | DG | 36 | 0.002 | 53 | 0.0005 | M5.8 | 1 | 0 | 69 | 1122 | |
| 2022 Oct 02, 02 | Oct 02, 02 | ... | DG | 39 | 0.003 | 56 | ... | M8.7 | 1 | 2 | 153 | 1222 | |
| 2022 Oct 02, 19 | Oct 02, 20 | ... | DG | 49 | 0.005 | 66 | 0.005 | X1.0 | 1 | 2 | 360 | 1086 | |
| 2022 Oct 04, 13 | Oct 04, 13 | ... | DG | 75 | 0.002 | 92 | ... | M1.6 | 1 | 1 | 67 | 1089 | |
| 2022 Oct 11, 08 | Oct 11, 08 | ... | DG | 35 | 0.0006 | 52 | 0.0003 | M3.9 | 1 | 0 | 88 | 252 | |
| 2022 Oct 12, 14 | Oct 12, 14 | ... | DG | 52 | 0.0002 | 69 | 0.0006 | C8.8 | 1 | 0 | 114 | 234 | |
| 2022 Nov 14, 02 | Nov 14, 03 | ... | DG | 35 | 0.0001 | 50 | ... | C3.3 | 1 | 0 | 74 | 321 | |
| 2022 Nov 19, 12 | Nov 19, 15 | ... | DG | 50 | 0.0001 | 65 | 0.0001 | M1.6 | 1 | 0 | 165 | 422 | |
| 2022 Dec 19, 22 | Dec 20, 03 | ... | DG | 55 | 0.0008 | 109 | 0.002 | C3.8 | 1 | 0 | 97 | 370 | |
| 2023 Jan 03, 06 | Jan 04, 06 | ... | DG | -131D | 0.0004 | -117D | 0.0006 | ... | 1 | 1 | 360 | 1129 | |
| 2023 Jan 08, 19 | Jan 08, 20 | ... | DG | -102D | BG | -88D | 0.005 | M1.0 | 1 | 0 | 106 | 705 | |
| 2023 Jan 09, 21 | Jan 09, 22 | ... | DG | -81? | 0.001 | -67? | BG | C2.6? | 1 | 0 | 43? | 586? | |
| 2023 Jan 12, 22 | Jan 12, 23 | ... | DG | 122D | 0.06 | 136D | 0.003 | ... | 1 | 1 | 198 | 1075 | |
| 2023 Jan 19, 19 | Jan 19, 20 | ... | DG | 94D | 0.0005 | 108D | ... | ... | 1 | 1 | 81 | 1073 | |
| 2023 Feb 01, 07 | Feb 01, 12 | ... | DG | 133D | 0.0005 | 146D | ... | ... | 1 | 0 | 360 | 1042 | |
| 2023 Feb 11, 11 | Feb 11, 15 | ... | DG | -18 | 0.0003 | -5 | 0.0002 | M1.0 | 1 | 2 | 360 | 1498 | |
| 2023 Feb 12, 16 | Feb 12, 19 | ... | DG | 144D | 0.0005 | 157D | ... | ... | 1 | 0 | 35 | 559 | |
| 2023 Feb 16, 10 | Feb 16, 10 | ... | DG | 44 | 0.0003 | 57 | ... | C9.0 | 1 | 0 | 149 | 1549 | |
| 2023 Feb 17, 20 | Feb 17, 21 | ... | DG | -64 | 0.002 | -51 | 0.005 | X2.2 | 1 | 2 | 360 | 1315 | |
| 2023 Feb 24, 20 | Feb 24, 20 | ... | DG | 28 | 0.1 | 41 | 0.2 | M3.7 | 1 | 1 | 360 | 1336 | |
| 2023 Feb 25, 19 | Feb 25, 20 | ... | DG | 43 | 1 | 56 | 4 | M6.3 | 1 | 0 | 360 | 1170 | |
| 2023 Mar 03, 18 | Mar 03, 18 | ... | DG | 80 | 0.0003 | 93 | ... | X2.1 | 1 | 1 | 360 | 709 | |
| 2023 Mar 06, 03 | Mar 06, 03 | ... | DG | 65 | 0.0002 | 77 | ... | M5.8 | 1 | 0 | 360 | 873 | |
| 2023 Mar 09, 12 | Mar 09, 14 | ... | DG | 160D | 0.0009 | 172D | 0.0006 | ... | 1 | 0 | 360 | 1030 | |
| 2023 Mar 13, 03 | Mar 13, 04 | ... | DG | -160D | 0.4 | -148D | 0.05 | ... | 1 | 2 | 360 | 1699 | |
| 2023 Mar 30, 07 | Mar 30, 07 | ... | DG | 81 | 0.004 | 93 | 0.001 | M5.4 | 1 | 0 | 224 | 487 | |
| 2023 Mar 31, 14 | Mar 31, 15 | ... | DG | 85 | 0.0006 | 96 | ... | C1.6 | 1 | 0 | 221 | 755 | |
| 2023 Apr 21, 18 | Apr 21, 19 | ... | DG | 11 | 0.01 | 21 | 0.01 | M1.7 | 1 | 0 | 360 | 1284 | |
| 2023 May 06, 00 | May 06, 00 | ... | DG | 102D | 0.001 | 111D | ... | ... | 1 | 0 | 139 | 655 | |
| 2023 May 07, 22 | May 07, 22 | ... | DG | 6 | 0.05 | 15 | 0.2 | M1.5 | 1 | 1 | 360 | 1075 | |
| 2023 May 09, 18 | May 09, 19 | ... | DG | 31 | 0.6 | 40 | 0.6 | M4.2 | 1 | 1 | 360 | 1209 | |
| 2023 May 16, 17 | May 16, 17 | ... | DG | 141 | 0.01 | 149 | 0.008 | M5.0S | 1 | 0 | 360 | 1099 | |

Table 11. ~ 25 MeV Proton Events at 1 AU During the STEREO Mission

| Solar Event (UT) | SEP Event (UT) | Solar Event-B (°) | 25 MeV I(B) | Solar Event-Earth (°) | 25 MeV I(Earth) | Solar Event-A (°) | 25 MeV I(A) | GOES X-Ray | Type III | Type II | Type CME | CME dA (°) | CME V km/s |
|------------------|----------------|-------------------|-------------|-----------------------|-----------------|-------------------|-------------|------------|----------|---------|----------|------------|------------|
| 2023 Jun 01, 00 | Jun 01, 02 | DG | 80 | 0.0002 | 87 | 0.0002 | C9.2 | 1 | 0 | 165 | 1565 | | |
| 2023 Jun 20, 16 | Jun 21, 00 | DG | -73 | 0.0002 | -68 | 0.0006 | X1.1 | 1 | 1 | 360 | 1113 | | |
| 2023 Jun 28, 02 | Jun 28, 06 | DG | 89 | 0.0001 | 93 | ... | C3.3 | 1 | 0 | 77 | 207 | | |
| 2023 Jul 03, 21 | Jul 03, 21 | DG | -34 | 0.0001 | -30 | ... | C8.9 | 1 | 0 | 140 | 208 | | |
| 2023 Jul 10, 03 | Jul 10, 05 | DG | 49 | 0.002 | 52 | 0.003 | M2.3 | 1 | 2 | 360 | 1160 | | |
| 2023 Jul 10, 12 | Jul 10, 13 | DG | 95D | 0.01 | 98D | 0.01 | C2.5 | 0 | 0 | 360 | 945 | | |
| 2023 Jul 13, 06 | Jul 13, 09 | DG | -179 | 0.001 | -177 | 0.002 | X1.0S | 1 | 0 | 360 | 663 | | |
| 2023 Jul 15, 20 | Jul 15, 21 | DG | 48 | 0.02 | 50 | 0.04 | C8.8 | 1 | 1 | 360 | 1815 | | |
| 2023 Jul 17, 23 | Jul 18, 00 | DG | 73 | 1 | 75 | 2 | M5.7 | 1 | 2 | 360 | 1385 | | |
| 2023 Jul 24, 17 | Jul 24, 18 | DG | 158D | 0.04 | 160D | 0.03 | X1.5S | 1 | 0 | 360 | 1204 | | |
| 2023 Jul 28, 15 | Jul 28, 16 | DG | 99 | 1.2 | 101 | 1.2 | M4.1 | 1 | 1 | 360 | 1896 | | |
| 2023 Aug 05, 07 | Aug 05, 07 | DG | 63 | 0.4 | 64 | 0.3 | M1.6 | 1 | 1 | 360 | 1000 | | |
| 2023 Aug 05, 22 | Aug 05, 22 | DG | 77 | 0.1 | 78 | 0.2 | X1.6 | 1 | 2 | 360 | 1647 | | |
| 2023 Aug 07, 20 | Aug 07, 21 | DG | 88 | 0.6 | 89 | 0.6 | X1.5 | 1 | 1 | 360 | 1851 | | |
| 2023 Aug 17, 02 | Aug 17, 03 | DG | 86 | 0.001 | 86 | 0.004 | C3.6 | 1 | 0 | 239 | 623 | | |
| 2023 Aug 18, 19 | Aug 18, 19 | DG | 41 | 0.0003 | 41 | ... | C3.7 | 1 | 1 | 85 | 456 | | |
| 2023 Sep 01, 03 | Sep 01, 03 | DG | 73 | 0.4 | 71 | 1.0 | M1.2 | 1 | 0 | 360 | 1339 | | |
| 2023 Sep 05, 14 | Sep 05, 18 | DG | 126D | 0.005 | 124D | 0.005 | ... | 1 | 0 | 360 | 1539 | | |
| 2023 Sep 11, 22 | Sep 12, 14 | DG | -170D | 0.001 | -173D | ... | ... | 1 | 0 | 360 | 1060 | | |
| 2023 Sep 14, 07 | Sep 14, 08 | DG | 45 | 0.004 | 42 | 0.006 | M1.4 | 1 | 0 | 360 | 804 | | |
| 2023 Sep 17, 12 | Sep 17, 21 | DG | 90D | 0.004 | 87D | 0.004 | ... | 0 | 0 | 214 | 590 | | |
| 2023 Sep 22, 07? | Sep 22, 16 | DG | 02 | 0.0004 | -1 | ... | ? | 1 | 0 | 86 | 729 | | |
| 2023 Oct 03, 12 | Oct 04, 00 | DG | -130 | 0.0002 | -134 | ... | C3.0S | 1 | 0 | 256 | 509 | | |
| 2023 Oct 10, 10 | Oct 11, 12 | DG | -125D | 0.0001 | -130D | ... | C2.8 | 1 | 0 | 360 | 1102 | | |
| 2023 Oct 19, 01 | Oct 19, 09 | DG | 71 | 0.001 | 66 | 0.001 | C1.5 | 1 | 0 | 227 | 636 | | |
| 2023 Oct 26, 23 | Oct 27, 12 | DG | -90 | 0.0006 | -95 | 0.0006 | M1.4 | 1 | 1 | 360 | 1238 | | |
| 2023 Nov 02, 19 | Nov 02, 20 | DG | -85 | 0.0004 | -91 | ... | M1.0 | 1 | 0 | 62 | 626 | | |
| 2023 Nov 03, 05 | Nov 03, 06 | DG | 32 | 0.005 | 26 | 0.006 | C3.3 | 1 | 0 | 226 | 693 | | |
| 2023 Nov 09, 11 | Nov 09, 15 | DG | 04 | 0.05 | -2 | 0.03 | C2.6 | 1 | 0 | 360 | 573 | | |
| 2023 Nov 23, 06? | Nov 24, 00 | DG | -90D? | 0.0001 | -96D? | ... | ? | 1 | 0 | 134? | 990? | | |
| 2023 Dec 14, 17 | Dec 14, 17 | DG | 53 | 0.08 | 46 | 0.08 | X2.8 | 1 | 2 | 360 | 948 | | |
| 2023 Dec 22, 04 | Dec 22, 08 | DG | 71 | 0.0003 | 64 | ... | C7.8 | 1 | 0 | 27 | 570 | | |
| 2023 Dec 24, 20 | Dec 25, 03 | DG | -115D | 0.001 | -122D | 0.002 | M1.1 | 1 | 0 | 141 | 384 | | |
| 2023 Dec 31, 09 | Dec 31, 15 | DG | 61D | 0.0004 | 54D | 0.0005 | ... | 0 | 0 | 146 | 729 | | |
| 2023 Dec 31, 22 | Dec 31, 22 | DG | -79 | 0.04 | -86 | 0.02 | X5.0 | 1 | 2 | 360 | 2852 | | |

B. A \sim 25 MeV SEP Event During Solar Minimum (May 3, 2018)

Figure 24 shows an example of a rare SEP event during the minimum between Solar Cycles 24 and 25 (see Figure 1) that nevertheless reached at least 25 MeV in protons. This event was observed on May 3, 2018 from \sim 19 UT and only detected at STEREO A - the top right panel of Figure 24 shows the HET-A proton intensity-time profiles at 13–21 and 21–40 MeV; individual instrument channels (not shown) suggest a maximum energy around 30 MeV. This was a short (\sim 1 day duration) event with a rapid rise and slower decay associated with a solar eruption at \sim E20° relative to STEREO A, based on observations by the Extreme Ultraviolet Imager (EUVI) on board STEREO-A (EUVI-A, Wuelser et al. 2004), corresponding to \sim E136° relative to Earth. The related flaring and erupting filament observed by EUVI-A at 17:46 UT at a wavelength of 304 Å are shown in the top left panel of Figure 24. The bottom panel shows the spacecraft configuration and location of this flaring (black arrow). This small “impulsive-like” SEP event from a source that was not well-connected to STEREO A was associated with a CME evident (Figure 25) in the STEREO-A COR2 (Howard et al. 2008) and EUVI-A 195 Å observations in the left panel (also showing the dimming associated with the eruption). The CME is also evident in observations from the SOHO/LASCO C2 coronagraph (right panel). Based on the LASCO observations, this CME is classified as a “partial halo” CME in the CDAW CME catalog with a width of 302° and speed of 533 km/s, though with a deceleration of 22.1 m s^{-2} in the C2 field of view suggesting that the speed was higher close to the Sun. The automated CACTus COR2 CME catalog gives a plane of the sky width of 102° and speed of 581 km/s. The DONKI database gives a CME speed of 650 km/s in a direction E155°, about 20° from, but not inconsistent with, the flare longitude. Type III radio emission (not shown) was detected at STEREO A but only weakly at Wind, consistent with the far side location relative to Earth. No type II emission is reported at either spacecraft (e.g., https://cdaw.gsfc.nasa.gov/CME_list/radio/waves_type2.html). Although the \sim 77° separation between the STEREO A nominal field line footpoint and the solar event does approach the 80° criterion used by Dresing et al. (2014) to define a “widespread” SEP event, the spacecraft configuration is not suitable to determine if this SEP event was actually detectable over a wide region of the heliosphere. However, we doubt that this was the case because of the low intensity and short duration of the event at STEREO A and also because, even though this spacecraft was close to the longitude of the solar event, no shock or ICME was detected in situ during the days following the solar event (<https://stereo-ssc.nascom.nasa.gov/data/insdata/impact/level3/STEREOLevel3Shock.pdf>; the associated “shock arrival” at 10:00 UT on May 7 reported in DONKI is clearly the forward shock of a CIR), and there is no evidence of any extended enhancement of shock-associated particles that might have been expected had this been a widespread event. Nevertheless, this event clearly illustrates that even a poorly-connected spacecraft can detect a such a small SEP event extending to tens of MeV arriving promptly after a modest solar eruption.

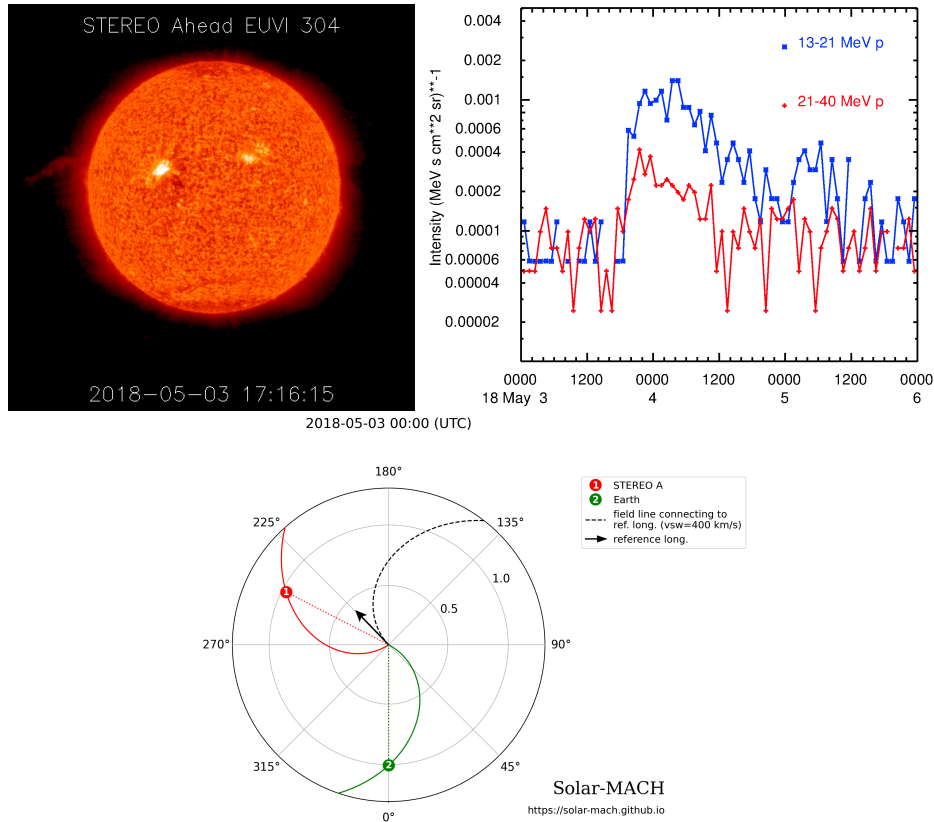


Figure 24. One hour averages (top right) of the proton intensity in two energy ranges for a small SEP event on May 3, 2018 detected by the STEREO A HET associated with flaring at $\sim 220^\circ$ relative to STEREO A ($\sim 136^\circ$ relative to Earth) and a filament eruption visible above the east limb observed by EUVI on STEREO A (top left). The bottom panel shows the spacecraft configuration and longitude of the flaring observed by STEREO A (black arrow). Interplanetary field lines assume a solar wind speed of 400 km/s.

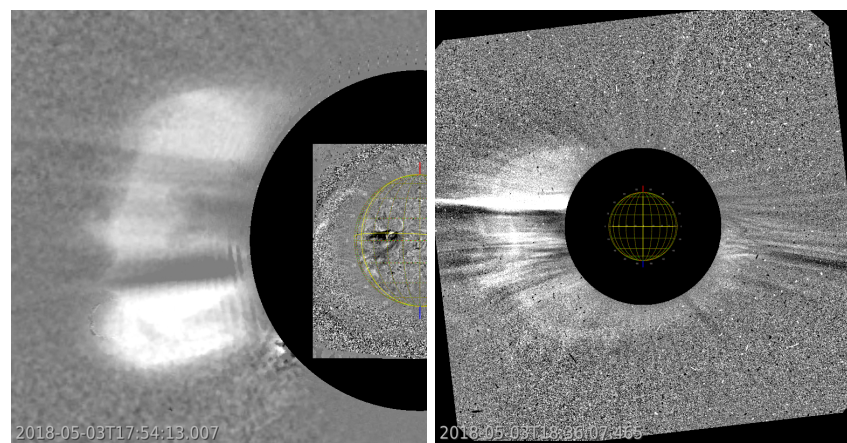


Figure 25. The CME associated with the SEP event on May 3, 2018 in Figure 24 observed by (left) STEREO A EUVI 195 Å at 16:48 UT in the low corona, also showing the dimming associated with the eastern eruption, and by STEREO A COR2 at 17:54 UT, and (right) by LASCO C2 at 18:36 UT. All images are base differences from pre-event images.

C. Several Problematic Events

While the likely associated solar event can be identified for nearly every SEP event, there are a few cases that are more challenging for various reasons. Three are discussed in this appendix.

C.1. September 30, 2015

As indicated in Table 8 of Appendix A, the origin of the SEP event on September 30, 2015 (Figure 26) is not completely clear. One complicating factor is the absence of data from STEREO A, then located on the far side of the Sun at 176° east of Earth (also, contact had been previously lost with STEREO B). This was a modest SEP event at Earth with a fairly prompt electron and proton onset at ~ 17 UT evident in the SOHO/EPHIN data (top left panel of Figure 26). However, no CME is reported at this time in the CDAW catalog (there were no LASCO data gaps on this day). The closest reported CMEs preceding the SEP onset were at 09:36 UT, going to the southwest with a plane of the sky speed of 586 km/s, and a partial halo CME at 10:00 UT going to the northwest with a speed of 602 km/s that overlap in the LASCO image in the top right panel of Figure 26. The DONKI database also identifies these two CMEs, with estimated longitudes relative to Earth of $W49^\circ$ and $W116^\circ$ (just over the west limb), respectively. Neither of these CMEs was associated with a GOES flare - the ongoing soft X-ray level was around C2. These CMEs were associated with the lift-off of a large filament above the west limb seen as a large erupting prominence in SDO AIA 304 Å observations (Figure 27). An M1.3 flare at $S20^\circ W50^\circ$ commencing at 10:49 UT was too late to be associated with these CMEs. There was also a brief M1.1 flare commencing at 13:18 UT located at $S20^\circ W55^\circ$. Examination of the CDAW LASCO running-difference movie suggests that this flare was associated with a further CME that is not recorded in the CDAW or DONKI catalogs but is indicated by an arrow in the LASCO C2 running difference image (at 14:00 UT) in the left-hand figure in the second row of Figure 26, superposed on the complex trailing regions of the previous CMEs. This CME is also evident in the C2 base difference image (14:36 UT minus the pre-event background) in the right-hand figure. The CME leading edge speed, based on a linear fit, is estimated to be 572 ± 8 km/s. There is no clear evidence of any additional CME around the time of the SEP onset.

Wind/WAVES (third row of Figure 26) observed brief type III emissions throughout the day. Some brighter emissions, generally weak at high frequencies (and therefore possibly occulted by the solar limb or indicating a lack of particle acceleration close to the Sun), commenced between ~ 5 and 11 UT, around the time of the two prominent CMEs and the filament liftoff. However, unusually, there were no radio emissions around the onset of the SEP event at ~ 17 UT. The most notable feature around SEP onset is the slow lift-off of a smaller filament above the southwest limb evident in the SDO observations in the bottom panel of Figure 26. Thus, although there were clearly eruptive structures on the western hemisphere of the Sun on September 30, 2015 that might have given rise to the SEP event, the SEP onset does not appear to be unambiguously associated with a specific filament eruption, CME, or X-ray or radio features.

We have also considered whether the onset of the SEP event on 30 September 2015, though associated with this activity, was delayed due to solar wind structures in the vicinity of Earth. An IMF sector boundary associated with a crossing of the heliospheric current sheet (HCS), was observed at ACE at ~ 19 UT, which is close to the SEP onset (a similar situation resulting in a delayed SEP onset is discussed by Lario et al. (2022)). Thus, it is also possible that the SEPs were largely confined to the region of anti-sunward fields following the sector boundary, i.e., north of the HCS. In the table, we have tentatively indicated the activity beginning at $\sim 9 - 10$ UT associated with the major filament eruption as the origin of this SEP event, but this association is uncertain for the reasons discussed above.

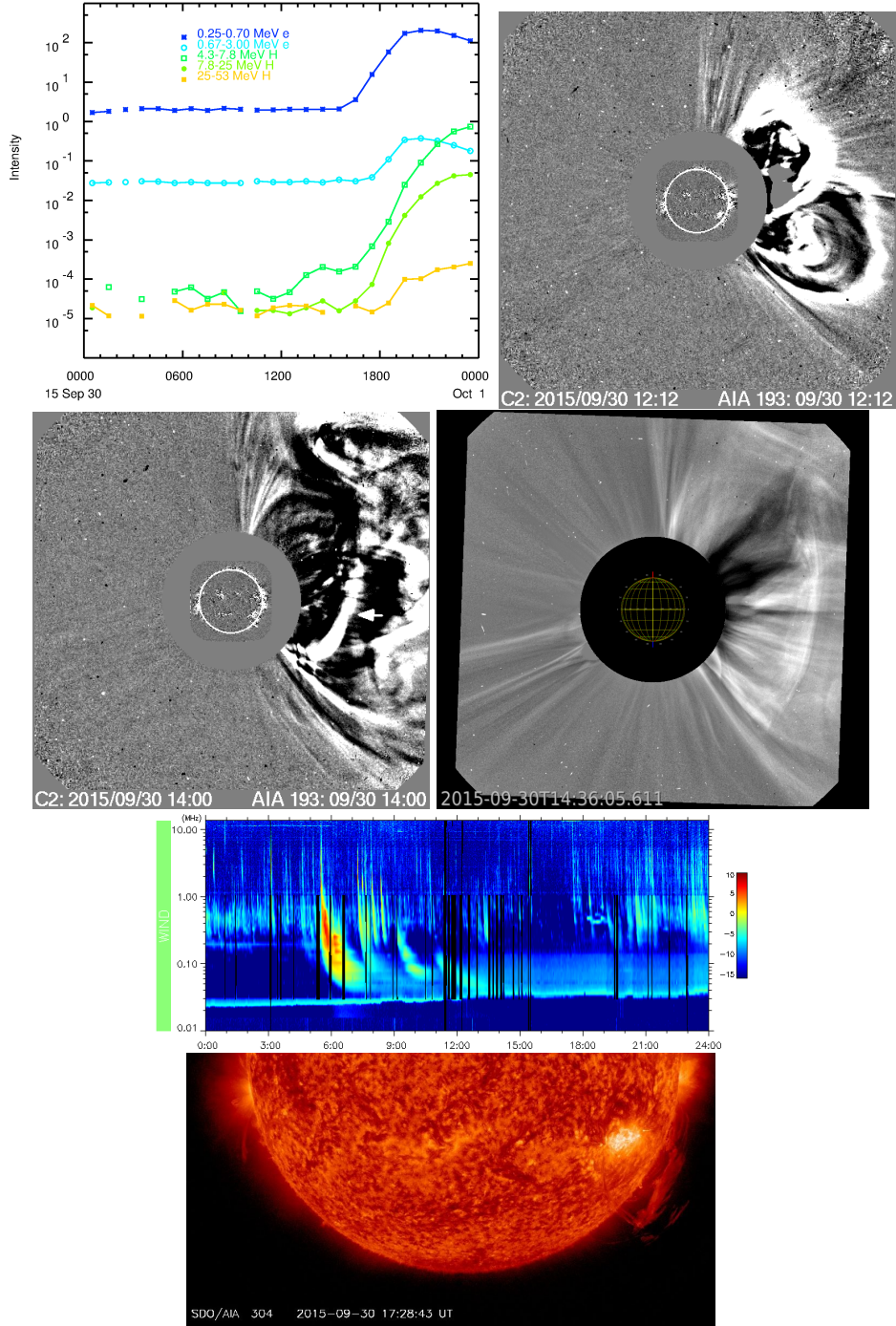


Figure 26. The SEP event of September 30, 2015, ~ 17 UT (top left; observations from SOHO/EPHIN), for which the associated solar event is uncertain and no STEREO observations are available. The nearest preceding CMEs were a pair at ~ 10 UT around 7 hours before the SEP event (top right, running difference image from the CDAW catalog) related to the lift off of a large filament (Figure 27). The left figure in the second row (also from the CDAW catalog) shows a likely CME (indicated by the arrow) trailing the first pair of CMEs that is not recorded in the CDAW or DONKI catalogs. This CME is also clearly evident in the right figure showing the base difference between C2 images at 14:36 UT and 09:12 UT. The Wind/WAVES radio data (third row) show only weak type III emissions at low frequencies early in the day, and no emissions around the time of SEP onset. There was a slow filament eruption above the southwest limb near the time of SEP onset (bottom figure) - SDO AIA 304 \AA observations at 17:29 UT are shown.

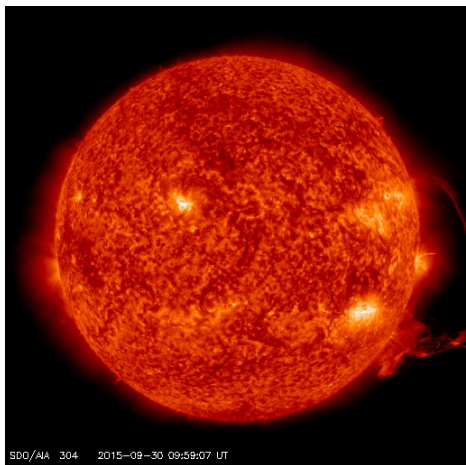


Figure 27. SDO AIA 304 Å observations at 9:59 UT on September 30, 2015, showing a large filament eruption above the west limb.

C.2. November 26, 2013

Another apparently anomalous SEP event is that on November 26, 2013 (Table 5) which unusually was not accompanied by a CME reported in the CDAW, DONKI or CACTus catalogs based on SOHO/LASCO and/or STEREO A/B COR2 coronagraph observations. This small prompt SEP event (Figure 28), just evident at proton energies of ~ 25 MeV, was observed only by STEREO A, with an electron onset time of $15:46$ UT ± 2 minutes. The event was associated with a small region of activity around 20° west of STEREO A and $\sim 44^\circ$ east of STEREO B seen by EUVI; the spacecraft were nearly 150° west or east of Earth, respectively, at this time (bottom panel of Figure 28). The SEP event was accompanied by a brief type III burst detected at both STEREO spacecraft (not shown) and also, occulted at high frequencies, at Wind (also not shown), consistent with the far side location. Despite the lack of a reported CME in the above catalogs, examination of the STEREO A and B COR1 coronagraph running difference movies clearly shows a CME (Figure 28, top right panel), first evident at STEREO B at 15:36 UT above the east limb, associated with the aforementioned active region and consistent with the SEP event onset. This CME, which became indistinct within the COR1 field of view, is recorded in the STEREO A and B COR1 CME lists at <https://cor1.gsfc.nasa.gov/catalog>. On close inspection of the STEREO A COR2 images, we do see evidence of the associated CME, but this “falls apart” in the field of view; we estimate the speed as 356 ± 10 km/s from a linear height-time fit. This CME observed at STEREO A is also noted in the “Dual-Viewpoint CME Catalog from the SECCHI/COR Telescopes” (Vourlidas et al. (2017); <http://solar.jhuapl.edu/Data-Products/COR-CME-Catalog.php>) but no parameters are given and the morphology is described as “other”. LASCO observations show outflows in the south, but no clear feature associated with this CME. Thus, this ~ 25 MeV proton event was associated with a CME observed close to the Sun that was not sufficiently distinct above $\sim 2 R_s$ to be recorded in the regular CME catalogs. Nevertheless, since there is clearly evidence of a CME in the lower corona, this SEP event is not an anomaly without an associated CME.

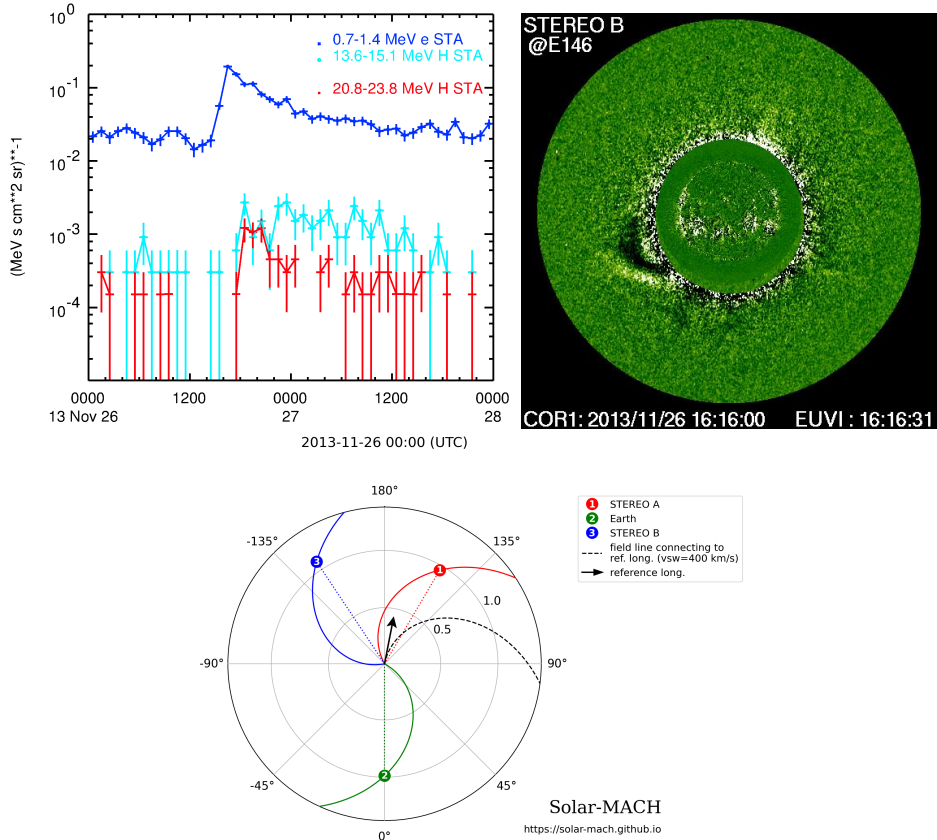


Figure 28. The small prompt SEP event on November 26, 2013 (top left), detected only at STEREO A (1 in the spacecraft location plot, bottom) that, unusually, was not associated with a reported CME in the LASCO C2 or STEREO A/B COR2 coronagraphs. The arrow in the bottom panel indicates the location of the related solar event observed by the STEREO A/B EUVIs. The top right panel shows that a CME associated with this event was evident in STEREO B COR1 (figure from the CDAW CME catalog). Although this faded by the edge of the COR1 field of view, close inspection suggests that the CME was observed by COR2 (not shown).

C.3. September 22, 2023

The associated solar event is also uncertain for the SEP event at L1 and STEREO A on September 22, 2023 (Figure 29) when STEREO A was separated by just 3° in longitude with respect to Earth/L1 (top right panel). This SEP event shows an indistinct onset and rise from ~ 16 UT (the top left panel shows observations from SOHO/ERNE) that is difficult to associate unambiguously with any of the frequent type III emissions, several overlapping CMEs and significant front side activity on this day; the ~ 25 MeV proton intensity rose to an ESP event associated with passage of an interplanetary shock on September 24, consistent with a front side origin. The fastest (983 km/s) CDAW CME on September 22 was at 02:24 UT associated with a long duration M1.2 flare at $E18^\circ$, but this is significantly earlier than the slow rise in proton intensity at Earth. At this time, PSP was at ~ 0.27 AU close to the Sun-Earth line and observed the SEP onset more clearly, at ~ 7 UT (bottom panel in Figure 29). This onset may be consistent with a faint CDAW CME observed at 07:36 UT with a recorded width of 86° . However, inspection of the LASCO observations suggests that it may have been expanding symmetrically around the occultor, though this is uncertain given the other structures in the field of view. The DONKI database gives a propagation longitude of $W04^\circ$ with a speed of 1508 km/s and an association with a flare at $N27W02$, though there was only limited brief \sim C-level flaring above the ongoing decay of the earlier long-duration flare. The height-time profile in the CDAW catalog indicates that the CME accelerated from around 500 km/s to 1000 km/s in the LASCO C2 field of view. We suggest in Table 11 that the SEP event at Earth and STEREO A was associated with this CME, though it is not possible to completely rule out a different association.

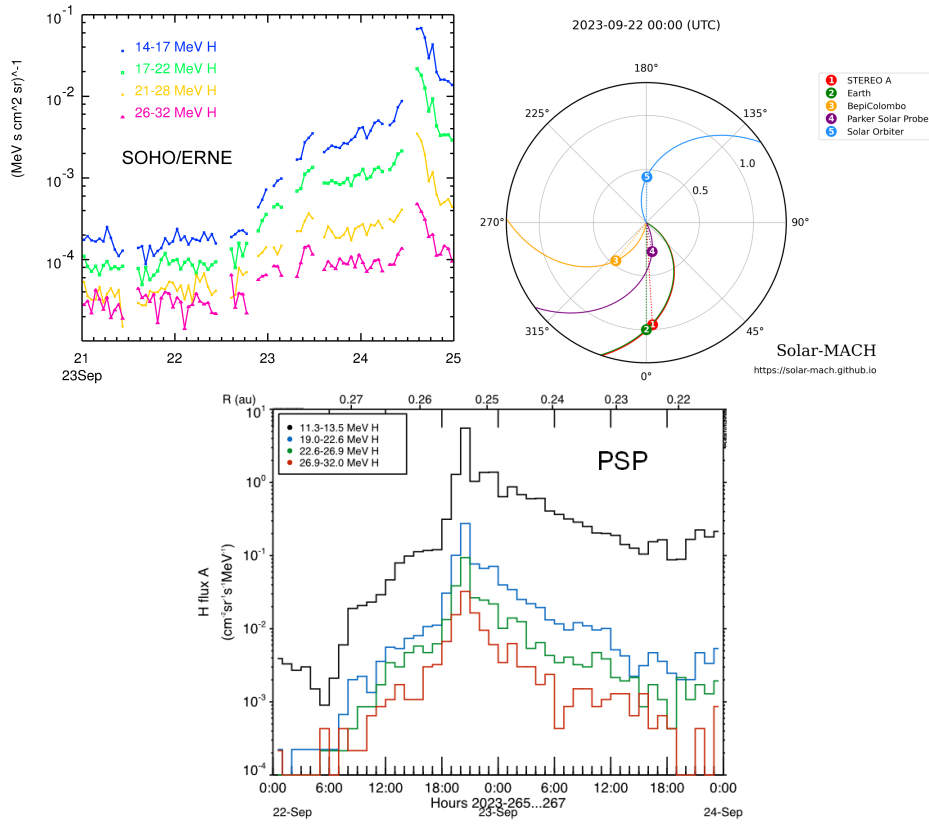


Figure 29. The SEP event observed at L1 (SOHO/ERNE observations are shown in the top left panel) and STEREO A (not shown) on September 22, 2023 with an indistinct onset. At this time, PSP was at ~ 0.27 AU, 11° west of the Sun-Earth line (top right). Hourly-averaged proton intensities from PSP HET A (bottom) show the SEP onset at ~ 7 UT on September 22. The proton intensity rose to the vicinity of a shock that passed PSP on September 22 and L1 and STEREO A on September 24.

Acknowledgements The authors thank the various researchers who have contributed to the success of the STEREO mission and have made their data available. We also acknowledge the contribution of data from instruments on near-Earth spacecraft, in particular SOHO EPHIN and ERNE. We thank members of the SERPENTINE collaboration for useful discussions. We particularly acknowledge the dedicated members of the CCMC and Moon to Mars Office at GSFC who have developed, contributed to, and maintain the DONKI database, and also the compilers of the CDAW CME database which is generated and maintained at the CDAW Data Center by NASA and The Catholic University of America in cooperation with the Naval Research Laboratory; SOHO is a project of international cooperation between ESA and NASA. We appreciate the helpful feedback provided by the reviewer.

Author Contribution IGR compiled the SEP event list, performed analysis of these events and wrote the manuscript. TvR contributed to the SEP event identifications and analysis. OCStC provided CME analysis and figures, and contributed to the SEP event, solar event and CME associations. DL and JGM contributed to the solar event identifications, and ERC contributed information on the STEREO mission. All authors read and reviewed the manuscript.

Funding IGR and DL acknowledge support from NASA Living With a Star program NNH19ZDA001N-■ LWS, Heliophysics Guest Investigators program NNH23ZDA001N-HGIO, and the NASA Heliophysics Space Weather Research Program's CLEAR SWx Center of Excellence, award 80NSSC23M0191. IGR also acknowledges support from the STEREO mission and NASA Heliophysics Supporting Research program NNH19ZDA001N-HSR. In addition, IGR and OCStC were supported by NASA program NNH17ZDA001N-LWS.

Data Availability The energetic particle data used are available from the NASA Space Physics Data Facility (<https://cdaweb.gsfc.nasa.gov/> and <https://spdf.gsfc.nasa.gov/research/vepo/>), and the STEREO HET website (<https://izwl.caltech.edu/STEREO/Public/HET-public.html>). We have also referred to SolO EPD data, generated and maintained by the EPD team; these data are available at https://espada.uah.es/epd/EPD_data.php. A machine readable version of the SEP event list is available at the Harvard Dataverse at <https://doi.org/10.7910/DVN/GQPCXZ>.

Declarations

Conflict of interest The authors declare that they have no conflicts of interest.

References

Aschwanden, M.J.: 2016, Global Energetics of Solar Flares. IV. Coronal Mass Ejection Energetics. *Astrophys. J.* **831**, 105. [DOI](#). [ADS](#).

Aschwanden, M.J., Xu, Y., Jing, J.: 2014, Global Energetics of Solar Flares. I. Magnetic Energies. *Astrophys. J.* **797**, 50. [DOI](#). [ADS](#).

Aschwanden, M.J., Boerner, P., Ryan, D., Caspi, A., McTiernan, J.M., Warren, H.P.: 2015, Global Energetics of Solar Flares: II. Thermal Energies. *Astrophys. J.* **802**, 53. [DOI](#). [ADS](#).

Aschwanden, M.J., Holman, G., O'Flannagain, A., Caspi, A., McTiernan, J.M., Kontar, E.P.: 2016, Global Energetics of Solar Flares. III. Nonthermal Energies. *Astrophys. J.* **832**, 27. [DOI](#). [ADS](#).

Aschwanden, M.J., Caspi, A., Cohen, C.M.S., Holman, G., Jing, J., Kretzschmar, M., Kontar, E.P., McTiernan, J.M., Mewaldt, R.A., O'Flannagain, A., Richardson, I.G., Ryan, D., Warren, H.P., Xu, Y.: 2017, Global Energetics of Solar Flares. V. Energy Closure in Flares and Coronal Mass Ejections. *Astrophys. J.* **836**, 17. [DOI](#). [ADS](#).

Bai, T., Cliver, E.W.: 1990, A 154 Day Periodicity in the Occurrence Rate of Proton Flares. *Astrophys. J.* **363**, 299. [DOI](#). [ADS](#).

Bain, H.M., Steenburgh, R.A., Onsager, T.G., Stitely, E.M.: 2021, A Summary of National Oceanic and Atmospheric Administration Space Weather Prediction Center Proton Event Forecast Performance and Skill. *Space Weather* **19**, e2020SW002670. e2020SW002670 2020SW002670. DOI. <https://agupubs.onlinelibrary.wiley.com/doi/abs/10.1029/2020SW002670>.

Benkhoff, J., Murakami, G., Baumjohann, W., Besse, S., Bunce, E., Casale, M., Cremosese, G., Glassmeier, K.-H., Hayakawa, H., Heyner, D., Hiesinger, H., Huovelin, J., Hüssmann, H., Iafolla, V., Iess, L., Kasaba, Y., Kobayashi, M., Milillo, A., Mitrofanov, I.G., Montagnon, E., Novara, M., Orsini, S., Quemerais, E., Reininghaus, U., Saito, Y., Santoli, F., Stramaccioni, D., Sutherland, O., Thomas, N., Yoshikawa, I., Zender, J.: 2021, BepiColombo - Mission Overview and Science Goals. *Space Sci. Rev.* **217**, 90. DOI. ADS.

Bruno, A., Richardson, I.G.: 2021, Empirical Model of 10 - 130 MeV Solar Energetic Particle Spectra at 1 AU Based on Coronal Mass Ejection Speed and Direction. *Sol. Phys.* **296**, 36. DOI. ADS.

Bruno, A., Bazilevskaya, G.A., Boezio, M., Christian, E.R., de Nolfo, G.A., Martucci, M., Merge, M., Mikhailov, V.V., Munini, R., Richardson, I.G., Ryan, J.M., Stochaj, S., Adriani, O., Barbarino, G.C., Bellotti, R., Bogomolov, E.A., Bongi, M., Bonvicini, V., Bottai, S., Cafagna, F., Campana, D., Carlson, P., Casolino, M., Castellini, G., De Santis, C., Di Felice, V., Galper, A.M., Karelina, A.V., Koldashov, S.V., Koldobskiy, S., Krutkov, S.Y., Kvashnin, A.N., Leonov, A., Malakhov, V., Marcelli, L., Mayorov, A.G., Menn, W., Mocchiutti, E., Monaco, A., Mori, N., Osteria, G., Panico, B., Papini, P., Pearce, M., Picozza, P., Ricci, M., Ricciarini, S.B., Simon, M., Sparvoli, R., Spillantini, P., Stozhkov, Y.I., Vacchi, A., Vannuccini, E., Vasilyev, G.I., Voronov, S.A., Yurkin, Y.T., Zampa, G., Zampa, N.: 2018, Solar Energetic Particle Events Observed by the PAMELA Mission. *Astrophys. J.* **862**, 97. DOI. ADS.

Bruno, A., Christian, E.R., de Nolfo, G.A., Richardson, I.G., Ryan, J.M.: 2019, Spectral Analysis of the September 2017 Solar Energetic Particle Events. *Space Weather* **17**, 419. DOI. <https://agupubs.onlinelibrary.wiley.com/doi/abs/10.1029/2018SW002085>.

Bruno, A., de Nolfo, G.A., Ryan, J.M., Richardson, I.G., Dalla, S.: 2023, Statistical Relationship between Long-duration High-energy Gamma-Ray Emission and Solar Energetic Particles. *Astrophys. J.* **953**, 187. DOI. ADS.

Bruno, A., Pesce-Rollins, M., Dalla, S., Omodei, N., Richardson, I.G., Ryan, J.M.: 2025, The 2024 July 16 solar event: a challenge to the coronal mass ejection origin of long-duration gamma-ray flares. *Astron. Astrophys.* **704**, A140. DOI. ADS.

Burkepile, J., St. Cyr, O.C., Richardson, I.G., de Toma, G., Thompson, B., Galloy, M.: 2025, Observations of SEP-Associated CMEs in the low and middle corona from Solar Dynamics Observatory AIA and the Mauna Loa K-Coronagraph. In: *SDO 2025 Science Workshop: A Gathering of the Helio-hive! Online at https://sdo2025.sdo-workshops.org*, 147. ADS.

Cane, H.V., Erickson, W.C.: 2005, Solar Type II Radio Bursts and IP Type II Events. *Astrophys. J.* **623**, 1180. DOI. ADS.

Cane, H.V., Lario, D.: 2006, An Introduction to CMEs and Energetic Particles. *Space Sci. Rev.* **123**, 45. DOI. ADS.

Cane, H.V., Erickson, W.C., Prestage, N.P.: 2002, Solar flares, type III radio bursts, coronal mass ejections, and energetic particles. *Journal of Geophysical Research (Space Physics)* **107**, 1315. DOI. ADS.

Cane, H.V., Reames, D.V., von Rosenvinge, T.T.: 1988, The role of interplanetary shocks in the longitude distribution of solar energetic particles. *J. Geophys. Res.* **93**, 9555. DOI. ADS.

Cane, H.V., Richardson, I.G., von Rosenvinge, T.T.: 1998, Interplanetary magnetic field periodicity of ~ 153 days. *Geophys. Res. Lett.* **25**, 4437. DOI. ADS.

Cane, H.V., Richardson, I.G., von Rosenvinge, T.T.: 2010, A study of solar energetic particle events of 1997-2006: Their composition and associations. *Journal of Geophysical Research (Space Physics)* **115**, A08101. DOI. ADS.

Cane, H.V., Stone, R.G., Fainberg, J., Steinberg, J.L., Hoang, S.: 1982, Type-II Solar Radio Events Observed in the Interplanetary Medium - Part One - General Characteristics. *Sol. Phys.* **78**, 187. DOI. ADS.

Chowdhury, P., Choudhary, D.P., Gosain, S., Moon, Y.-J.: 2015, Short-term periodicities in interplanetary, geomagnetic and solar phenomena during solar cycle 24. *Astrophys. Space Sci.* **356**, 7. DOI. ADS.

Cohen, C.M.S., Mason, G.M., Mewaldt, R.A.: 2017, Characteristics of Solar Energetic Ions as a Function of Longitude. *Astrophys. J.* **843**, 132. DOI. ADS.

Cohen, C.M.S., Mason, G.M., Christian, E.R., Cummings, A.C., de Nolfo, G.A., Desai, M.I., Giacalone, J., Hill, M.E., Labrador, A.W., Leske, R.A., McComas, D.J., McNutt, R.L. Jr., Mitchell, D.G., Mitchell, J.G., Muro, G.D., Rankin, J.S., Schwadron, N.A., Shen, M.M., Wiedenbeck, M.E., Xu, Z.G., Ho, G.C., Wimmer-Schweingrüber, R.F.: 2025, Longitudinal Dependence of Heavy Ion Composition in the 2021 October 28 Ground Level Enhancement Event. *Astrophys. J. Lett.* **978**, L35. [DOI](#). [ADS](#).

Cucinotta, F.A., Hu, S., Schwadron, N.A., Kozarev, K., Townsend, L.W., Kim, M.-H.Y.: 2010, Space radiation risk limits and Earth-Moon-Mars environmental models. *Space Weather* **8**, S00E09. [DOI](#). [ADS](#).

Dalla, S., Balogh, A., Heber, B., Lopate, C.: 2001, Further indications of a ~140 day recurrence in energetic particle fluxes at 1 and 5 AU from the Sun. *J. Geophys. Res.* **106**, 5721. [DOI](#). [ADS](#).

Dikpati, M., McIntosh, S.W.: 2020, Space Weather Challenge and Forecasting Implications of Rossby Waves. *Space Weather* **18**, e02109. [DOI](#). [ADS](#).

Domingo, V., Fleck, B., Poland, A.I.: 1995, The SOHO Mission: an Overview. *Sol. Phys.* **162**, 1. [DOI](#). [ADS](#).

Dresing, N., Gómez-Herrero, R., Heber, B., Klassen, A., Malandraki, O., Dröge, W., Kartavykh, Y.: 2014, Statistical survey of widely spread out solar electron events observed with STEREO and ACE with special attention to anisotropies. *Astron. Astrophys.* **567**, A27. [DOI](#). [ADS](#).

Dresing, N., Rodríguez-García, L., Jebaraj, I.C., Warmuth, A., Wallace, S., Balmaceda, L., Podladchikova, T., Strauss, R.D., Kouloumvakos, A., Palmroos, C., Krupar, V., Gieseler, J., Xu, Z., Mitchell, J.G., Cohen, C.M.S., de Nolfo, G.A., Palmerio, E., Carcaboso, F., Kilpua, E.K.J., Trotta, D., Auster, U., Asvestari, E., da Silva, D., Dröge, W., Getachew, T., Gómez-Herrero, R., Grande, M., Heyner, D., Holmström, M., Huovelin, J., Kartavykh, Y., Laurenza, M., Lee, C.O., Mason, G., Maksimovic, M., Mieth, J., Murakami, G., Oleynik, P., Pinto, M., Pulupa, M., Richter, I., Rodríguez-Pacheco, J., Sánchez-Cano, B., Schuller, F., Ueno, H., Vainio, R., Vecchio, A., Veronig, A.M., Wijsen, N.: 2023, The 17 April 2021 widespread solar energetic particle event. *Astron. Astrophys.* **674**, A105. [DOI](#). [ADS](#).

Dresing, N., Yli-Laurila, A., Valkila, S., Gieseler, J., Morosan, D.E., Farwa, G.U., Kartavykh, Y., Palmroos, C., Jebaraj, I., Jensen, S., Kühl, P., Heber, B., Espinosa, F., Gómez-Herrero, R., Kilpua, E., Linho, V.-V., Oleynik, P., Hayes, L.A., Warmuth, A., Schuller, F., Collier, H., Xiao, H., Asvestari, E., Trotta, D., Mitchell, J.G., Cohen, C.M.S., Labrador, A.W., Hill, M.E., Vainio, R.: 2024, The solar cycle 25 multi-spacecraft solar energetic particle event catalog of the SERPENTINE project. *Astron. Astrophys.* **687**, A72. [DOI](#). [ADS](#).

Dresing, N., Jebaraj, I.C., Wijsen, N., Palmerio, E., Rodríguez-García, L., Palmroos, C., Gieseler, J., Jarry, M., Asvestari, E., Mitchell, J.G., Cohen, C.M.S., Lee, C.O., Wei, W., Ramstad, R., Riihonen, E., Oleynik, P., Kouloumvakos, A., Warmuth, A., Sánchez-Cano, B., Ehrmann, B., Dunn, P., Dudnik, O., Mac Cormack, C.: 2025, The reason for the widespread energetic storm particle event of 13 March 2023. *Astron. Astrophys.* **695**, A127. [DOI](#). [ADS](#).

Farwa, G.U., Dresing, N., Gieseler, J., Vuorinen, L., Richardson, I.G., Palmroos, C., Valkila, S., Heber, B., Jensen, S., Kühl, P., Rodriguez-García, L., Vainio, R.: 2025, Electron and proton peak intensities as observed by a five-spacecraft fleet in solar cycle 25. *Astron. Astrophys.* **693**, A198. [DOI](#). [ADS](#).

Fox, N.J., Velli, M.C., Bale, S.D., Decker, R., Driesman, A., Howard, R.A., Kasper, J.C., Kinnison, J., Kusterer, M., Lario, D., Lockwood, M.K., McComas, D.J., Raouafi, N.E., Szabo, A.: 2016, The Solar Probe Plus Mission: Humanity's First Visit to Our Star. *Space Sci. Rev.* **204**, 7. [DOI](#). [ADS](#).

Gieseler, J., Dresing, N., Palmroos, C., Freiherr von Forstner, J.L., Price, D.J., Vainio, R., Kouloumvakos, A., Rodríguez-García, L., Trotta, D., Génot, V., Masson, A., Roth, M., Veronig, A.: 2023, Solar-MACH: An open-source tool to analyze solar magnetic connection configurations. *Frontiers in Astronomy and Space Sciences* **9**, 384. [DOI](#). [ADS](#).

Gnevyshev, M.N.: 1967, On the 11-Years Cycle of Solar Activity. *Sol. Phys.* **1**, 107. [DOI](#). [ADS](#).

Gnevyshev, M.N.: 1977, Essential features of the 11-year solar cycle. *Sol. Phys.* **51**, 175. [DOI](#). [ADS](#).

Gómez-Herrero, R., Dresing, N., Klassen, A., Heber, B., Lario, D., Agueda, N., Malandraki, O.E., Blanco, J.J., Rodríguez-Pacheco, J., Banjac, S.: 2015, Circumsolar Energetic Particle Distribution on 2011 November 3. *Astrophys. J.* **799**, 55. [DOI](#). [ADS](#).

Gurgenashvili, E., Zaqrashvili, T.V., Kukhianidze, V., Reiners, A., Oliver, R., Lanza, A.F., Reinhold, T.: 2021, Rieger-type periodicity in the total irradiance of the Sun as a star during solar cycles 23–24. *Astron. Astrophys.* **653**, A146. [DOI](#) [ADS](#).

Hassler, D.M., Zeitlin, C., Wimmer-Schweingruber, R.F., Böttcher, S., Martin, C., Andrews, J., Böhm, E., Brinza, D.E., Bullock, M.A., Burmeister, S., Ehresmann, B., Epperly, M., Grinspoon, D., Köhler, J., Kortmann, O., Neal, K., Peterson, J., Posner, A., Rafkin, S., Seimetz, L., Smith, K.D., Tyler, Y., Weigle, G., Reitz, G., Cucinotta, F.A.: 2012, The Radiation Assessment Detector (RAD) Investigation. *Space Sci. Rev.* **170**, 503. [DOI](#) [ADS](#).

Howard, R.A., Moses, J.D., Vourlidas, A., Newmark, J.S., Socker, D.G., Plunkett, S.P., Kondryke, C.M., Cook, J.W., Hurley, A., Davila, J.M., Thompson, W.T., St Cyr, O.C., Mentzell, E., Mehalick, K., Lemen, J.R., Wuelser, J.P., Duncan, D.W., Tarbell, T.D., Wolfson, C.J., Moore, A., Harrison, R.A., Waltham, N.R., Lang, J., Davis, C.J., Eyles, C.J., Mapson-Menard, H., Simnett, G.M., Halain, J.P., Defise, J.M., Mazy, E., Rochus, P., Mercier, R., Ravet, M.F., Delmotte, F., Auchere, F., Delaboudiniere, J.P., Bothmer, V., Deutsch, W., Wang, D., Rich, N., Cooper, S., Stephens, V., Maahs, G., Baugh, R., McMullin, D., Carter, T.: 2008, Sun Earth Connection Coronal and Heliospheric Investigation (SECCHI). *Space Sci. Rev.* **136**, 67. [DOI](#) [ADS](#).

Iucci, N., Levitin, A.E., Belov, A.V., Eroshenko, E.A., Ptitsyna, N.G., Villoresi, G., Chizhenkov, G.V., Dorman, L.I., Gromova, L.I., Parisi, M., Tyasto, M.I., Yanke, V.G.: 2005, Space weather conditions and spacecraft anomalies in different orbits. *Space Weather* **3**. [DOI](#) <https://agupubs.onlinelibrary.wiley.com/doi/abs/10.1029/2003SW000056>.

Jiggens, P., Clavie, C., Evans, H., O'Brien, T.P., Witasse, O., Mishev, A.L., Nieminen, P., Daly, E., Kalegaev, V., Vlasova, N., Borisov, S., Benck, S., Poivey, C., Cyamukungu, M., Mazur, J., Heynderickx, D., Sandberg, I., Berger, T., Usoskin, I.G., Paassilta, M., Vainio, R., Straube, U., Müller, D., Sánchez-Cano, B., Hassler, D., Praks, J., Niemelä, P., Leppinen, H., Punkkinen, A., Aminalragia-Giamini, S., Nagatsuma, T.: 2019, In Situ Data and Effect Correlation During September 2017 Solar Particle Event. *Space Weather* **17**, 99. [DOI](#) <https://agupubs.onlinelibrary.wiley.com/doi/abs/10.1029/2018SW001936>.

Kahler, S.W.: 1982, The role of the big flare syndrome in correlations of solar energetic proton fluxes and associated microwave burst parameters. *J. Geophys. Res.* **87**, 3439. [DOI](#) [ADS](#).

Kahler, S.W., Hildner, E., Van Hollebeke, M.A.I.: 1978, Prompt solar proton events and coronal mass ejections. *Sol. Phys.* **57**, 429. [DOI](#) [ADS](#).

Kaiser, M.L., Kucera, T.A., Davila, J.M., St. Cyr, O.C., Guhathakurta, M., Christian, E.: 2008, The STEREO Mission: An Introduction. *Space Sci. Rev.* **136**, 5. [DOI](#) [ADS](#).

Khoo, L.Y., Sánchez-Cano, B., Lee, C.O., Rodríguez-García, L., Kouloumvakos, A., Palmerio, E., Carcaboso, F., Lario, D., Dresing, N., Cohen, C.M.S., McComas, D.J., Lynch, B.J., Fraschetti, F., Jebaraj, I.C., Mitchell, J.G., Nieves-Chinchilla, T., Krupar, V., Pacheco, D., Giacalone, J., Auster, H.-U., Benkhoff, J., Bonnin, X., Christian, E.R., Ehresmann, B., Fedeli, A., Fischer, D., Heyner, D., Holmström, M., Leske, R.A., Maksimovic, M., Mieth, J.Z.D., Oleynik, P., Pinto, M., Richter, I., Rodríguez-Pacheco, J., Schwadron, N.A., Schmid, D., Telloni, D., Vecchio, A., Wiedenbeck, M.E.: 2024, Multispacecraft Observations of a Widespread Solar Energetic Particle Event on 2022 February 15–16. *Astrophys. J.* **963**, 107. [DOI](#) [ADS](#).

Kollhoff, A., Kouloumvakos, A., Lario, D., Dresing, N., Gómez-Herrero, R., Rodríguez-García, L., Malandraki, O.E., Richardson, I.G., Posner, A., Klein, K.-L., Pacheco, D., Klassen, A., Heber, B., Cohen, C.M.S., Laitinen, T., Cernuda, I., Dalla, S., Espinosa Lara, F., Vainio, R., Köberle, M., Kühl, R., Xu, Z.G., Berger, L., Eldrum, S., Brüdern, M., Laurens, M., Kilpua, E.J., Aran, A., Rouillard, A.P., Bućik, R., Wijesen, N., Pomoell, J., Wimmer-Schweingruber, R.F., Martin, C., Böttcher, S.I., Freiherr von Forstner, J.L., Terasa, J.-C., Boden, S., Kulkarni, S.R., Ravanbakhsh, A., Yedla, M., Janitzek, N., Rodríguez-Pacheco, J., Prieto Mateo, M., Sánchez Prieto, S., Parra Espada, P., Rodríguez Polo, O., Martínez Hellín, A., Carcaboso, F., Mason, G.M., Ho, G.C., Allen, R.C., Bruce Andrews, G., Schlemm, C.E., Seifert, H., Tyagi, K., Lees, W.J., Hayes, J., Bale, S.D., Krupar, V., Horbury, T.S., Angelini, V., Evans, V., O'Brien, H., Maksimovic, M., Khotyaintsev, Y.V., Vecchio, A., Steinvall, K., Asvestari, E.: 2021, The first widespread solar energetic particle event observed by Solar Orbiter on 2020 November 29. *Astron. Astrophys.* **656**, A20. [DOI](#) [ADS](#).

Kouloumvakos, A., Wijesen, N., Jebaraj, I.C., Afanasiev, A., Lario, D., Cohen, C.M.S., Riley, P., Mitchell, D.G., Ding, Z., Vourlidas, A., Giacalone, J., Chen, X., Hill, M.E.: 2025, Shock and SEP Modeling Study for the 2022 September 5 SEP Event. *Astrophys. J.* **979**, 100. [DOI](#) [ADS](#).

Krucker, S., Hurford, G.J., Grimm, O., Kögl, S., Gröbelbauer, H.-P., Etesi, L., Casadei, D., Csillaghy, A., Benz, A.O., Arnold, N.G., Molendini, F., Orleanski, P., Schori, D., Xiao, H., Kuhar, M., Hochmuth, N., Felix, S., Schramka, F., Marcin, S., Kobler, S., Iseli, L., Dreier, M., Wiehl, H.J., Kleint, L., Battaglia, M., Lastufka, E., Sathiapal, H., Lapadula, K., Bednarzik, M., Birrer, G., Stutz, S., Wild, C., Marone, F., Skup, K.R., Cichocki, A., Ber, K., Rutkowski, K., Bujwan, W., Juchnikowski, G., Winkler, M., Darmetko, M., Michalska, M., Seweryn, K., Bialek, A., Osica, P., Sylwester, J., Kowalinski, M., Ścisłowski, D., Siarkowski, M., Stęlicki, M., Mrozek, T., Podgórski, P., Meuris, A., Limousin, O., Gevin, O., Le Mer, I., Brun, S., Strugarek, A., Vilmer, N., Murret, S., Maksimović, M., Fárník, F., Kozáček, Z., Kašparová, J., Mann, G., Onel, H., Warmuth, A., Rendtel, J., Anderson, J., Bauer, S., Dionies, F., Paschke, J., Plüschke, D., Woche, M., Schuller, F., Veronig, A.M., Dickson, E.C.M., Gallagher, P.T., Maloney, S.A., Bloomfield, D.S., Piana, M., Massone, A.M., Benvenuto, F., Massa, P., Schwartz, R.A., Dennis, B.R., van Beek, H.F., Rodríguez-Pacheco, J., Lin, R.P.: 2020, The Spectrometer/Telescope for Imaging X-rays (STIX). *Astron. Astrophys.* **642**, A15. [DOI](#) [ADS](#).

Krupar, V., Kruparova, O., Szabo, A., Nemec, F., Maksimovic, M., Martinez Oliveros, J.C., Lario, D., Bonnin, X., Vecchio, A., Pulupa, M., Bale, S.D.: 2024, Comparative Analysis of Type III Radio Bursts and Solar Flares: Spatial Localization and Correlation with Solar Flare Intensity. *Astrophys. J.* **961**, 88. [DOI](#) [ADS](#).

Kühl, P., Dresing, N., Heber, B., Klassen, A.: 2017, Solar Energetic Particle Events with Protons Above 500 MeV Between 1995 and 2015 Measured with SOHO/EPHIN. *Sol. Phys.* **292**, 10. [DOI](#) [ADS](#).

Kwon, R.-Y., Zhang, J., Olmedo, O.: 2014, New Insights into the Physical Nature of Coronal Mass Ejections and Associated Shock Waves within the Framework of the Three-dimensional Structure. *Astrophys. J.* **794**, 148. [DOI](#) [ADS](#).

Lara, A., Borgazzi, A., Mendes, O. Jr., Rosa, R.R., Domingues, M.O.: 2008, Short-Period Fluctuations in Coronal Mass Ejection Activity during Solar Cycle 23. *Sol. Phys.* **248**, 155. [DOI](#) [ADS](#).

Lario, D., Karelitz, A.: 2014, Influence of interplanetary coronal mass ejections on the peak intensity of solar energetic particle events. *Journal of Geophysical Research (Space Physics)* **119**, 4185. [DOI](#) [ADS](#).

Lario, D., Aran, A., Gómez-Herrero, R., Dresing, N., Heber, B., Ho, G.C., Decker, R.B., Roelof, E.C.: 2013, Longitudinal and Radial Dependence of Solar Energetic Particle Peak Intensities: STEREO, ACE, SOHO, GOES, and MESSENGER Observations. *Astrophys. J.* **767**, 41. [DOI](#) [ADS](#).

Lario, D., Kwon, R.-Y., Riley, P., Raouafi, N.E.: 2017, On the Link between the Release of Solar Energetic Particles Measured at Widespread Heliolongitudes and the Properties of the Associated Coronal Shocks. *Astrophys. J.* **847**, 103. [DOI](#) [ADS](#).

Lario, D., Kwon, R.Y., Balmaceda, L., Richardson, I.G., Krupar, V., Thompson, B.J., Cyr, O.C.S., Zhao, L., Zhang, M.: 2020, Fast and Wide CMEs without Observed ≥ 20 MeV Protons. *Astrophys. J.* **889**, 92. [DOI](#) [ADS](#).

Lario, D., Wijsen, N., Kwon, R.Y., Sánchez-Cano, B., Richardson, I.G., Pacheco, D., Palmerio, E., Stevens, M.L., Szabo, A., Heyner, D., Dresing, N., Gómez-Herrero, R., Carcaboso, F., Aran, A., Afanasiev, A., Vainio, R., Riihonen, E., Poedts, S., Brüden, M., Xu, Z.G., Kollhoff, A.: 2022, Influence of Large-scale Interplanetary Structures on the Propagation of Solar Energetic Particles: The Multispacecraft Event on 2021 October 9. *Astrophys. J.* **934**, 55. [DOI](#) [ADS](#).

Lario, D., Richardson, I.G., Aran, A., Wijsen, N.: 2023, High-energy (> 40 MeV) Proton Intensity Enhancements Associated with the Passage of Interplanetary Shocks at 1 au. *Astrophys. J.* **950**, 89. [DOI](#) [ADS](#).

Laurenza, M., Cliver, E.W., Hewitt, J., Storini, M., Ling, A.G., Balch, C.C., Kaiser, M.L.: 2009, A technique for short-term warning of solar energetic particle events based on flare location, flare size, and evidence of particle escape. *Space Weather* **7**, S04008. [DOI](#) [ADS](#).

Lean, J.: 1990, Evolution of the 155 Day Periodicity in Sunspot Areas during Solar Cycles 12 to 21. *Astrophys. J.* **363**, 718. [DOI](#) [ADS](#).

Lobzin, V.V., Cairns, I.H., Robinson, P.A.: 2012, Rieger-type Periodicity in the Occurrence of Solar Type III Radio Bursts. *Astrophys. J. Lett.* **754**, L28. [DOI](#) [ADS](#).

Logachev, Y.I., Bazilevskaya, G.A., Vlasova, N.A., Ginzburg, E.A., Daibog, E.I., Ishkov, V.N., Lazutin, L.L., Nguen, M.D., Surova, G.M., Yakovchuk, O.S.: 2022, Catalog of solar proton events in the 24th cycle of solar activity (2009–2019). Technical report, ESDB repository, GC RAS, Moscow. [DOI](#).

Lomb, N.R.: 1976, Least-Squares Frequency Analysis of Unequally Spaced Data. *Astrophys. Space Sci.* **39**, 447. [DOI](#). [ADS](#).

Lou, Y.-Q., Wang, Y.-M., Fan, Z., Wang, S., Wang, J.X.: 2003, Periodicities in solar coronal mass ejections. *Mon. Not. R. Astron. Soc.* **345**, 809. [DOI](#). [ADS](#).

MacDowall, R.J., Lara, A., Manoharan, P.K., Nitta, N.V., Rosas, A.M., Bougeret, J.L.: 2003, Long-duration hectometric type III radio bursts and their association with solar energetic particle (SEP) events. *Geophys. Res. Lett.* **30**, 8018. [DOI](#). [ADS](#).

MacDowall, R.J., Richardson, I.G., Hess, R.A., Thejappa, G.: 2009, Re-examining the correlation of complex solar type III radio bursts and solar energetic particles. In: Gopalswamy, N., Webb, D.F. (eds.) *Universal Heliophysical Processes* **257**, 335. [DOI](#). [ADS](#).

Matthiä, D., Meier, M.M., Berger, T.: 2018, The Solar Particle Event on 10–13 September 2017: Spectral Reconstruction and Calculation of the Radiation Exposure in Aviation and Space. *Space Weather* **16**, 977. [DOI](#). <https://agupubs.onlinelibrary.wiley.com/doi/abs/10.1029/2018SW001921>.

Mavromichalaki, H., Gerontidou, M., Paschalis, P., Paouris, E., Tezari, A., Sgouropoulos, C., Crosby, N., Dierckxsens, M.: 2018, Real-Time Detection of the Ground Level Enhancement on 10 September 2017 by A.Ne.Mo.S.: System Report. *Space Weather* **16**, 1797. [DOI](#). <https://agupubs.onlinelibrary.wiley.com/doi/abs/10.1029/2018SW001992>.

McIntosh, S.W., Leamon, R.J., Krista, L.D., Title, A.M., Hudson, H.S., Riley, P., Harder, J.W., Kopp, G., Snow, M., Woods, T.N., Kasper, J.C., Stevens, M.L., Ulrich, R.K.: 2015, The solar magnetic activity band interaction and instabilities that shape quasi-periodic variability. *Nature Communications* **6**, 6491. [DOI](#). [ADS](#).

Mishev, A.L., Usoskin, I.G.: 2018, Assessment of the Radiation Environment at Commercial Jet-Flight Altitudes During GLE 72 on 10 September 2017 Using Neutron Monitor Data. *Space Weather* **16**, 1921. [DOI](#). <https://agupubs.onlinelibrary.wiley.com/doi/abs/10.1029/2018SW001946>.

Mitchell, J.G., Cohen, C.M.S., Eddy, T.J., Joyce, C.J., Rankin, J.S., Shen, M.M., de Nolfo, G.A., Christian, E.R., McComas, D.J., McNutt, R.L., Wiedenbeck, M.E., Schwadron, N.A., Hill, M.E., Labrador, A.W., Leske, R.A., Mewaldt, R.A., Mitchell, D.G., Szalay, J.R.: 2023, A Living Catalog of Parker Solar Probe IS \odot IS Energetic Particle Enhancements. *Astrophys. J. Suppl.* **264**, 31. [DOI](#). [ADS](#).

Miteva, R., Samwel, S.W., Costa-Duarte, M.V.: 2018, The Wind/EPACT Proton Event Catalog (1996 - 2016). *Sol. Phys.* **293**, 27. [DOI](#). [ADS](#).

Müller, D., St. Cyr, O.C., Zouganelis, I., Gilbert, H.R., Marsden, R., Nieves-Chinchilla, T., Antonucci, E., Auchère, F., Berghmans, D., Horbury, T.S., Howard, R.A., Krucker, S., Maksimovic, M., Owen, C.J., Rochus, P., Rodriguez-Pacheco, J., Romoli, M., Solanki, S.K., Bruno, R., Carlsson, M., Fludra, A., Harra, L., Hassler, D.M., Livi, S., Louarn, P., Peter, H., Schühle, U., Teriaca, L., del Toro Iniesta, J.C., Wimmer-Schweingruber, R.F., Marsch, E., Velli, M., De Groof, A., Walsh, A., Williams, D.: 2020, The Solar Orbiter mission: Science overview. *Astron. Astrophys.* **642**, A1. [DOI](#). [ADS](#).

Müller-Mellin, R., Kunow, H., Fleißner, V., Pehlke, E., Rode, E., Röschmann, N., Scharnberg, C., Sierks, H., Rusznyak, P., McKenna-Lawlor, S., Elendt, I., Sequeiros, J., Meziat, D., Sanchez, S., Medina, J., Del Peral, L., Witte, M., Marsden, R., Henrion, J.: 1995, COSTEP - Comprehensive Suprathermal and Energetic Particle Analyser. *Sol. Phys.* **162**, 483. [DOI](#). [ADS](#).

Nelson, G.J., Melrose, D.B.: 1985, Type II bursts. In: McLean, D.J., Labrum, N.R. (eds.) *Solar Radiophysics: Studies of Emission from the Sun at Metre Wavelengths*, 333. [ADS](#).

Paassilta, M., Raukunen, O., Vainio, R., Valtonen, E., Papaioannou, A., Siipola, R., Riihonen, E., Dierckxsens, M., Crosby, N., Malandraki, O., Heber, B., Klein, K.-L.: 2017, Catalogue of 55-80 MeV solar proton events extending through solar cycles 23 and 24. *Journal of Space Weather and Space Climate* **7**, A14. [DOI](#). [ADS](#).

Paassilta, M., Papaaoannou, A., Dresing, N., Vainio, R., Valtonen, E., Heber, B.: 2018, Catalogue of > 55 MeV Wide-longitude Solar Proton Events Observed by SOHO, ACE, and the STEREOs at ≈ 1 AU During 2009 - 2016. *Sol. Phys.* **293**, 70. [DOI](#). [ADS](#).

Palmerio, E., Lee, C.O., Mays, M.L., Luhmann, J.G., Lario, D., Sánchez-Cano, B., Richardson, I.G., Vainio, R., Stevens, M.L., Cohen, C.M.S., Steinvall, K., Möstl, C., Weiss, A.J., Nieves-Chinchilla, T., Li, Y., Larson, D.E., Heyner, D., Bale, S.D., Galvin, A.B., Holmström, M., Khotyaintsev, Y.V., Maksimovic, M., Mitrofanov, I.G.: 2022, CMEs and SEPs During November-December 2020: A Challenge for Real-Time Space Weather Forecasting. *Space Weather* **20**, e2021SW002993. [DOI](#). [ADS](#).

Palmerio, E., Luhmann, J.G., Mays, M.L., Caplan, R.M., Lario, D., Richardson, I.G., Whitman, K., Lee, C.O., Sánchez-Cano, B., Wijsen, N., Li, Y., Cardoso, C., Pinto, M., Heyner, D., Schmid, D., Auster, H.-U., Fischer, D.: 2024, Improved modelling of SEP event onset within the WSA-Enlil-SEPMOD framework. *Journal of Space Weather and Space Climate* **14**, 3. [DOI](#). [ADS](#).

Pande, B., Pande, S., Chandra, R., Chandra Mathpal, M.: 2018, Solar flares, CMEs and solar energetic particle events during solar cycle 24. *Advances in Space Research* **61**, 777. [DOI](#). [ADS](#).

Paouris, E., Vourlidas, A., Kouloumvakos, A., Papaioannou, A., Jagarlamudi, V.K., Horbury, T.: 2023, The Space Weather Context of the First Extreme Event of Solar Cycle 25, on 2022 September 5. *Astrophys. J.* **956**, 58. [DOI](#). [ADS](#).

Papaioannou, A., Malandraki, O.E., Dresing, N., Heber, B., Klein, K.-L., Vainio, R., Rodríguez-Gasén, R., Klassen, A., Nindos, A., Heynderickx, D., Mewaldt, R.A., Gómez-Herrero, R., Vilmer, N., Kouloumvakos, A., Tziotziou, K., Tsiroupolou, G.: 2014, SEPServer catalogues of solar energetic particle events at 1 AU based on STEREO recordings: 2007-2012. *Astron. Astrophys.* **569**, A96. [DOI](#). [ADS](#).

Papaioannou, A., Kouloumvakos, A., Mishev, A., Vainio, R., Usoskin, I., Herbst, K., Rouillard, A.P., Anastasiadis, A., Gieseler, J., Wimmer-Schweingruber, R., Kühl, P.: 2022, The first ground-level enhancement of solar cycle 25 on 28 October 2021. *Astron. Astrophys.* **660**, L5. [DOI](#). [ADS](#).

Park, J., Innes, D.E., Bucik, R., Moon, Y.-J.: 2013, The Source Regions of Solar Energetic Particles Detected by Widely Separated Spacecraft. *Astrophys. J.* **779**, 184. [DOI](#). [ADS](#).

Pesnell, W.D., Thompson, B.J., Chamberlin, P.C.: 2012, The Solar Dynamics Observatory (SDO). *Sol. Phys.* **275**, 3. [DOI](#). [ADS](#).

Posner, A., Richardson, I.G., Strauss, R.D.-T.: 2024, The "SEP Clock": A Discussion of First Proton Arrival Times in Wide-Spread Solar Energetic Particle Events. *Sol. Phys.* **299**, 126. [DOI](#). [ADS](#).

Posner, A., Richardson, I.G., Zeitlin, C.J.: 2025, Mars Ground Level Enhancements in the Context of the Solar Energetic Particle Clock. *Sol. Phys.* **300**, 102. [DOI](#). [ADS](#).

Prise, A.J., Harra, L.K., Matthews, S.A., Long, D.M., Aylward, A.D.: 2014, An Investigation of the CME of 3 November 2011 and Its Associated Widespread Solar Energetic Particle Event. *Sol. Phys.* **289**, 1731. [DOI](#). [ADS](#).

Reames, D.V.: 1999, Particle acceleration at the Sun and in the heliosphere. *Space Sci. Rev.* **90**, 413. [DOI](#). [ADS](#).

Richardson, I.G.: 2018, Solar wind stream interaction regions throughout the heliosphere. *Living Reviews in Solar Physics* **15**, 1. [DOI](#). [ADS](#).

Richardson, I.: 2024, Solar Energetic Particle Events Including \sim 25 MeV Protons Observed at STEREO and/or Earth since 2006. [DOI](https://doi.org/10.7910/DVN/GQPCXZ). <https://doi.org/10.7910/DVN/GQPCXZ>.

Richardson, I.G., Mays, M.L., Thompson, B.J.: 2018, Prediction of Solar Energetic Particle Event Peak Proton Intensity Using a Simple Algorithm Based on CME Speed and Direction and Observations of Associated Solar Phenomena. *Space Weather* **16**, 1862. [DOI](#).

Richardson, I.G., von Rosenvinge, T.T., Cane, H.V.: 2015, The Properties of Solar Energetic Particle Event-Associated Coronal Mass Ejections Reported in Different CME Catalogs. *Sol. Phys.* **290**, 1741. [DOI](#). [ADS](#).

Richardson, I.G., von Rosenvinge, T.T., Cane, H.V.: 2016, North/South Hemispheric Periodicities in the $>$ 25 MeV Solar Proton Event Rate During the Rising and Peak Phases of Solar Cycle 24. *Sol. Phys.* **291**, 2117. [DOI](#). [ADS](#).

Richardson, I.G., von Rosenvinge, T.T., Cane, H.V.: 2017, 25 MeV solar proton events in Cycle 24 and previous cycles. *Advances in Space Research* **60**, 755. [DOI](#). [ADS](#).

Richardson, I.G., von Rosenvinge, T.T., Cane, H.V., Christian, E.R., Cohen, C.M.S., Labrador, A.W., Leske, R.A., Mewaldt, R.A., Wiedenbeck, M.E., Stone, E.C.: 2014, $>$ 25 MeV Proton Events Observed by the High Energy Telescopes on the STEREO A and B Spacecraft and/or at Earth During the First \sim Seven Years of the STEREO Mission. *Sol. Phys.* **289**, 3059. [DOI](#). [ADS](#).

Richardson, I.G., St. Cyr, O.C., Burkepile, J.T., Xie, H., Thompson, B.J.: 2023, Solar Energetic-Particle-Associated Coronal Mass Ejections Observed by the Mauna Loa Solar Observatory Mk3 and Mk4 Coronameters. *Sol. Phys.* **298**, 105. [DOI](#). [ADS](#).

Rieger, E., Share, G.H., Forrest, D.J., Kanbach, G., Reppin, C., Chupp, E.L.: 1984, A 154-day periodicity in the occurrence of hard solar flares? *Nature* **312**, 623. [DOI](#). [ADS](#).

Rodríguez-Pacheco, J., Wimmer-Schweingruber, R.F., Mason, G.M., Ho, G.C., Sánchez-Prieto, S., Prieto, M., Martín, C., Seifert, H., Andrews, G.B., Kulkarni, S.R., Panitzsch, L., Boden,

S., Böttcher, S.I., Cernuda, I., Elftmann, R., Espinosa Lara, F., Gómez-Herrero, R., Terasa, C., Almena, J., Begley, S., Böhm, E., Blanco, J.J., Boogaerts, W., Carrasco, A., Castillo, R., da Silva Fariña, A., de Manuel González, V., Drews, C., Dupont, A.R., Eldrum, S., Gordillo, C., Gutiérrez, O., Haggerty, D.K., Hayes, J.R., Heber, B., Hill, M.E., Jüngling, M., Kerem, S., Knierim, V., Köhler, J., Kolbe, S., Kulemzin, A., Lario, D., Lees, W.J., Liang, S., Martínez Hellín, A., Meziat, D., Montalvo, A., Nelson, K.S., Parra, P., Paspirgilis, R., Ravankakhsh, A., Richards, M., Rodríguez-Polo, O., Russu, A., Sánchez, I., Schlemm, C.E., Schuster, B., Seimetz, L., Steinhagen, J., Tammen, J., Tyagi, K., Varela, T., Yedla, M., Yu, J., Agueda, N., Aran, A., Horbury, T.S., Klecker, B., Klein, K.-L., Kontar, E., Krucker, S., Maksimovic, M., Malandraki, O., Owen, C.J., Pacheco, D., Sanahuja, B., Vainio, R., Connell, J.J., Dalla, S., Dröge, W., Gevin, O., Gopalswamy, N., Kartavykh, Y.Y., Kudela, K., Limousin, O., Makela, P., Mann, G., Önel, H., Posner, A., Ryan, J.M., Soucek, J., Hofmeister, S., Vilmer, N., Walsh, A.P., Wang, L., Wiedenbeck, M.E., Wirth, K., Zong, Q.: 2020, The Energetic Particle Detector. Energetic particle instrument suite for the Solar Orbiter mission. *Astron. Astrophys.* **642**, A7. [DOI](#) [ADS](#).

Rotti, S., Aydin, B., Georgoulis, M.K., Martens, P.C.: 2022, Integrated Geostationary Solar Energetic Particle Events Catalog: GSEP. *Astrophys. J. Suppl.* **262**, 29. [DOI](#) [ADS](#).

Ryan, J.M., Lee, M.A.: 1991, On the Transport and Acceleration of Solar Flare Particles in a Coronal Loop. *Astrophys. J.* **368**, 316. [DOI](#) [ADS](#).

Scargle, J.D.: 1982, Studies in astronomical time series analysis. II. Statistical aspects of spectral analysis of unevenly spaced data. *Astrophys. J.* **263**, 835. [DOI](#) [ADS](#).

St. Cyr, O.C., Howard, R.A., Plunkett, S.P., Lawrence, G., Stenborg, G., Yashiro, S., Michalek, G., Sheeley, N., Gopalswamy, N., Vourlidas, A.: 2005, The Last Word: The Definition of Halo Coronal Mass Ejections. *Eos, Transactions American Geophysical Union* **86**, 281.

St. Cyr, O.C., Richardson, I.G., Burkepile, J.T., Gallo, M., Nieves-Chinchilla, T., Thompson, B.J.: 2025, Mauna Loa Solar Observatory K-Cor Coronagraph Observations of Coronal Mass Ejections Associated with Solar Energetic Particles. *Submitted to Solar Physics*.

Stone, E.C., Frandsen, A.M., Mewaldt, R.A., Christian, E.R., Margolies, D., Ormes, J.F., Snow, F.: 1998, The Advanced Composition Explorer. *Space Sci. Rev.* **86**, 1. [DOI](#) [ADS](#).

Storini, M., Bazilevskaya, G.A., Fluckiger, E.O., Krainev, M.B., Makhmutov, V.S., Sladkova, A.I.: 2003, The GNEVYSHEV gap: A review for space weather. *Advances in Space Research* **31**, 895. [DOI](#) [ADS](#).

Strauss, R.D., Dresing, N., Richardson, I.G., van den Berg, J.P., Steyn, P.J.: 2023, On the Onset Delays of Solar Energetic Electrons and Protons: Evidence for a Common Accelerator. *Astrophys. J.* **951**, 2. [DOI](#) [ADS](#).

Sun, X., Bobra, M.G., Hoeksema, J.T., Liu, Y., Li, Y., Shen, C., Couvidat, S., Norton, A.A., Fisher, G.H.: 2015, Why Is the Great Solar Active Region 12192 Flare-rich but CME-poor? *Astrophys. J. Lett.* **804**, L28. [DOI](#) [ADS](#).

Torsti, J., Valtonen, E., Lumme, M., Peltonen, P., Eronen, T., Louhola, M., Riihonen, E., Schultz, G., Teittinen, M., Ahola, K., Holmlund, C., Kelhä, V., Leppälä, K., Ruuska, P., Strömmér, E.: 1995, Energetic Particle Experiment ERNE. *Sol. Phys.* **162**, 505. [DOI](#) [ADS](#).

Vainio, R., Valtonen, E., Heber, B., Malandraki, O.E., Papaioannou, A., Klein, K.-L., Afanasiev, A., Agueda, N., Aurass, H., Battarbee, M., Braune, S., Dröge, W., Ganse, U., Hamadache, C., Heynderickx, D., Huttunen-Heikinmaa, K., Kiener, J., Kilian, P., Kopp, A., Kouloumavakos, A., Maisala, S., Mishev, A., Miteva, R., Nindos, A., Oittinen, T., Raukunen, O., Riihonen, E., Rodríguez-Gasén, R., Saloniemi, O., Sanahuja, B., Scherer, R., Spanier, F., Tatischeff, V., Tziotziou, K., Usoskin, I.G., Vilmer, N.: 2013, The first SEPServer event catalogue ~68-MeV solar proton events observed at 1 AU in 1996–2010. *Journal of Space Weather and Space Climate* **3**, A12. [DOI](#) [ADS](#).

Van Hollebeke, M.A.I., Ma Sung, L.S., McDonald, F.B.: 1975, The Variation of Solar Proton Energy Spectra and Size Distribution with Heliolongitude. *Sol. Phys.* **41**, 189. [DOI](#) [ADS](#).

von Rosenvinge, T.T., Reames, D.V., Baker, R., Hawk, J., Nolan, J.T., Ryan, L., Shuman, S., Wortman, K.A., Mewaldt, R.A., Cummings, A.C., Cook, W.R., Labrador, A.W., Leske, R.A., Wiedenbeck, M.E.: 2008, The High Energy Telescope for STEREO. *Space Sci. Rev.* **136**, 391. [DOI](#) [ADS](#).

von Rosenvinge, T.T., Richardson, I.G., Reames, D.V., Cohen, C.M.S., Cummings, A.C., Leske, R.A., Mewaldt, R.A., Stone, E.C., Wiedenbeck, M.E.: 2009, The Solar Energetic Particle Event of 14 December 2006. *Sol. Phys.* **256**, 443. [DOI](#) [ADS](#).

von Rosenvinge, T., Richardson, I.G., Cane, H.V., Christian, E., Cohen, C., Cummings, A., Labrador, A.W., Leske, R., Mewaldt, R., Stone, E., Wiedenbeck, M.: 2015, The Longitudinal

Distribution of Solar Energetic Particles. In: *34th International Cosmic Ray Conference (ICRC2015), International Cosmic Ray Conference* **34**, 104. [DOI](#). [ADS](#).

Vourlidas, A., Balmaceda, L.A., Stenborg, G., Dal Lago, A.: 2017, Multi-viewpoint Coronal Mass Ejection Catalog Based on STEREO COR2 Observations. *Astrophys. J.* **838**, 141. [DOI](#). [ADS](#).

Vršnak, B., Sudar, D., Ruždjak, D.: 2005, The CME-flare relationship: Are there really two types of CMEs? *Astron. Astrophys.* **435**, 1149. [DOI](#). [ADS](#).

Whitman, K., Egeland, R., Richardson, I.G., Allison, C., Quinn, P., Barzolla, J., Kitiashvili, I., Sadykov, V., Bain, H.M., Dierckxsens, M., Mays, M.L., Tadesse, T., Lee, K.T., Semones, E., Luhmann, J.G., Nunez, M., White, S.M., Kahler, S.W., Ling, A.G., Smart, D.F., Shea, M.A., Tenishev, V., Boubrahimi, S.F., Aydin, B., Martens, P., Angryk, R., Marsh, M.S., Dalla, S., Crosby, N., Schwadron, N.A., Kozarev, K., Gorby, M., Young, M.A., Laurens, M., Cliver, E.W., Alberti, T., Stumpo, M., Benella, S., Papaioannou, A., Anastasiadis, A., Sandberg, I., Georgoulis, M.K., Ji, A., Kempton, D., Pandey, C., Li, G., Hu, J., Zank, G.P., Lavasa, E., Giannopoulos, G., Falconer, D., Kadadi, Y., Fernandes, I., Dayeh, M.A., Munoz-Jaramillo, A., Chatterjee, S., Moreland, K.D., Sokolov, I.V., Rousset, I.I., Taktakishvili, A., Effenberger, F., Gombosi, T., Huang, Z., Zhao, L., Wijsen, N., Aran, A., Poedts, S., Kouloumvakos, A., Paassilta, M., Vainio, R., Belov, A., Eroshenko, E.A., Abunina, M.A., Abunin, A.A., Balch, C.C., Malandraki, O., Karavolos, M., Heber, B., Labrenz, J., Kuhl, P., Kosovichev, A.G., Oria, V., Nita, G.M., Illarionov, E., O'Keefe, P.M., Jiang, Y., Fereira, S.H., Ali, A., Paouris, E., Aminalragia-Giamini, S., Jiggens, P., Jin, M., Lee, C.O., Palmerio, E., Bruno, A., Kasapis, S., Wang, X., Chen, Y., Sanahuja, B., Lario, D., Jacobs, C., Strauss, D.T., Steyn, R., van den Berg, J., Swalwell, B., Waterfall, C., Nedal, M., Miteva, R., Dechev, M., Zucca, P., Engell, A., Maze, B., Farmer, H., Kerber, T., Barnett, B., Loomis, J., Grey, N., Thompson, B.J., Linker, J.A., Caplan, R.M., Downs, C., Török, T., Lionello, R., Titov, V., Zhang, M., Hosseinzadeh, P.: 2023, Review of solar energetic particle models. *Advances in Space Research* **72**, 5161. [DOI](#).

Wijsen, N., Lario, D., Sánchez-Cano, B., Jebaraj, I.C., Dresing, N., Richardson, I.G., Aran, A., Kouloumvakos, A., Ding, Z., Niemela, A., Palmerio, E., Carcaboso, F., Vainio, R., Afanasiev, A., Pinto, M., Pacheco, D., Poedts, S., Heyner, D.: 2023, The Effect of the Ambient Solar Wind Medium on a CME-driven Shock and the Associated Gradual Solar Energetic Particle Event. *Astrophys. J.* **950**, 172. [DOI](#). [ADS](#).

Wild, J.P., Smerd, S.F., Weiss, A.A.: 1963, Solar Bursts. *Ann. Rev. Astron. Astrophys.* **1**, 291. [DOI](#). [ADS](#).

Wilson III, L.B., Brosius, A.L., Gopalswamy, N., Nieves-Chinchilla, T., Szabo, A., Hurley, K., Phan, T., Kasper, J.C., Lugaz, N., Richardson, I.G., Chen, C.H.K., Verscharen, D., Wicks, R.T., TenBarge, J.M.: 2021, A Quarter Century of Wind Spacecraft Discoveries. *Reviews of Geophysics* **59**, e2020RG000714. [DOI](#). [ADS](#).

Winter, L.M., Ledbetter, K.: 2015, Type II and Type III Radio Bursts and their Correlation with Solar Energetic Proton Events. *Astrophys. J.* **809**, 105. [DOI](#). [ADS](#).

Wuelser, J.-P., Lemen, J.R., Tarbell, T.D., Wolfson, C.J., Cannon, J.C., Carpenter, B.A., Duncan, D.W., Gradwohl, G.S., Meyer, S.B., Moore, A.S., Navarro, R.L., Pearson, J.D., Rossi, G.R., Springer, L.A., Howard, R.A., Moses, J.D., Newmark, J.S., Delaboudiniere, J.-P., Artzner, G.E., Auchere, F., Bougnet, M., Bouyries, P., Bridou, F., Clotaire, J.-Y., Colas, G., Delmotte, F., Jerome, A., Lamare, M., Mercier, R., Mullot, M., Ravet, M.-F., Song, X., Bothmer, V., Deutsch, W.: 2004, EUVI: the STEREO-SECCHI extreme ultraviolet imager. In: Fineschi, S., Gummin, M.A. (eds.) *Telescopes and Instrumentation for Solar Astrophysics, Society of Photo-Optical Instrumentation Engineers (SPIE) Conference Series* **5171**, 111. [DOI](#). [ADS](#).

Xie, H., Mäkelä, P., St. Cyr, O.C., Gopalswamy, N.: 2017, Comparison of the coronal mass ejection shock acceleration of three widespread SEP events during solar cycle 24. *Journal of Geophysical Research: Space Physics* **122**, 7021. [DOI](#). <https://agupubs.onlinelibrary.wiley.com/doi/abs/10.1002/2017JA024218>.

Zhao, L., Zhang, M.: 2018, Effects of Coronal Magnetic Field Structures on the Transport of Solar Energetic Particles. *Astrophys. J. Lett.* **859**, L29. [DOI](#). [ADS](#).